THESIS FOR THE DEGREE OF LICENTIATE OF ENGINEERING

Applicability of thermal energy storage in future district heating system

Design methodologies and performance evaluations

Yichi Zhang

Division of Building Technology

Department of Architecture and Civil Engineering

CHALMERS UNIVERSITY OF TECHNOLOGY

Gothenburg, Sweden 2021

Applicability of thermal energy storage in future district heating system

Design methodologies and performance evaluations

Yichi Zhang

Technical report no 2021:6

Lic /Architecture and Civil Engineering / Chalmers University of Technology

Department of Architecture and Civil Engineering
Division of Building Technology
Chalmers University of Technology
SE-412 96 Gothenburg
Sweden
Telephone + 46 (0)31-772 1000

Author e-mail: yichi@chalmers.se

Cover:

Graphical explanation of the design procedures for TES

Chalmers Reproservice
Gothenburg, Sweden 2021

Applicability of thermal energy storage in future district heating system

Design methodologies and performance evaluations

YICHI ZHANG
Department of Architecture and Civil Engineering
Division of Building Technology, Building Physics Modelling
Chalmers University of Technology

Abstract

District heating (DH) enables efficient and economical utilization of energy resources to satisfy the heat and hot water demands in buildings and is, thereby, well-established in Northern European countries. To achieve the future renewable energy system, the current DH systems are proved to undergo transitions towards the future DH systems, with major characteristics including renewable-based heat sources, low temperature networks, lower heating demands and smart controls. An important step is the coordination of heating and electricity sectors to achieve synergies and optimal solutions for the overall energy system, which is also known as the smart energy systems. Such goal could be achieved in a cost-effective manner by the flexibilities added from short-term thermal energy storage (TES) technologies. Despite the importance of TES has been demonstrated in previous studies, giving drastic changes compared to the current systems, the practical applicability of TES in the future DH systems remains unknown. The proposed benefits of TES might deviate from expectation considering the future characteristics, such as the low storage temperature levels and short space-heating period. Furthermore, the current studies about the TES applications have mostly focused on specific case studies. The findings are of limited applicability because they cannot be easily generalized and extrapolated to other future conditions.

To explore the practical challenges and optimal applications of short-term TES units in the future, a systematic design framework that considers the diverse factors from top-level targets to bottom-level implementations is developed in this study. The top-level theoretical analysis method is developed to identify the load shifting potentials and associated storage capacities for the whole energy system, by comparing and matching energy supply and demand profiles. Compared to current bottom-up detailed system models, the proposed method requires only the energy profiles, which has resulted in much shorter analysis time. The method is further validated by complex system models, and because a good agreement has been achieved, it can be applied in various scenarios to efficiently pre-study the storage potentials. Then, the design of the practical TES capacity is derived from the theoretical result by considering performance indicators during realistic operations, such as power-to-heat conversion efficiency and heat loss efficiency.

On bottom-level implementations, four typical short-term TES technologies were investigated including central water tank (CWT), district heating network inertia (DHNI), domestic hot water tank (DHWT), and building thermal mass (BTM). For this purpose, an integrated bottom-

level model to simulate the operation dynamics of the district heating systems and to optimize the use of the TES units is developed. Techno-economic analysis and comparisons of TES technologies were performed on a variety of scenarios, which are representatives of the main characteristics of the current middle-temperature district heating system and future low-temperature district heating system. The changes in the source side, transportation networks and end-use building demands are considered. As a result, a performance map of the TES technologies indicating the strong links between the system characteristics and optimal TES applications has been identified. Based on that, the optimal combinations of TES technologies were proposed for a LTDH system. Consequently, combining this with top-level methods, the overall potentials and roles of short-term TES were identified by a systematic design framework.

Key words:

Thermal energy storage; district heating; low-temperature district heating; variable renewable energy; demand-side management; low energy buildings

Termiska energilager i framtidens fjärrvärmesystem

Metoder för utformning och utvärdering av prestanda

YICHI ZHANG
Institutionen för Arkitektur och samhällsbyggnadsteknik
Avdelningen för Byggnadsteknologi, Byggnadsfysikalisk modellering
Chalmers tekniska högskola

Sammanfattning

Fjärrvärme möjliggör ett effektivt och ekonomiskt hållbart energiförsörjningssystem för att tillgodose uppvärmnings- och varmvattenbehovet i byggnader. Det är därför välutbyggt i de nordeuropeiska länderna. För att uppnå framtidens förnyelsebara energisystem måste nuvarande fjärrvärmesystem utvecklas i flera avseenden, såsom integration av förnyelsebara energikällor, system med låg temperatur, framtida lägre värmebehov och smarta styrsystem. Ett viktigt steg för att uppnå detta är att koppla samman värme- och elsektorerna. Detta kan ge viktiga synergier och optimala lösningar för det övergripande energisystemet. En sådan sammankoppling skulle kunna möjliggöras på ett kostnadseffektivt sätt genom den flexibilitet som termiska energilager (TES) ger till fjärrvärmesystemet. Trots att betydelsen av TES jämfört med de nuvarande systemen har påvisats i tidigare studier med dramatiska förändringar är den praktiska potentialen av TES i framtidens fjärrvärmesystem fortfarande outforskad. De föreslagna fördelarna med TES kan komma att avvika från förväntningarna med tanke på de framtida systemegenskaperna, till exempel lägre temperaturer och kortare uppvärmningsperioder. Dessutom har de nuvarande studierna om TES-tillämpningar mestadels varit inriktade på specifika fallstudier. Resultaten är av begränsad tillämpbarhet eftersom de inte lätt kan generaliseras och extrapoleras till andra förhållanden.

I denna studie utvecklas en systematisk designmodell för systemutformning som beaktar de olika faktorerna från mål på övergripande nivå till genomförbarhet. Målet är att utforska de praktiska utmaningarna för att identifiera de optimala tillämpningarna av TES-enheter med kort laddningsfrekvens. Den teoretiska analysmetoden utvecklas på övergripande nivå för att identifiera potentialen och för att matcha energitillgångs- och efterfrågeprofiler med tillhörande lagringskapacitet för hela energisystemet. Jämfört med nuvarande systemmodeller som utgår från detaljerad simulering av de enskilda byggnaderna kräver denna metod endast energiprofilerna vilket leder till en kortare simuleringstid. Metoden har validerats med god överensstämmelse mot mer komplexa systemmodeller vilken gör metoden tillämpbar för att effektivt studera lagringspotentialen i olika scenarier. Därefter härleds utformningen av den praktiska TES-kapaciteten från det teoretiska resultatet genom att beakta prestandan under realistisk drift, till exempel förluster vid energiomvandlingen från el till värme.

För genomförandet undersöktes fyra typiska kortsiktiga TES-tekniker; central ackumulatortank, termisk tröghet i fjärrvärmenätet, ackumulatortank för hushållsbruk och termisk massa i byggnader. En integrerad modell utvecklades för att simulera dynamiken i

fjärrvärmesystemet och optimera användningen av TES-enheterna. En teknisk och ekonomisk analys av TES-teknikerna utfördes baserat på olika scenarier som representerar de viktigaste egenskaperna hos det nuvarande fjärrvärmesystemet med medelhög temperatur, och det framtida fjärrvärmesystemet med låg temperatur. Förändringar på produktionssidan, i transportnät och i förändrade krav på byggnader beaktas. En prestandakarta för TES-tekniken visar de starka kopplingarna mellan systemegenskaperna och optimala TES-tillämpningar. Därefter har de optimala kombinationerna av TES-tekniker föreslagits för ett fjärrvärmesystem med låg temperatur. Genom att kombinera detta med analyser på systemnivå identifierades de övergripande möjligheterna och rollerna för TES med kort laddningsfrekvens.

Nyckelord:

Termisk energilagring, fjärrvärme, fjärrvärme med låg temperatur, variabel förnybar energi, styrning av efterfrågan, lågenergibyggnader

Acknowledgment

Firstly, I would like to express my sincere thanks to my supervisors, Angela Sasic Kalagasidis and Pär Johansson for their continuing help and support. The supervision meetings with you are always inspiring and beneficial for my research career. I would also like to thank Carl-Eric Hagentoft for his help on the models regarding the building physics.

Thanks also go to the colleagues of the Division of Building Technology for the help during daily work and relaxing fika time (physical and virtual) before and during corona period. In particular to colleagues from the building physics modelling group, for help on my project and licentiate thesis.

I would like to thank my friends who are always supporting me. Special thanks to my coding doge, for the accompanies and encouraging words when I was in stuck with problems. Finally, I would like to thank my family. You're always in my heart.

The research project has been funded by the Swedish Research Council for Environment, Agricultural Sciences and Spatial Planning (FORMAS) [Grant No. 2018-01228]. The financial support is gratefully acknowledged. The author also thank the Chalmers Energy Area of Advance, Profile area: Energy in Urban Development for the additional financial support.

Yichi Zhang

Gothenburg, May 2021

List of Publications

This licentiate thesis is based mainly on the work presented in the following publications:

I. Yichi Zhang, Pär Johansson, Angela Sasic Kalagasidis, "Applicability of thermal energy storage in future low-temperature district heating systems - multi-scenarios analysis and evaluations" preprint submitted to the Journal of *Energy Conversion and Management*, May 2021.
II. Yichi Zhang, Pär Johansson, Angela Sasic Kalagasidis, "Utilizing the thermal inertia of district heating networks to improve energy system flexibility: potentials and feasibilities", preprint to be submitted, 2021.

Additional Publications

Other publications that are related to the content of the thesis are listed below.

III. Yichi Zhang, Pär Johansson, Angela Sasic Kalagasidis. " Techno-economic assessment of thermal energy storage technologies for demand-side management in low-temperature individual heating systems" Submitted to the Journal of *Energy*, December 2020 (postprint under review)
IV. Yichi Zhang, Xingli Ding, Angela Sasic Kalagasidis. " Intermittent individual heating based on realistic occupancies – A performance comparison of all-air, radiator, and floor heating systems" Submitted to the *Journal of Building Engineering*, March 2021 (preprint under review)

Contents

Abbreviations

BTM	Building Thermal Mass
CHP	Combined Heat and Power
COP	Coefficient of Performance
CWT	Central Water Tank
DH	District Heating
DHNI	District Heating Network Inertia
DHW	Domestic Hot Water
DHWT	Domestic Hot Water Tank
ES	Electric Storage
IWH	Industrial Waste Heat
LTDH	Low-temperature District Heating
MTDH	Middle-temperature District Heating
SEK	Swedish Kronor
SFH	Single-family House
SH	Space Heating
TES	Thermal Energy Storage
VRE	Variable Renewable Energy

Part I

Summary

1 Introduction

This chapter introduces shortly the background of the energy system transitions from current to future highly interoperable systems operated solely on renewable energy sources. Based on literature reviews, thermal energy storage (TES) technologies are identified as one of key enables of this transition. The challenges related to the applicability of TES technologies under such transitions are summarized and formulated as aims of this study. Finally, the research framework and limitations are presented.

1.1 Background

The target of a 100% renewable energy system brings drastic challenges for the whole society [1]. With the increasing share of variable renewable energy (VRE) suppliers, the whole energy systems including the transportation networks and consumers shall be re-designed and planned to efficiently utilize the VRE sources while maintaining secured energy supplies and acceptable economic expenditures [2]. It is acknowledged that the integrated design of energy conversions and management between energy sub-sectors are becoming increasingly important for achievable and affordable strategies.

Currently, the heating sector accounts for 50% of Europe's final energy consumption [3] and is expected to remain so for the forecasted future. Among solutions to decarbonize the heating sector and increase the renewable energy integration, the concept of the future low temperature district heating (LTDH) is discussed in several studies [4–6]. A low temperature of the circulating water in combination with low heating demands in buildings can enable key benefits of LTDH, including better utilization of low-temperature waste heat and of renewable energy sources, as well as lower losses in transportation networks. Furthermore, the heating sector of the LTDH system can be coordinated with the electricity and transportation sectors. Together they can form what is today referred to as a smart energy system and enable an optimal transition towards the future 100% renewable energy system [2,7].

In order to achieve such synergies between sectors, TES technologies are widely studied since they can offer flexibilities in matching the energy supply and demand on various time scales [8]. Combined with CHP plants and power-to-heat technologies such as heat pumps, TES technologies can increase the VRE integration and reduce the operational cost in existing

systems [9,10] and future smart energy systems [11–14]. TES technologies can be classified into long-term seasonal storage units and short-term storage units according to the period of storage cycles. The latter is a common choice that can be installed at the supply side or demand side to deal with diurnal variations of power and demand caused by the intermittent nature of variable renewable energy (VRE). These variations have strong influence on the marginal operation costs and performances of the DH systems [15]. Thus, the short-term storage units are chosen as study objects. According to their connections to the DH systems, the TES units can be classified into three categories, as shown in Figure 1.1. In this study, four short-term sensible TES technologies, which are the central water tank (CWT), district heating network inertia (DHNI), building thermal mass (BTM), and distributed domestic hot water tank (DHWT), are investigated.

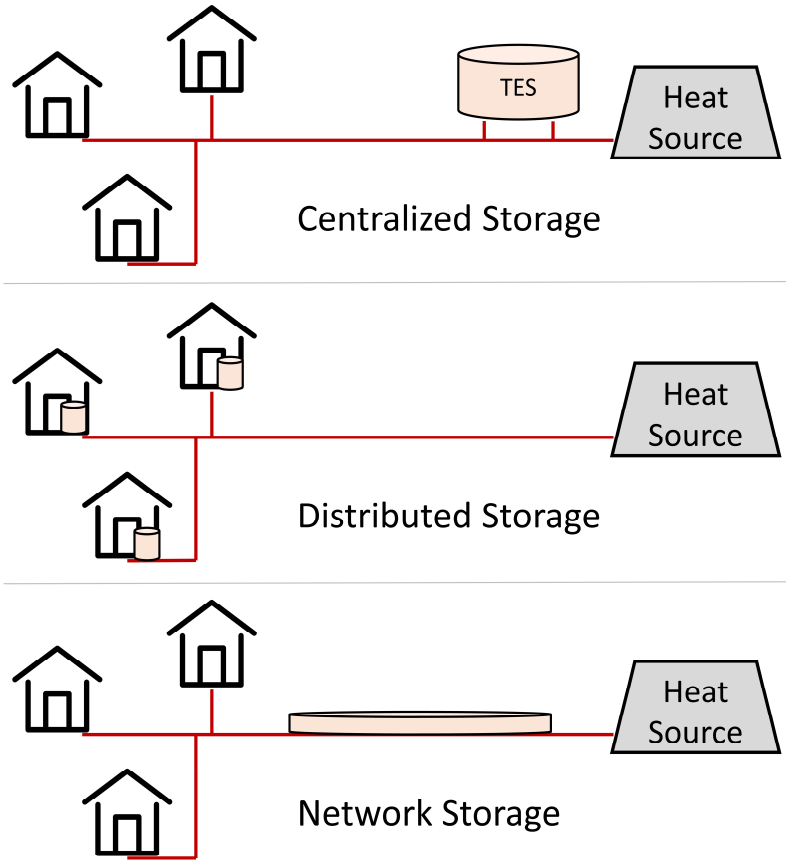

Figure 1.1. TES connections to DH systems.

Despite the importance of TES and future LTDH systems imposed by previous top-down studies [4–6,11–14], relatively less attention has been put on how different TES technologies are adapted and performed in future DH systems. In recent reviews summarizing the applications of TES technologies in district heating and cooling systems [8,16], the majority of examples refer to the TES applications in the current middle and high temperature district heating (DH) systems. It is, however, worth noting some important changes in the future LTDH systems. Because of lower system temperatures, the heat source efficiency will be more

sensitive to temperature changes. Furthermore, the networks and substations are to be re-designed to maintain the return water temperature and avoid bypass heat loses. Meanwhile, space-heating demand and heating periods will be reduced due to better energy efficiency of the future buildings. Considering the above-mentioned changes in the LTDH system, whether the planned TES technologies can work as expected in the future LTDH systems remains as a question.

From the perspective of bottom-level TES applications details, as the storage temperature difference becomes smaller in LTDH systems, the use of sensible active storage units becomes less profitable [15]. Since the system efficiency is more sensitive to temperature levels, the current plausible storage technologies that have influences on the network working temperatures, such as the use of the district heating network inertia (DHNI) and domestic hot water tank (DHWT), might lose attractiveness in the future. Based on literature research, the challenges for the current short-term TES technologies in future LTDH systems are summarized in Table 1.1. However, these issues were mostly only mentioned or qualitatively discussed, implying strong need for the quantitative investigations of the applicability of TES technologies in the future.

Table 1.1. Overview of the challenges for current short-term TES technologies in future LTDH systems

TES	Challenges in the future LTDH systems
Central water tank (CWT)	1) Smaller energy storage density due to reduced temperature differences [15] 2) Mixture of hot and cold water inside the tank increases the return water temperatures and influences the source efficiency [17]
District heating network inertia (DHNI)	1) Less storage potentials due to reduced heating demand densities [18] 2) Active network temperature changes influence the source efficiency [16] 3) Infeasible during low-demand period [19]
Building thermal mass (BTM)	1) Only feasible during space-heating period. Less potentials in the future due to reduced space heating demand 2) More influenced by the residents' behaviours [20]
Domestic hot water tank (DHWT)	1) Smaller energy storage density due to reduced temperature differences 2) Large circulation losses in the demand side [21] 3) Alternative designs to assure comfort and sanitary hot water supply, while maintaining required return water temperatures [22,23]

As for the top-level planning of the TES and energy systems, most studies are still taking the current TES technologies into account, without considering their technical details and applicability in the future. In ref [11], the potential of DHNI is evaluated based on a fixed temperature increase of 10 K in the network, which is not appropriate according to aforementioned reasons. Limitations also exist for evaluating the storage potential of building thermal mass (BTM) [24], since the practical storage capacity is reduced as the heating demand becomes lower in the future. Without the knowledge about operational conditions of TES technologies in the future, there are risks for the exaggerated or underestimated potentials of the TES, which further influences the energy balance and overall planning of the energy systems. The proposed pathways towards the 100% renewable energy target might deviate from the reality. Hence, to prevent biased conclusions for the future energy systems, the technological development and planning of TES shall be in high accordance with the changes in the future.

According to the roadmap studies for the sustainable energy target in Europe [6,14], various system types are to exist on the future market, including both middle-temperature district heating (MTDH) systems and LTDH systems. The system design is based on several practical issues, such as the types of heat sources, the demand densities, and the thermal performance of end-users, i.e. the buildings. However, the current studies about the TES applications have mostly focused on specific case studies. The findings are thus of limited applicability because they are not conceptualized and cannot be extrapolated to other future conditions. In consequence, the roles of TES technologies are not clear. The diverse factors and application scenarios associated with the TES performances shall be systematically analysed. In other words, a design framework that can specify the potentials and explain the applications is need.

1.2 Aim and objectives

This study aims to evaluate the applicability of TES technologies in future DH systems. A systematic design framework for the short-term TES units, from top-level targets to bottom-level implementations, is developed for that purpose. The top-level theoretical analysis method can easily identify the load shifting potentials and associated storage capacities, based on the matching of energy supply and demand profiles. The bottom-up techno-economic analysis and comparisons of four typical short-term TES technologies were performed on a variety of scenarios, which are representing the main characteristics of the current and future DH systems. Based on the results, the potentials and roles of short-term TES technologies in the future are illustrated.

The presented work answers the following questions:

1. How do the current TES technologies perform in different DH systems in the future?

2. How to design the suitable TES technologies according to the specific targets and practical conditions?

3. What is the role of short-term TES technologies in the future?

1.3 Methodological framework

The design framework for the TES units can be summarized into three levels, as shown in Figure 1.2. The top-level factors decide the general target of the TES unit, such as the maximum shiftable load and economic benefit. Then, the target is converted to the practical storage capacity of the TES units in the middle level, by considering the realistic heating systems and heat sources. The implementations of the TES units belong to the bottom level, where the design details of the different storage choices are specified. Practical issues such as the buildings and demand densities are influencing the choice of the TES units on this bottom level. A graphical explanation of the design procedures is shown in Figure 1.3.

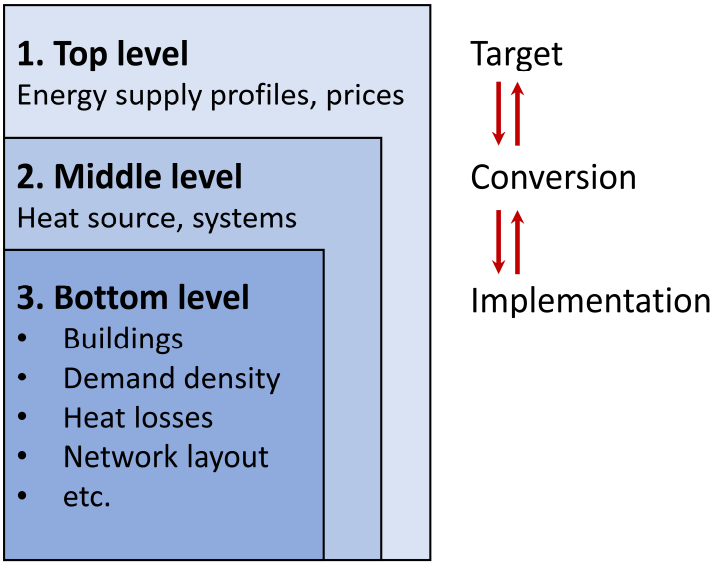

Figure 1.2. Three levels of design for the short-term TES technologies.

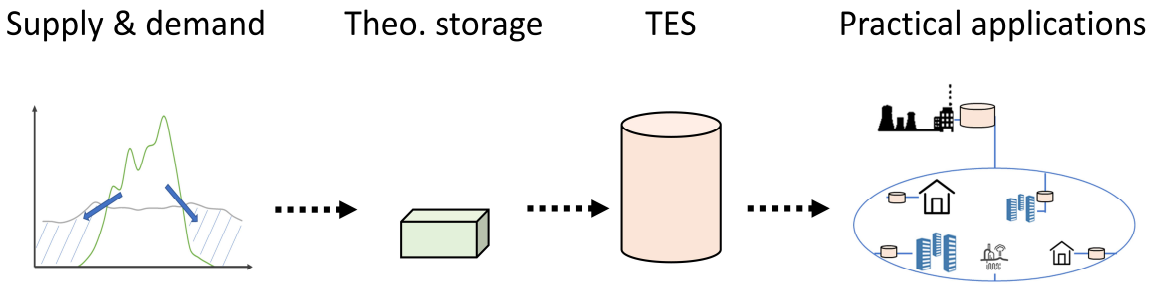

Figure 1.3. Graphical explanation of the design procedures for TES.

The thesis is organized as the design framework shown in Figure 1.4. The research questions are raised in the introductory chapter. Chapter 2 presents a novel method for defining design targets of the storage unit, by matching the supply and demand profiles. The middle-level conversion of the design target is also explained in Chapter 2. Then, bottom-level implementations of TES technologies are explained in Chapter 3 and Chapter 4 by considering different DH systems. Chapter 3 introduces the main bottom-level modelling methodologies and evaluates the applications of TES technologies under multiple scenarios in a case LTDH system. The suggestions for the TES in future LTDH systems were also qualitatively discussed in this chapter. In Chapter 4, the TES performances in a MTDH system were evaluated and further compared to that in the LTDH system, to investigate the influences of bottom-level technical details on the TES applications. Based on the findings from the multi-scenarios' studies, the design suggestions for the short-term TES units were discussed, as well as forecasted storage potentials and benefits. Finally, the conclusions and recommendations for future research are presented in Chapter 5.

The main content of Chapter 3 is based on the study presented in Paper I. Part of the methodologies and results in Chapter 4 were reported in the appended Paper II.

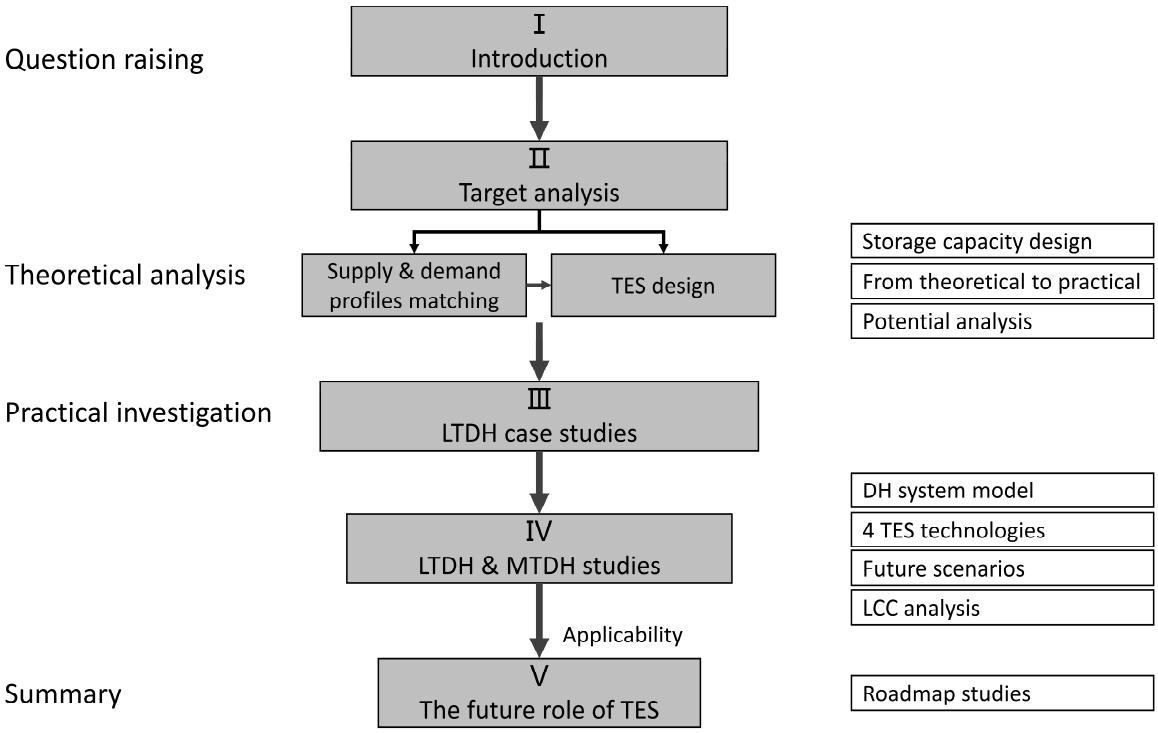

Figure 1.4. Illustrative flowchart of the structures of this thesis.

1.4 Limitations

In this thesis, the investigated DH systems have only one centralized location for heat sources. Although there are growing interests in the multi-sources DH systems, they are not considered in this study to limit the scope of the work. For the same reason, this study only investigated the heating technologies at the source-side, while such technologies can be installed at the demand-side as peak heater, to reduce the system operation costs and required system sizes. As pointed out in [25], various types of energy systems will co-exist on the market. Together, they form an overview of the future sustainable energy systems. Thus, the investigated scenarios in this study are still part of this big picture. The applicability of TES technologies in other scenarios shall be further investigated, which is the future research objective of this project, as explained in Chapter 5.

This study only focused on the short-term TES technologies, as the common methods to handle the diurnal load variations. The long-term storage units, such as those designed for balancing the seasonal demand and supply, are not considered. These storage units can also shift the diurnal load variations, but their practical feasibilities related to the specific projects shall be carefully investigated. Besides, only sensible storage units are included in this study, while e.g. the latent phase-change material storage units are not addressed. The applicability of these alternative storage units shall be further studied.

2 Target analysis

In this chapter, a novel simplified method is presented to identify the design target of the storage unit, by matching the energy supply and demand profiles. With this method, the maximum benefit from balancing the energy profiles and the associated maximum storage capacity can be acquired by simple calculations, based on the information of energy profiles. The results obtained thereby are validated by the case study results from complex dynamic models in later chapters, which proves the reliability and application prospects of the proposed simplified method. Then, the analyzed target is converted to the design of the practical TES. The key performance indicators regarding the design process are also described.

2.1 Simplified stationary analysis methodology

The benefits from the TES units can be classified into three points [26]: (1) reduced investment and usage of peak capacity. (2) smoother operation of equipment and reduced running costs. (3) flexible load shifting to utilize non-dispatchable VRE or electricity with lower prices.

For the first and second points, the benefits of the TES units are basically related to the characteristics of the heat sources, such as the operational costs and investments. However, regarding the third point, the benefits are decided by the relations between the energy supply and demand profiles, which have more complex conditions than the fixed characteristics of the heat sources. Thus, this chapter focuses on the matching of energy profiles to evaluate the maximum load shifting potentials. Such process is also the pre-requisite for storage designs.

2.1.1 Profile matching analysis

For an energy storage unit, the load shifting target is to transfer the surplus VRE supply to the period when the VRE is insufficient, as shown in Figure 2.1. The main question is how much energy can be theoretically shifted. The potential is influenced by the following factors: (1) the relations between the amount of the surplus and deficit energy; (2) the length of one storage cycle; (3) the charging and discharging power of the storage unit. To evaluate the theoretical load shifting potential, several assumptions are made:

(1) The operation is made up of several separate charging-discharging cycles, noted as storage cycles. Within each cycle, the storage capacity is fully utilized to shift the surplus energy to deficit period. The surplus or deficit potential cannot be transferred to other storage cycles, due to the limitations of the storage unit.

(2) Energy loss is not considered. The analysis refers to theoretical charging and discharging process.

(3) The analysis is about the theoretical electric storage and the electricity supply and demand. The conversion between heat and electricity sectors, and the heat source efficiencies are illustrated in Section 2.3.

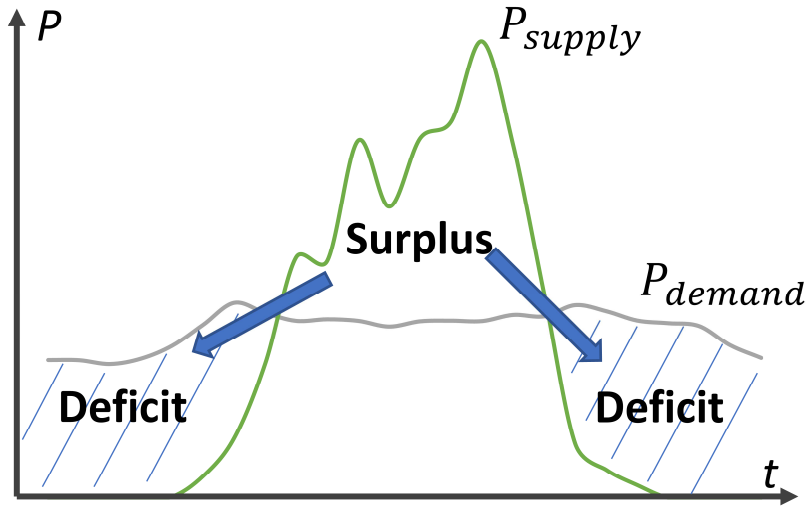

Figure 2.1. Illustrative figure for the matching of energy supply and demand.

By subtracting the demand $P_{demand,t}$ from VRE supply profile $P_{VRE,supply,t}$, a baseline usage of the VRE, which doesn't require any active load shifting measure, is acquired, as written in Eq. (1). Within each storage cycle, the cumulative amount of the deficit VRE $Q_{deficit,cycle}$ and surplus VRE $Q_{sur,cycle}$ is calculated according to Eq. (2) and Eq. (3). The matching potential in every cycle is defined as the minimal value of the deficit and surplus energy. Thus, for each storage, there is an associated matching potential.

$$P_{base,t} = P_{VRE,supply,t} - P_{demand,t} \tag{1}$$

$$Q_{deficit,cycle} = \min\left(\left|\sum_{t\in cycle} P_{base,t}\right|, \Delta\tau_{deficit} \cdot P_{storage,max}\right) \quad (P_{base,t} < 0) \tag{2}$$

$$Q_{sur,cycle} = \min\left(\sum_{t\in cycle} P_{base,t}, \Delta\tau_{sur} \cdot P_{storage,max}\right) \quad (P_{base,t} > 0) \tag{3}$$

t	Time (s, h)
$P_{base,t}$	Baseline demand profile (W)
$\Delta\tau_{deficit}$	Length of the deficit period (s, h)
$\Delta\tau_{sur}$	Length of the surplus period (s, h)
$P_{storage,max}$	Maximum charging and discharging power for the virtual storage unit (W)

To illustrate the application of the above method, a small-scale LTDH system with 165 SFHs is considered as an example. This system is also the case for bottom-level investigations and the detailed descriptions can be found in Chapter 3. The heat sources in this system are heat pumps, so the heating demand is converted to electricity demand. The household electricity demand profile is defined according to previous investigations of the electric appliances in Sweden [27], with an installed capacity of 94 kW. As for energy supply, the regular electric grid and the wind power with the installed capacity of 450 kW are considered. Table 2.1 presents the general information about the energy supply and demand profiles, derived from the energy system models from Chapter 3. Without active load management 841.4 MWh of VRE can be utilized, which is equivalent to around 66.7% of the total VRE supply. The total surplus VRE is 420 MWh.

Table 2.1. The annual accumulated energy and maximum power of the energy demand and supply in the case LTDH system

Annual energy (MWh)				Max power (kW)			
Heat	H2P demand	VRE	Household	Heat	H2P demand	VRE	Household
2064	425	1261	743	720	157	450	94

Assuming a fixed storage cycle per day, the amount of deficit and surplus energy for each day is shown in Figure 2.2. Accordingly, the theoretical matching potentials are presented in Figure 2.3. The maximum daily potential is 977 kWh, which is also the maximum design capacity for the virtual daily storage unit. Under this scenario, the annual integrated VRE is 900 MWh, which is larger than without profile matching but still lower than the total supply of 1261 MWh. The remaining VRE supply cannot be integrated into the storage due to the limitations of the demand profiles and discharging powers. The accumulated annual matching potential is 58.7 MWh, which is 14% of the total surplus VRE.

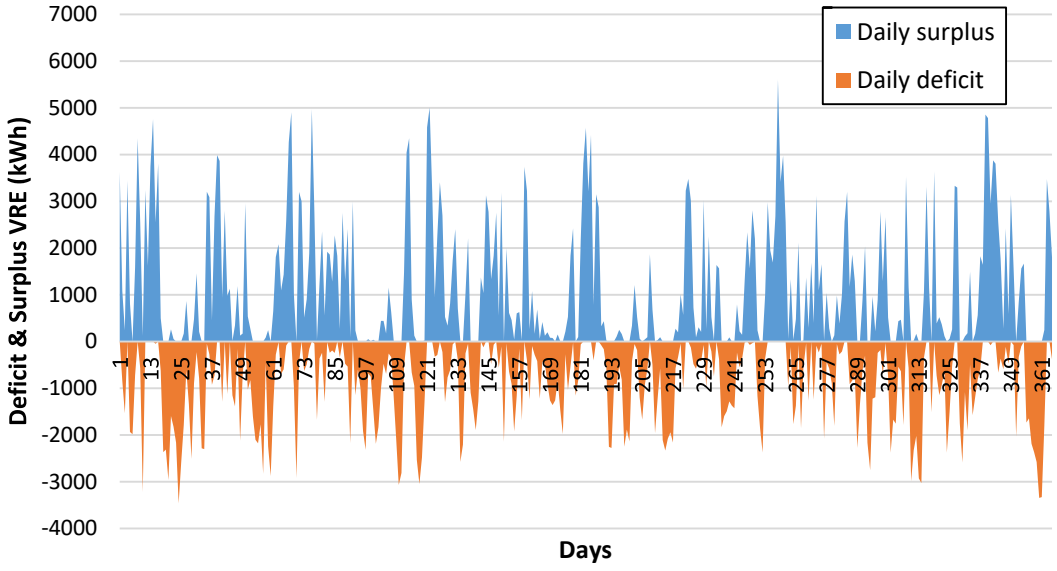

Figure 2.2. Daily deficit and surplus amount of VRE in the LTDH case with a fixed storage cycle per day.

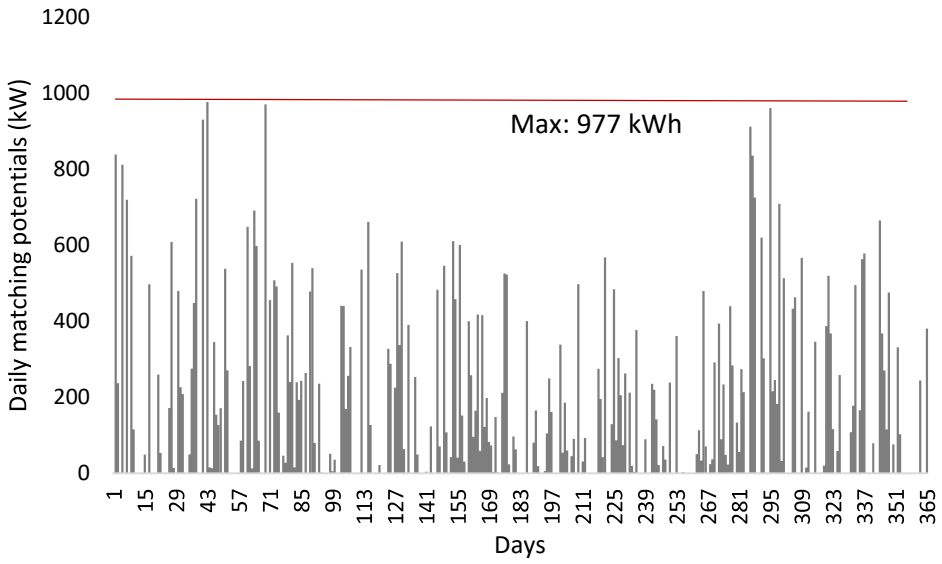

Figure 2.3. Theoretical matching potentials for LTDH case with a fixed storage cycle of one day.

2.1.2 Influence of storage cycles and validations

As illustrated in the above Section 2.1.1, the matching potential is influenced by the length of the storage cycle and the storage capacity. To investigate such influences, the simplified stationary analysis method is applied to the case LTDH system with different storage capacities and storage cycles, as shown in Figure 2.4 and Figure 2.5. The VRE integration rate, which is the percentage of the integrated VRE in the total production, is shown to compare the storage performance. The storage capacities are designed from 0% to 200% of the daily average H2P demand, which is 1,164 kWh according to Table 2.1. However, as shown in the results, there is a maximum feasible storage capacity for every scenario. As the design storage cycle is larger, the maximum capacity and the associated VRE integration benefits are also becoming larger. For small-sized storage unit whose storage capacity is less than 40% of the daily demand, the storage benefit is not related to the length of storage cycles but more influenced by the limited storage capacities and charging powers.

Table 2.2. Utilized days and VRE potentials for different cycle lengths under the wind and solar power conditions

Cycle length	Solar		Wind	
	Utilized days	Potentials	Utilized days	Potentials
1 day cycle	281	61%	203	20%
2 days cycle	84	39%	162	80%

Regarding the storage cycles, four different maximum lengths were considered. For each scenario, the storage cycle is not a fixed value, i.e., the cycle can be shorter than the maximum value according to the preferrable matching conditions. With the maximum cycle length of two days as an example, the distributions of the one-day cycle and two-days cycle are shown in Table 2.2. Due to the diurnal characteristics of the VRE, the majority of the annual operation has used one-day cycle. However, the wind power scenario shows stronger tendency to use the two-days cycle. This phenomenon is also reflected in the difference of VRE integration benefits, as shown in Figure 2.4 and Figure 2.5, for the wind power and solar power conditions, respectively. For the system that has wind power and a storage unit with large storage capacity,

the switch from one-day cycle to two-days cycle almost doubled the integrated VRE. However, such switch of storage cycles can only integrate around 40% more of the VRE. This can be explained by the insignificant diurnal characteristics of the wind power. Based on the results of the two-days cycle, the increase of cycle length can only bring in limited benefits. This also explains the necessity of using the short-term storage units to shift the diurnal load variations.

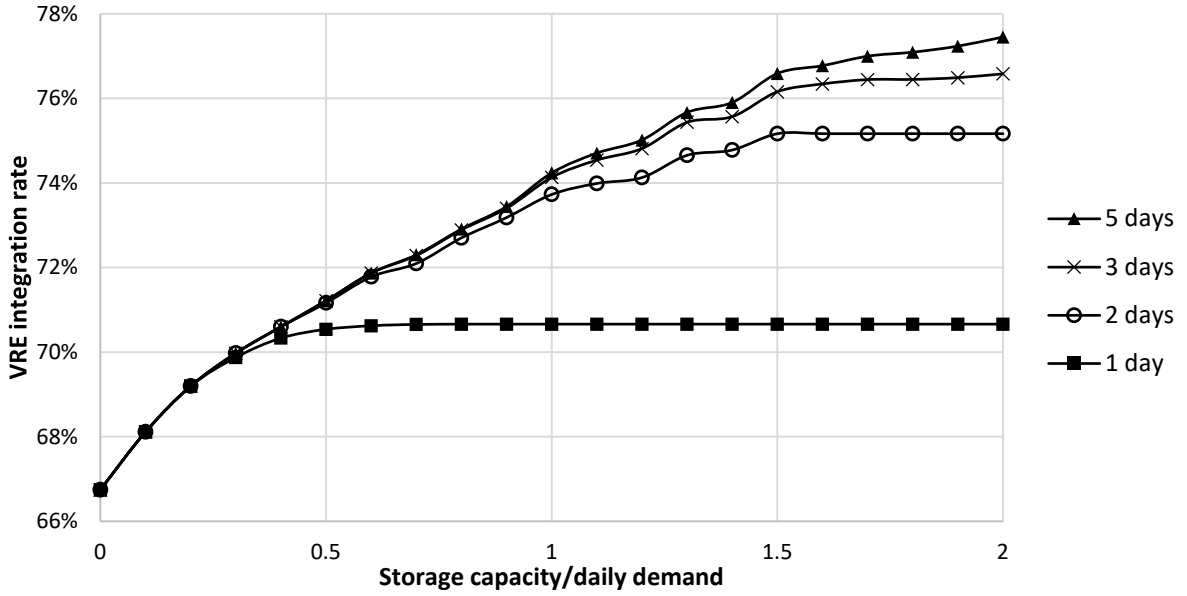

Figure 2.4. VRE integration rate with different storage capacities and storage cycles, under the wind power condition.

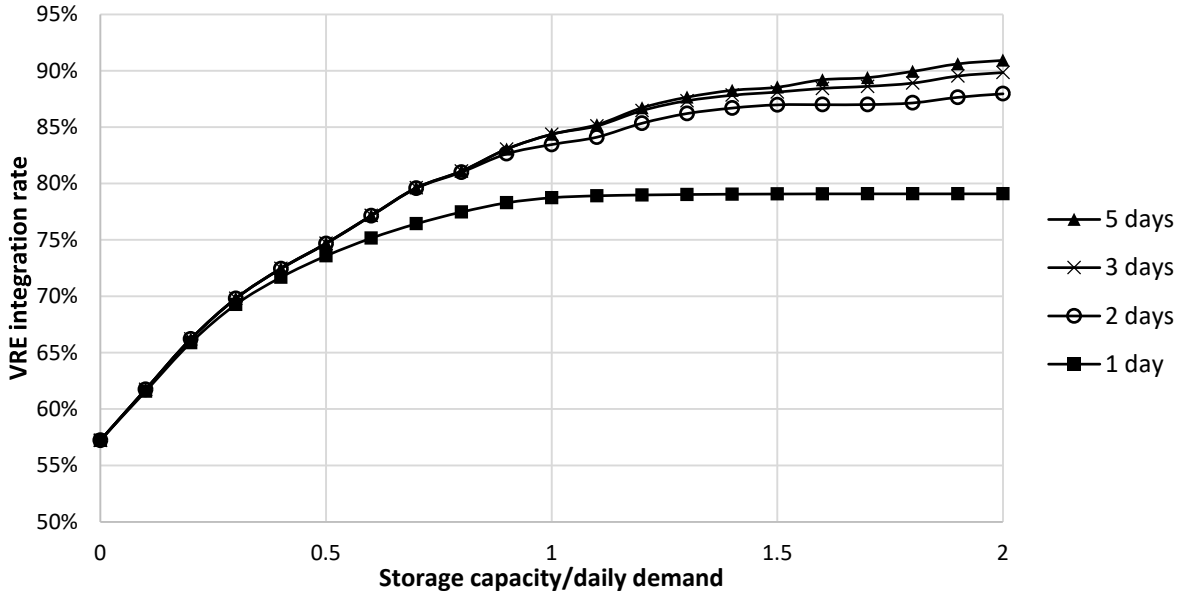

Figure 2.5. VRE integration rate with different storage capacities and storage cycles, under the solar power condition.

To validate the analysis method, the simplified results were compared with the results from detailed dynamic systems models, which are further explained in Chapter 3 and Chapter 4. The scenarios with wind powers are used as examples. The indicator of full-load storage cycles, defined according to Eq. (4), is used to compare the performances of storage units.

$$full-load\ storage\ cycles = \frac{\Delta Q_{VRE,year}}{C_{design}} = \frac{Q_{VRE,storage} - Q_{VRE,baseline}}{C_{design}} \quad (4)$$

$\Delta Q_{VRE,year}$ Increased VRE integrations by the storage unit (kWh)

C_{design} Design storage capacity (kWh)

As shown in Figure 2.6, the difference between the simplified results and dynamic modelling results becomes smaller as the storage capacity is larger. In general, the difference of improved VRE is around 20% of the total integrated VRE. The reasons can be concluded into following parts:

1) The simplified stationary analysis assumes virtual electric storage (cf. Figure 1.4) while the dynamic models used TES units with practical issues such as heat losses and utilization efficiency. An overall thermal efficiency of 70% and heat-to-power of 4.8 are assumed to convert the virtual electric storage to TES. However, the practical efficiency during operation can be influenced by dynamic conditions such as water temperatures and control strategies.

2) The limit of the charging and discharging power for the storage unit is also simplified in the stationary analysis. The maximum charging/discharging power is assumed for all surplus/deficit hours. However, this is not feasible in real cases for many reasons, such as the unavoidable mixtures of temperatures inside TES units which can degrade the storage levels. Thus, the simplified results are exaggerated in some ways. The power constraints are in linear relationship with the storage sizes. Thus, the performances' differences become smaller for larger storage units.

3) There are limitations for the optimization solvers and the control systems in the dynamic models, which are further explained in later chapters.

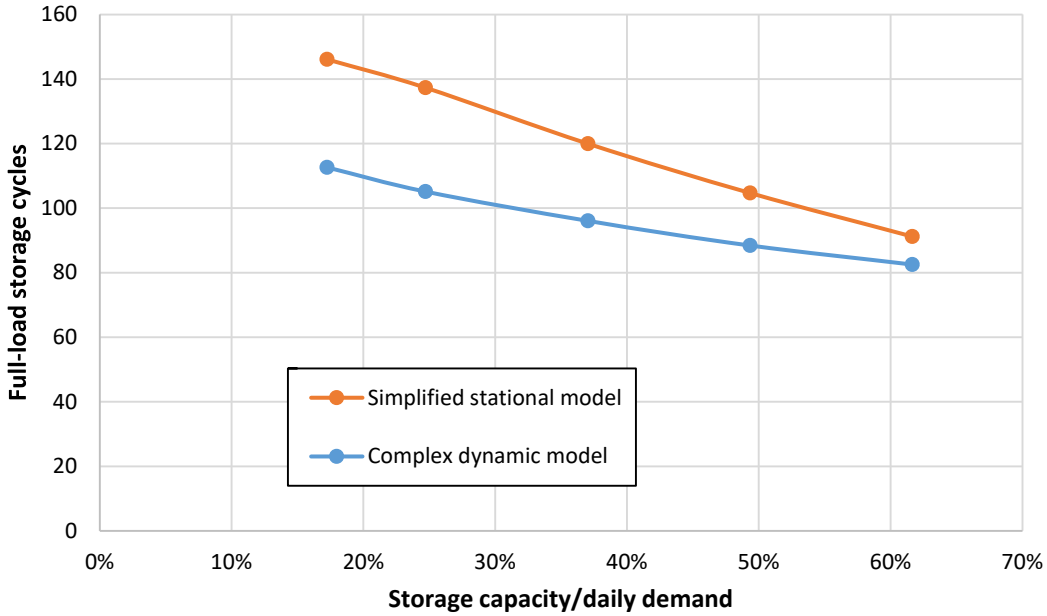

Figure 2.6. Full-load discharge cycles for the theoretical and practical scenarios.

2.2 Applications of the target analysis method

Since the load shifting benefits are influenced by the relationships between the energy supply and demand, a pre-study and matching of the profiles can help to identify the storage potentials and proposed benefits. In this section, various scenarios with different VRE supply profiles are investigated as applications of the theoretical analysis. The installed capacities and total annual generations of the investigated VRE profiles are presented in Table 2.3.

Table 2.3. Investigated solar power and wind power scenarios with identical installed electric power production capacity for both cases.

Scenario name	Generation (MWh)	Scenario name	Generation (MWh)	Power (kW)
Solar-300	308	Wind-300	840	300
Solar-400	410	Wind-400	1121	400
Solar-500	513	Wind-500	1401	500
Solar-600	615	Wind-600	1681	600
Solar-700	718	Wind-700	1961	700

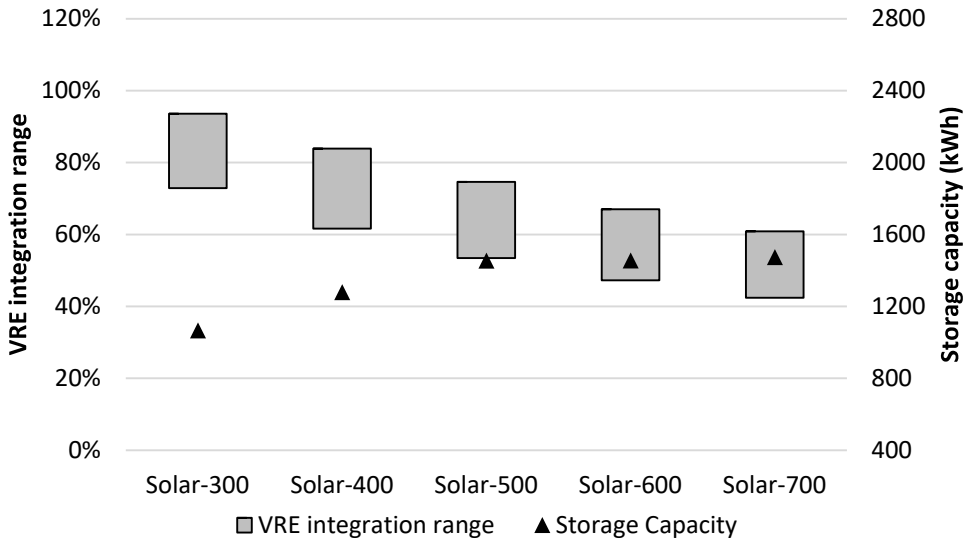

Figure 2.7. VRE integrations and design storage capacity for different solar power scenarios.

The VRE integrations and design capacities of the storage unit under the solar power and wind power scenarios are presented in Figure 2.7 and Figure 2.8, respectively.

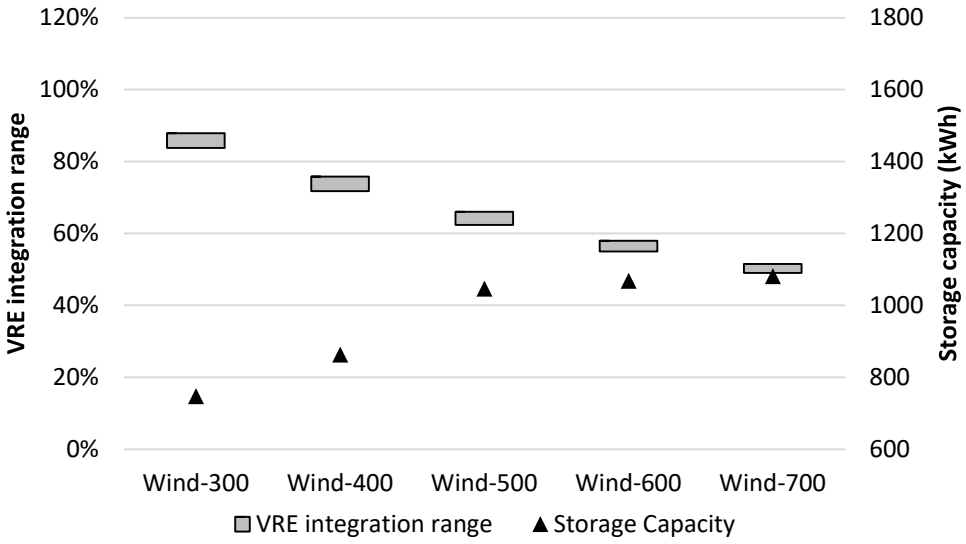

Figure 2.8. VRE integrations and design storage capacity for different wind power scenarios.

Under the same power generation capacity, the integrated surplus solar power is much larger than the integrated surplus wind power. This can be explained by the energy generation profiles. The generation curve of solar power has larger difference between the maximum and minimum values. Thus, the surplus power is easily consumed during the deficit period. However, the wind power generation curve is more flattened and the matching of deficit and surplus VRE becomes difficult. As a result, the efficiency of the storage unit is also influenced, as presented in Figure 2.9 regarding the full-load storage cycles. The differences between the solar and wind scenarios imply the importance of supply and demand matching for making suitable storage designs.

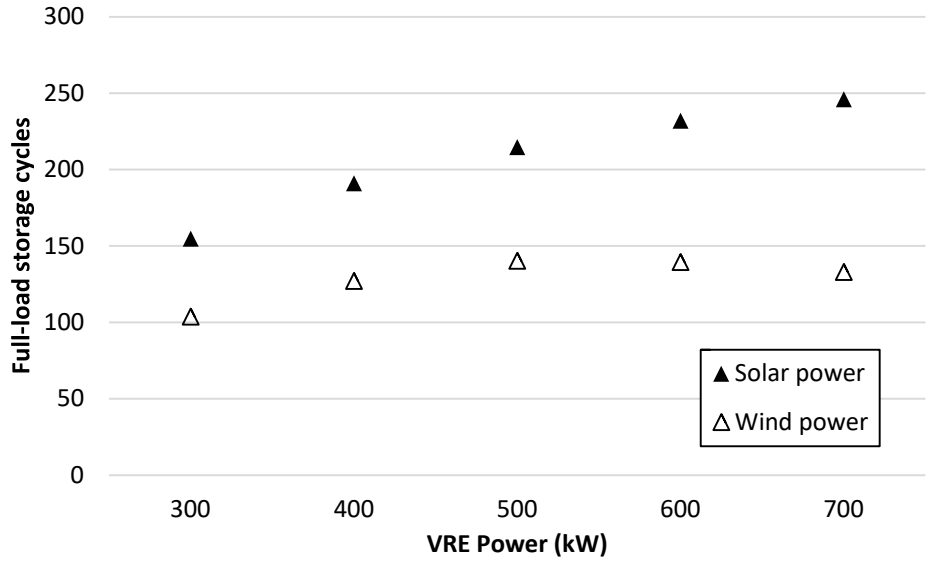

Figure 2.9. Full-load storage cycles for the design storage unit under different solar power and wind power scenarios.

2.3 Target conversion: TES designs

The storage target and theoretical electric storage capacity are analyzed in the above sections. To convert the target into practical TES design, considerations over the conversion process and practical storage efficiencies are needed, as illustrated in Eq. (5). An overview of the design process is shown in Figure 2.10.

$$C_{TES} = \frac{1}{\eta_{thermal} \cdot \eta_{usable}} \cdot C_{TES,theo} = \frac{1}{\eta_{thermal} * \eta_{usable}} \cdot (\eta_{h2p} \cdot C_{ES}) \quad (5)$$

C_{TES} Design storage capacity (kWh)

$\eta_{thermal}$ Thermal efficiency due to heat losses (%)

η_{usable} Usable part of the storage capacity (%)

$C_{TES,theo}$ Theoretical TES capacity from simplified analysis (kWh)

η_{h2p} Heat-to-power conversion efficiency

C_{ES} Electric storage capacity (kWh)

Table 2.4. Common heat sources and their heat-to-power ratios

Heat source	Heat to power ratio η_{h2p}
Electric heater	1
CHP plant, extraction	2~3
CHP plant, back pressure	4~5
Heat pump, air source	2~3
Heat pump, water source	3~5

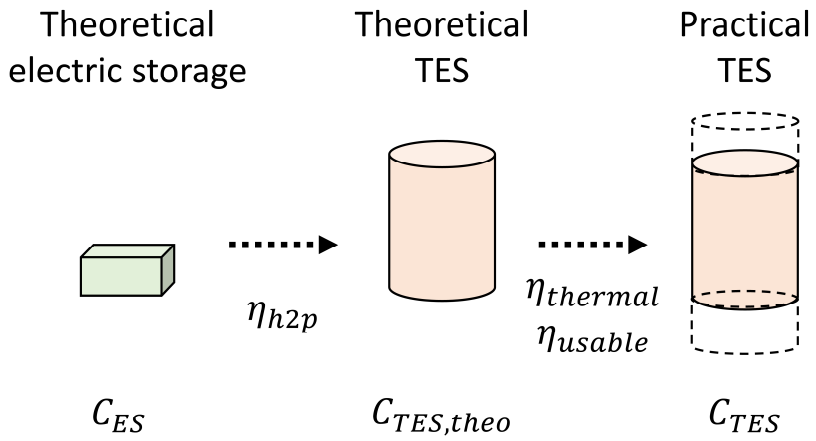

Figure 2.10. Overview of the design method from theoretical electric storage to practical thermal energy storage.

From theoretical electric storage to theoretical TES, the heat-to-power ratio η_{h2p} of the heat source is considered. The ranges of the heat-to-power ratios in common heat sources are shown in Table 2.4. The use of TES is more economically attractive in systems with lower heat-to-

power ratios, such as those with direct electric heaters. However, it is not correct to say that the choice of heat sources is only decided by the economic attractiveness of the TES. Indeed, it is a rather complex process that requires considerations over the whole system performances.

The thermal efficiency $\eta_{thermal}$ describes the available storage capacity considering heat losses, influenced by the storage characteristics and practical thermal insulation levels. For large central storage unit, this value could be around 90% due to better insulations. Whilst in small-sized distributed household water tanks, the insulation investment per unit volume becomes much higher and the efficiency is reduced to around 80%.

Due to the unavoidable mixtures inside the storage unit and the requirements for the supply and return water temperatures, only part of the total storage capacity can be actively used, described by the efficiency η_{usable}. The value ranges between 70% to 90% [28]. This efficiency can be improved by enhancing the temperature stratifications inside the storage unit through novel structural designs [29].

The above-explained methodologies refer to the design condition when the storage capacity is fully utilized within a storage cycle. Thus, the shifted energy during this typical period has certain relationship with the design capacity, as explained in Eq. (6). However, during the whole year's operation, due to the control precisions, the heat storage is used more frequently than the theoretically assumed condition. Thus, the practical full-load discharge cycles of the TES unit are often larger than that of the theoretical electric storage unit, as shown in Eq. (7).

$$\frac{Q_{dch,cycle}}{C_{TES}} = \frac{E_{shift,cycle}}{C_{ES}} \approx 1 \quad design\ condition \tag{6}$$

$$\frac{Q_{dch,year}}{C_{TES}} > \frac{E_{shift,year}}{C_{ES}} \quad whole\ year's\ operation \tag{7}$$

2.4 Conclusions

This chapter introduces the methodologies and applications of the theoretical target analysis and TES designs. By matching the energy supply and demand profiles, the load shifting potentials and associated storage capacity designs can be identified. The assumptions regarding the storage cycles and storage capacities are investigated and validated in this chapter. It has been proved that the proposed method can be applied in various scenarios to pre-study the energy profiles and to identify suitable storage designs. Besides, the theoretical analysis method is based on virtual electric systems, so it can be applied for analyzing both the heating and electricity sectors. The method can be even extended with costs and benefits associated with the energy systems to pre-evaluate the economic benefits of storage units.

The practical TES design process builds a connection between the theoretical storage target and the bottom-level TES implementations. With the proposed analysis indicators such as the heat loss efficiency and storage capacity efficiency, the practical storage capacity and sizes are acquired. Then, the specific bottom-level choice of storage technologies and their applications in different heating systems are explained in following chapters.

3 Applicability of TES in future LTDH systems

This chapter introduces the bottom-level implementations of four TES technologies in the current and future district heating networks, based on a LTDH system in Roskilde, Denmark. The four TES units are the central water tank (CWT), district heating network inertia (DHNI), building thermal mass (BTM) and domestic hot water tank (DHWT). An integrated model to simulate the operation dynamics of the district heating systems and to optimize the use of the TES units is developed. Based on the system model, techno-economic analysis is conducted on a variety of scenarios, created as representatives of the possible changes from the heat sources to the end-users in the future. The content of Chapter 3 is based on the study presented in Paper I.

3.1 LTDH case description

As reported in [6], the small-scale DH systems with small heat demand densities have promising potentials to be upgraded into the LTDH systems. Thus, a LTDH system, located in the suburban area of Trekroner in the municipality of Roskilde in Denmark, derived from a previous study [30], is chosen as the study case. The DH system is supplying heat through a branched network to 165 single-family houses (SFHs), aggregated into 31 substations, as shown in Figure 3.1. This case represents the common residential area with a relatively low heating demand in Europe, where the benefits of the LTDH, such as the reduction of heat losses and the improved heat source efficiency, can be well-assured. The heated floor area is set as 120 m^2 for each SFH and the total heated area for the case LTDH system is 19,800 m^2. The network has a total length of 1.9 km and the pipe sizes are designed by an optimization process, explained in Section 3.2.

For simplicity reasons, the secondary circulation network between the substation and the end-user SFHs is represented by a 20 m long pipe which is omitted in the figure. Several heat source options are centred in one plant in the network and the specific characteristics of them are introduced in Section 3.3 as representative scenarios of the future LTDH systems. The whole year of 2019 is selected as the study period and all external input data, such as the historical weather data and energy prices, are referring to the year 2019.

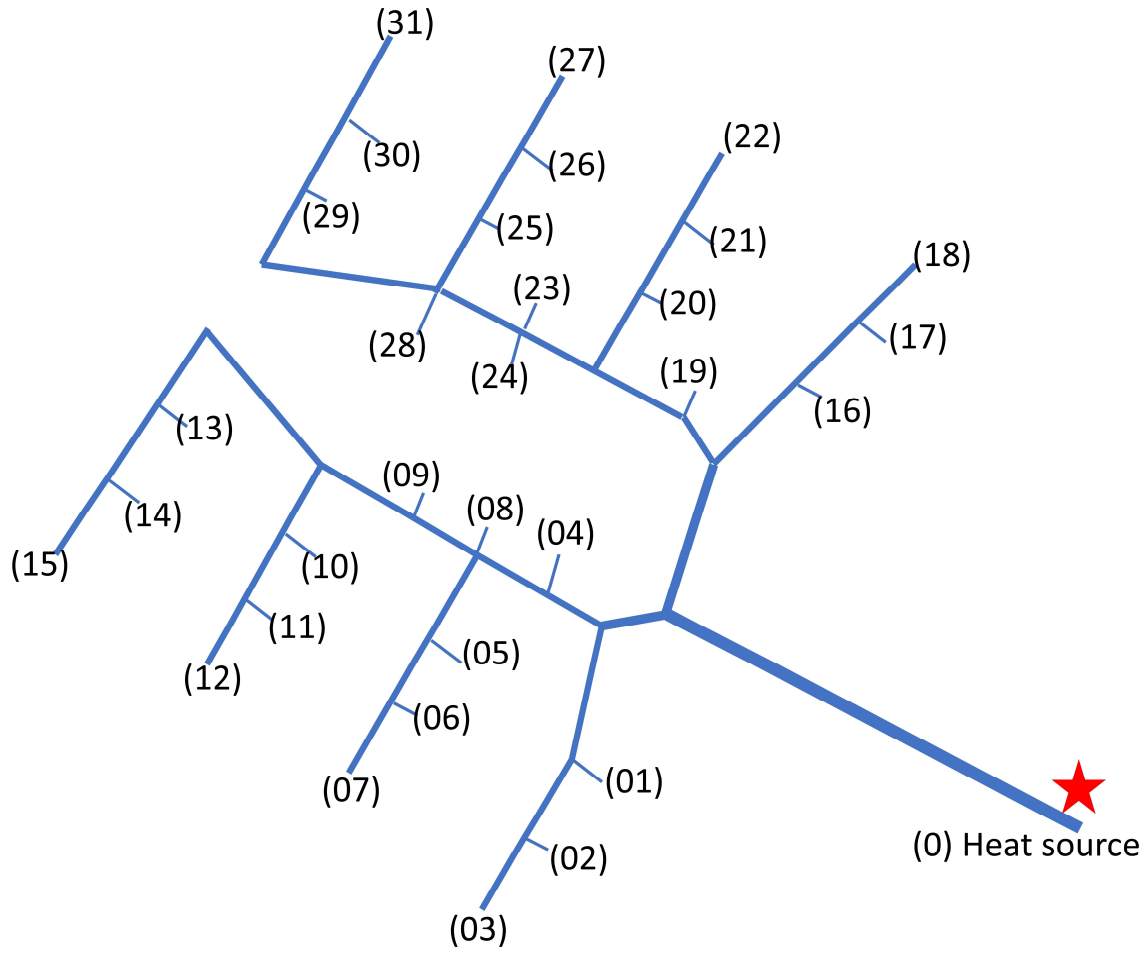

Figure 3.1. Network layout of the case DH system, with substations and heat source marked.

3.2 Methods

3.2.1 DH system model

The DH system model has four main steps, as shown in Figure 3.2. The general modelling methodologies are briefly explained in this section, while the detailed modelling principles, variables and functions can be found in appended Paper I. Based on the input building properties and the weather data, the demand profiles for space-heating and domestic hot water are generated by stochastic modelling method in the first step. Then, based on the theoretical demand profiles, the compartments in the DH systems, such as the heat sources, substations and circulating pipes, are designed in the second step. In the third step, the temperatures and flow dynamics of the networks are modelled by the node method [31,32], with considerations of the transport delay and heat loss. This scenario is also named the reference (REF) scenario, where the active load management is not implemented. Then, in the step function, the active usage of the four TES technologies is optimized. The multi-scenarios analysis is conducted on this model by changing parameters according to specific designs. The model is developed and performed in MATLAB.

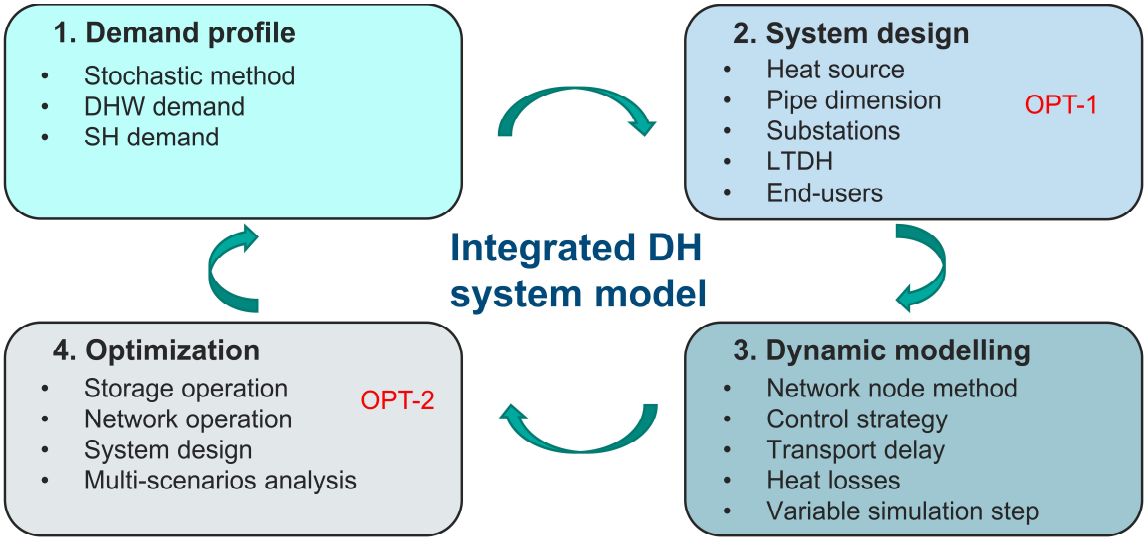

Figure 3.2. Schematic of the main steps of the integrated DH system model developed in this study.

To simplify the computation process, the end-users connected to the same substation are aggregated into one representative end-user. This simplification is acceptable since the end-users connected to one substation are often the buildings with similar properties and load profiles. The SH demand is calculated by a lumped capacitance building model with five resistances (5R1C), written in Eq. (8), according to EN ISO 13790 [33]. In this representation, each building is considered as one thermal zone with a uniform air temperature. The indoor setpoint temperature is 21°C.

$$C_{eff}\frac{dT_{in}(t)}{dt} = (K_{tr} + K_{vent}) \cdot \left(T_{out}(t) - T_{in}(t)\right) + \dot{Q}_{gain} \tag{8}$$

K_{tr} and K_{vent} Total conductance for the heat transmission and ventilation part (W/K)

T_{out} and T_{in} Outdoor and indoor air temperature (°C)

$\dot{Q}_{gain}$ Power of the total heat gains (W)

C_{eff} lumped heat storage capacity (J/K)

In order to consider fairly realistic conditions of DHW usage, the draw-off profile is generated with a time-step of one minute by a stochastic modelling tool called DHWcalc [34], built upon statistical methods and realistic draw-off profiles. The daily mean load for the case SFHs is randomly chosen within the range of 140 to 160 litres/day, which represents the average DHW usage for SFHs in Northern Europe [35].

The SH part and the DHW part are coupled parallelly to the substation. Related heat loss for each branch pipeline is calculated by considering linear heat loss coefficient, pipe length, and temperature differences between the water and surrounding soil. The case system is designed to have a fixed supply water temperature and variable flowrate. The outlet water temperature

from the heat source is set as 55°C and the maximum allowable temperature drop on the primary pipeline due to heat losses is set as 5°C.

To simulate the temperature and flow dynamics of the large DH system, the models of junction nodes, pipes, and energy balances are applied in this study. Based on the Kirchhoff balance laws, the node model has been developed [31,32] and since then applied in dynamic network models [19,36,37]. Thus, only the general modelling approach is illustrated here, while other modelling details can be found in the cited works. The topology of the network is described by a graph approach. Each pipe is defined as a branch, with an inlet node and an outlet node. The end-use substation is also simplified to a pipe that connects the supply branch and return branch, as shown in Figure 3.3.

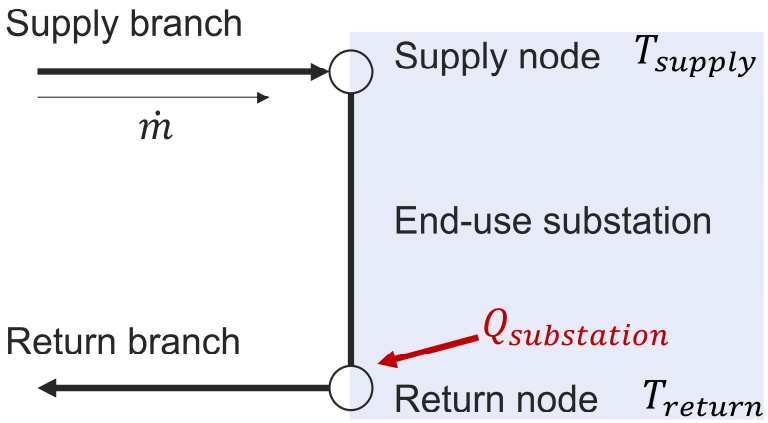

Figure 3.3. Schematic diagram of the node model in end-use substations.

For the entire network, the mass balance equation and pressure balance equation can be written in the matrix form in Eq. (9) and Eq. (10).

$$\mathbf{A}\boldsymbol{G_B} = \boldsymbol{G_{ext}} \tag{9}$$

$$\boldsymbol{B_f}\Delta\boldsymbol{H} = \mathbf{0} \tag{10}$$

$\boldsymbol{G_B}$	Flowrate vector for all branches
$\boldsymbol{G_{ext}}$	Vector that expresses the mass flowrates leaving or entering the node
$\Delta\boldsymbol{H}$	Pressure drops vector
$\mathbf{A}$	Incidence matrix expressing the connections between the nodes and branches
$\boldsymbol{B_f}$	Route matrix expressing the connections between the routes and branches

Considering the heat loss and transportation delay, the outlet temperature of the branch pipe at current time step $T_{B,out}(\tau)$, can be expressed as a step response to the temperature difference between the inlet temperature and the environment, written in Eq. (11). A schematic diagram of the pipe model can be found in Figure 3.4. K_p is expressed through Eq. (12).

$$T_{B,out}(\tau) = T_{B,in}(\tau - \Delta\tau)e^{\frac{-K_p L_B}{u}} + T_e\left(1 - e^{\frac{-K_p L_B}{u}}\right) \quad (11)$$

$$K_p = \frac{K_L}{A_{cross} C_p \rho} \quad (12)$$

$T_{B,in}$ Inlet temperature for the branch (°C)

$T_{B,out}(\tau)$ The outlet temperature of the branch pipe at current time step (°C)

T_e Outdoor climate temperature for calculating the heat losses (°C)

$\Delta\tau$ Transmission delay (s, h)

K_L Linear heat loss coefficient (W/m)

L_B Pipe length (m)

A_{cross} Cross-sectoral area of the pipes (m^2)

C_p Thermal capacity of water (J/(kg·K))

ρ Density of water (kg/m^3)

u Flow velocity (m/s)

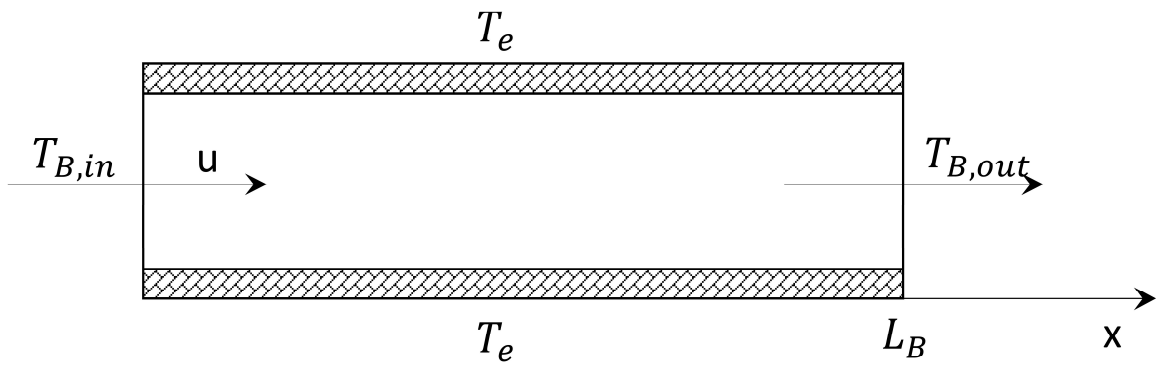

Figure 3.4. Schematic diagram of the pipe model.

For each node, the inlet energy equals the outlet energy. Thus, the energy balance equation for the network can be written in the matrix form as Eq. (13). Due to the coupling between mass and energy equations, the problem is solved by the iterative algorithm.

$$\boldsymbol{A_i R_B T_{out} - A_o R_B A_o^T T_N = \dot{Q}_N} \quad (13)$$

$\boldsymbol{A_i}$ and $\boldsymbol{A_o}$ Inflow and outflow matrix, derived from incidence matrix $\boldsymbol{A}$

$\boldsymbol{R_B}$ Diagonal matrix that contains the heat capacity of branches

$\boldsymbol{T_N}$ Vector that contains the node temperatures at current time step, unknown variable

$\dot{\boldsymbol{Q}}_{\boldsymbol{N}}$ The energy exchange between the node network and the exterior environment

Based on the dynamic system model, the practical system performance at the reference (REF) scenario can be acquired, where active management is not applied. The system is operated to directly fulfil the consumers' demand. However, by utilizing the TES units, additional flexibility to shift the supply and demand profiles is implemented in the system. The lowest system running cost is set as the target to find the optimal operation scheme of the TES units, as well as the whole LTDH systems. Due to the non-linear characteristics of the TES units and the complex DH system, it is complicated to find a global optimal result for the non-convex problem that consider the decisions of all TES units. Thus, a combined central optimization and local control strategy is applied to simplify the optimization process while maintaining realistic characteristics of the control system. The basic idea is shown by the schematic diagram in Figure 3.5. The detailed descriptions of the optimization problem, including the cost-function, constraints, and variables, can be found in the appended Paper I.

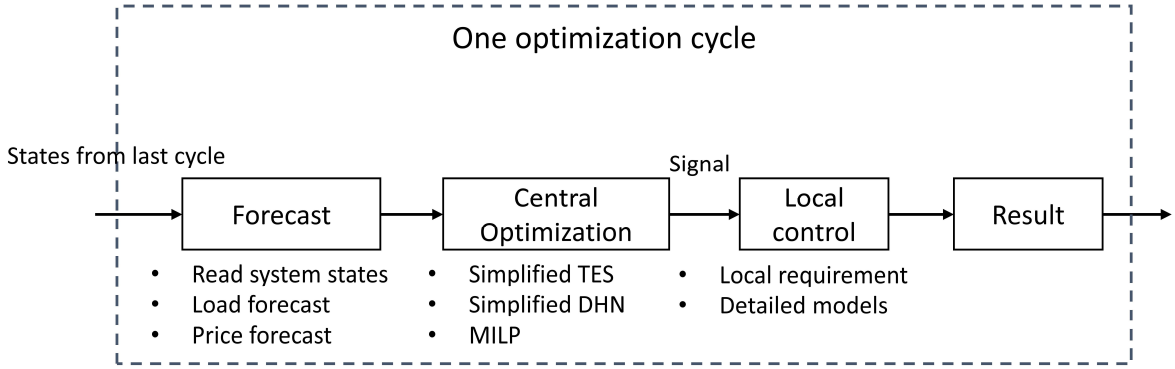

Figure 3.5. Schematic diagram of the combined central optimization and local control strategy.

3.2.2 TES model

The design parameters of the four TES technologies are presented in Table 3.1. To make the evaluations fair, the volume of the CWT and the total volume of the distributed DHWTs are set the same. However, since the DHWT is placed in the consumer side with a 10°C inlet cold water, it has a higher storage temperature difference and a larger designed storage capacity compared to the CWT. The design parameters of the DHNI and the BTM are derived from the network structures and the building properties, illustrated in the following sections.

Table 3.1. Design parameters of the TES units in LTDH system

Parameters	CWT	DHNI	DHWT	BTM
Size (m^3)	27.9	2.2	27.9	-
Storage temperature difference (K)	25	10	40	0.5
Storage capacity (kWh)	814	26.1	1302	785
Percent in average daily load (%)	14.3%	0.5%	23.0%	13.8%

As for the CWT, a one-dimensional vertically stratified WT model with 20 layers was used , which has been commonly applied in several WT optimization studies [38,39]. For each layer, heat and mass transfer by convection and conduction are considered, as explained in Eq. (14).

For simplicity, the heat losses are calculated by the temperature difference between the hot water and surrounding environment.

$$\rho V C_p \frac{\partial T}{\partial t} = A_{cross}\lambda \frac{\partial^2 T}{\partial x^2} - G\rho C_p \frac{\partial T}{\partial x} - K_{cwt,loss}A_{ext}(T - T_e) \quad (14)$$

x Vertical coordinate (m)

G Water mass flowrate (kg/s)

$K_{cwt,loss}$ Heat loss factor of the CWT, assumed to be 0.3 W/(m^2·K) [40]

During the discharging period, the outlet water temperature from the CWT will gradually decrease due to inevitable mixtures of hot and cold water inside the tank. The lower limit for the outlet water temperature from the top of the CWT is set as 53°C, which is 2°C lower than the design supply water temperature. During the charging period, the upper limit for the outlet water temperature from the bottom of the CWT is set as 35°C, to keep an efficient operation of the heat sources.

The modelling approach for the DHWT is the same as the CWT. However, the DHWT only has 10 layers to suit the practical stratifications in small-sized water tank [38]. Unlike the CWT that has an extensive thermal insulation to reduce the heat loss factor to 0.3 W/(m^2·K), the DHWT has poorer insulation due to relatively high investment cost per volume and the extra space the insulation layer takes. Thus, the heat loss factor of the DHWT is set as 1 W/(m^2·K), according to a previous field measurement study [41]. To guarantee the comfortable and safe DHW supply, a deterministic local controller is applied for the DHWT, as shown in Figure 3.6.

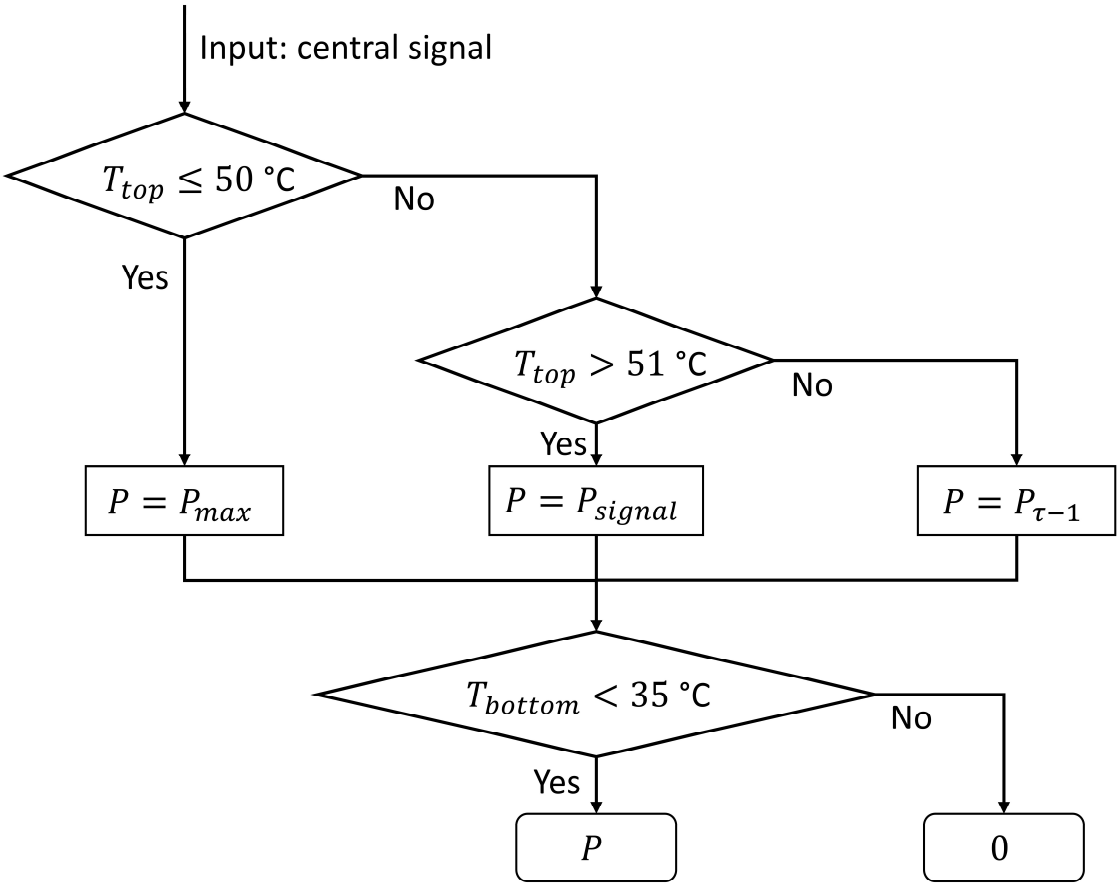

Figure 3.6. Local control strategy for the DHWT.

For the use of BTM, the available storage capacity of the BTM is decided by the effective (interior) heat capacity of the building and the indoor temperature deviations from the setpoint. Results from a previous field measurement of BTM in Gothenburg, Sweden [20], showed that the indoor temperature deviation of 0.5 K above the setpoint temperature is acceptable and thus used in this study. Otherwise, if indoor temperature changes below the setpoint are allowed, the systems tend to reduce the thermal comfort levels for lower energy consumption.

As for the use of DHNI as storage unit, an active temperature increase of 10 K in the transportation pipes, which is recommended by previous study [11] as a reasonable value, is assumed in this study. However, the return water temperatures are kept the same as is illustrated in the above control strategies (Figure 3.6), to avoid negative impact on the source efficiency. Thus, only half of the network storage capacity can be utilized. The total volume of the water in the supply transportation pipes is calculated as 2.2 m^3. Hence, the theoretical storage capacity is 26.1 kWh, which is relatively small compared to the other three TES options. To avoid frequent changes in the network temperature, the minimum charging period is set as 5 hours, which is also in accordance with the charging period of other TES units. Then, the maximum charging power is also defined.

3.3 LTDH characteristics and scenarios design

The concepts and main characteristics of LTDH systems are summarized in several studies [4–6]. With the aim of evaluating the applicability of TES, the performances of the LTDH system were investigated under several scenarios, which represent the possible future changes in the DH system, including the sources, substations, and end-use buildings, as shown in Table 3.2.

Table 3.2. Summary of the investigated scenarios for the LTDH system.

Heat sources	Substations	End-use buildings
Peak scenario	Current design with bypass loss	Current buildings
Variable renewable energy (VRE) scenario	Triple-pipes design	Future low-energy buildings
Industrial waste heat (IWH) scenario		

3.3.1 Heating sources

At the source side, due to the reduction of return water temperatures, the low-grade waste heat from multiple sources can be recovered. Besides, the integration of VRE can be improved through the implementation and smart control of power-to-heat technologies such as heat pumps. Thus, three typical scenarios of the heat sources are investigated, as summarized in Table 3.3. In general, there are three heat sources in every scenario, including two baseload sources that supply 90% of the heat demand and one heat-only boiler that supplies the remaining 10% peak demand. The cost for the peak boiler, considering the practical fuel cost and taxes [42], is significantly higher than that of the two baseload sources.

Table 3.3 Descriptions of the three heat sources scenarios.

Scenario Name	Source 1	Source 2	Source 3
Peak	150 kW HP, COP[1] 4.8 0.31 SEK/kWh heat[2]	200 kW HP, COP[1] 4.0 0.38 SEK/kWh heat[2]	500 kW Wood-pellets boiler 0.75 SEK/kWh heat
VRE	Same as peak scenario	Same as peak scenario	Same as peak scenario
IWH	150 kW Waste heat 0.18 SEK/kWh heat	200 kW Waste heat 0.25 SEK/kWh heat	Same as peak scenario

1 Nominal COP with output water temperature of 55°C

2 Reference cost for heating, calculated under the nominal COP and the average electricity price of 1.5 SEK/kWh

In the peak scenario, two waste-water source HPs are designed for the baseload. The COP is calculated by the empirical equation with the condensing temperature and evaporating temperature [43]. The waste-water temperature at the source side is set as a stable value of 15°C. The thermodynamic efficiency is set as 0.65 and 0.55 for the source 1 and source 2, respectively. The operation costs of the two HPs are the electricity bills, calculated by the hourly variable electricity prices from the NordPool spot market [44].

The HPs in the VRE scenario are the same as the peak scenario. However, 900 m^2 of crystalline solar PV panels, which have a total power generation capacity of 178.2 kW, are assumed in the case system. The active load shifting performance of TES units to integrate the intermittent VRE is investigated in this scenario. The hourly power generation profile at the case location is calculated by the Photovoltaic Geographical Information System-interactive (PVGIS) tools [45]. The feed-in price for the residual PV power is set as 0.

In the IWH scenario, the two baseload sources are changed to directly exchanged waste heat from industrial processes, as an efficient step towards the sustainable future [4,7,14]. The industrial process is assumed to have a constant temperature of 60°C, which can heat the network circulation water to 55°C. The heating capacity shown in Table 3.3 is defined based on the average return water temperature of 30°C. Thus, the reduction of the return water temperature will directly increase the recovered waste heat and reduce the usage of peak boilers.

3.3.2 Substations

As pointed out in previous studies [21,22], one important cause for the existing high return water temperatures is the preparation of DHW demand. As shown in Figure *3.7* the instantaneous heat exchanger type and domestic hot water tank (DHWT) type are two traditional designs that are widely applied in the current DH systems. The pipes are filled with hot water to assure an acceptable waiting time, which significantly increase the heat losses and return water temperatures.

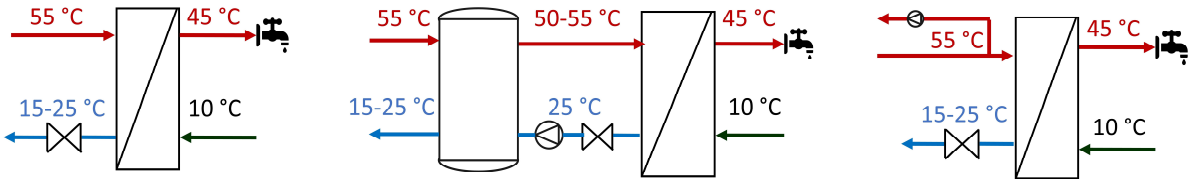

Figure 3.7. Three typical substation types for preparing the DHW demand.

In order to maintain the required return water temperature, several solutions were provided by researchers [23,46,47]. One idea is based on the maximum cooling concept, where the supply water is bypassed to the floor heating pipes in the bathroom to be cooled down to the required return water temperature level, set to 25°C in this study. This design is also named "comfortable bathroom" in some studies [23,46]. Thus, the bypass loss is inevitably created by this design. This design is applied to the instantaneous heat exchanger types and DHWT types in this study.

Alternatively, the triple-pipes design with a re-circulation pipe can eliminate the bypass heat loss while maintaining the thermal comfort [22], as shown in Figure 3.7 (c). There are also other alternative designs, such as inclusion of the electrical supplementary system [23]. They are currently omitted in this study.

3.3.3 End-use heating demand

Another key characteristic of the future LTDH system is the improved energy performance of buildings through building renovations and newly built low-energy buildings. With less SH demand and shorter SH period, there are more variations in the demand profile, induced by the intermittent nature of the DHW demand. Besides, the storage potential of the BTM is also reduced in well-insulated buildings [48]. Two scenarios that represent the current building stock and the future low-energy building stock are studied.

For simplicity, in all scenarios, the SFHs have the same structures and properties. A constant ventilation rate of 0.5 h^{-1} is assumed in both scenarios. However, heat recovery measures are implemented in the future low-energy buildings to further reduce the ventilation loss. The accumulated SH demand and other key performance indexes are summarized in Table 3.4.

Table 3.4. Performances of the current and low-energy buildings.

Buildings	Heat loss (W/K)	Internal capacity (kWh/K)	Time constant (h)	SH period (h)	Heating demand (kWh/m^2)	Heating power (W/m^2)
Current	128.4	9.5	74	5715	80.6	28.2
Low-energy	67.3	9.5	141	4159	34.7	14.1

Based on the integrated DH system models, the heat supply under the current and future building stocks are simulated, as presented in Figure 3.8. The network loss refers to the transmission heat loss through the transportation pipes, while the bypass loss refers to the heat loss due to return water temperature requirement, as explained in the previous sections. It can be noticed that as the SH demand decreases, the heat losses and DHW demands become increasingly important. In the future low-energy building stock, the non-space-heating period becomes longer, and a certain flowrate of hot water is required during this period, which increases the bypass loss. In general, the heat losses in two building stocks are 13% and 28% of the total heat supply, respectively.

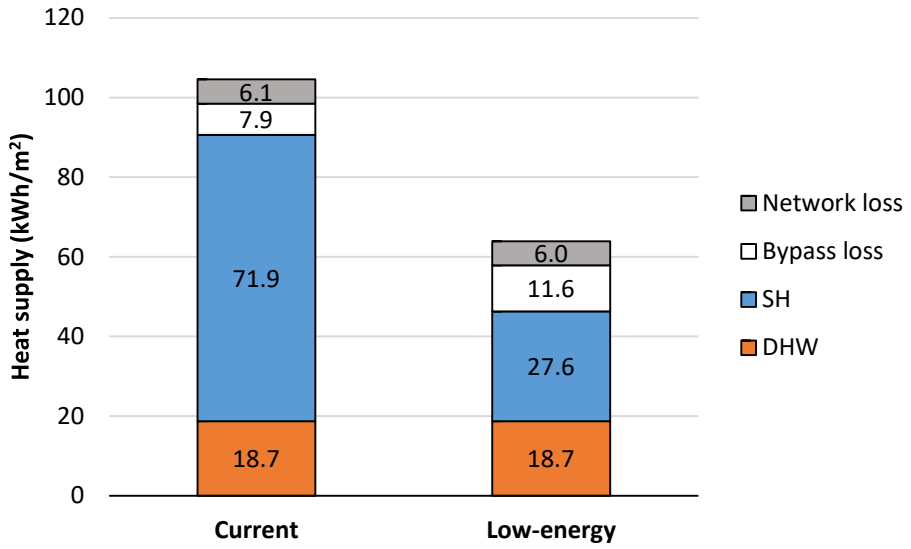

Figure 3.8. Annual heat supply per unit heated area under the current and future low-energy building stocks.

3.4 Results

The most important findings from the appended Paper I are presented in this section. The applicability of TES technologies under the different heating sources are firstly introduced. Then, the influences of substation designs and the end-use demand are analyzed.

3.4.1 The influence of heat sources

The annual cost-savings for the systems with four TES technologies, under three heat sources scenarios, are presented in Figure 3.9.

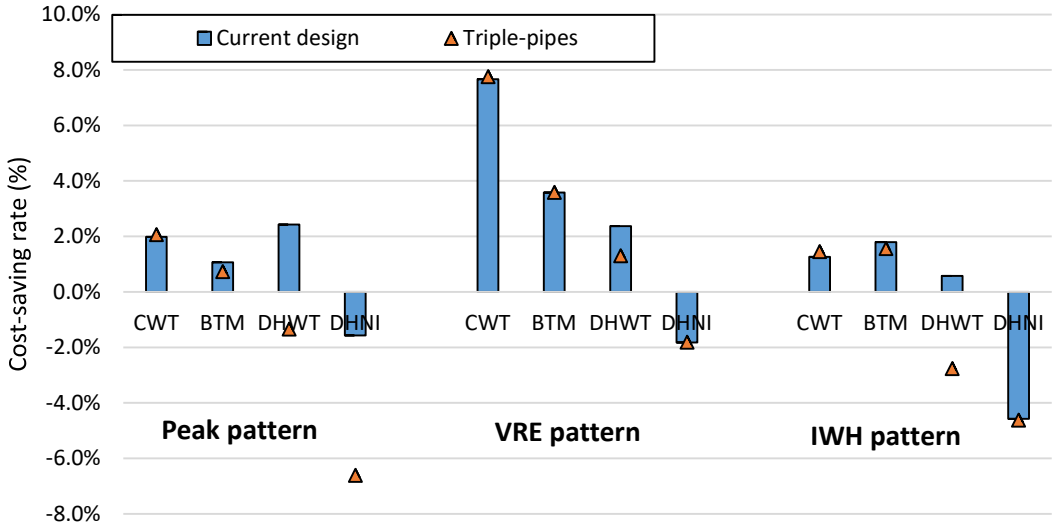

Figure 3.9. Annual cost-savings for the systems with the current substation design and the triple-pipes design.

In the peak scenario, the objective of the optimization is to reduce the use of peak boiler by shifting the demand to the baseload plants during off-peak periods. The BTM has the lowest full-load discharge cycles because it is only used during the SH period. The CWT has the highest storage efficiency while the DHNI has the lowest, due to the network losses. Although the peak load reduction by the DHWT is smaller than the CWT and the BTM, the saved operation cost is the highest among the four TES units. This can be explained by the heat losses in the whole system. During the non-space-heating period, the original bypass heat loss as required to maintain the low return water temperature is collected and used in the DHWT. Although the DHWT system has larger TES loss, its total heat loss is approximately 4 kWh/m^2 lower than the other investigated systems, as shown in Figure 3.10. For the system with DHNI, the total operation cost is even higher than the reference system without any TES options due to the reduced source efficiency by raising the network supply water temperature.

Table 3.5. Storage performances and annual cost-savings of the TES units under the peak scenario.

TES units	Efficiency (%)	Cycles (n)	Peak load (kWh)
REF	-	-	169,005
CWT	97%	134	-33,018
BTM	83%	52	-20,329
DHWT	88%	244	-8,066
DHNI	61%	267	-2,687

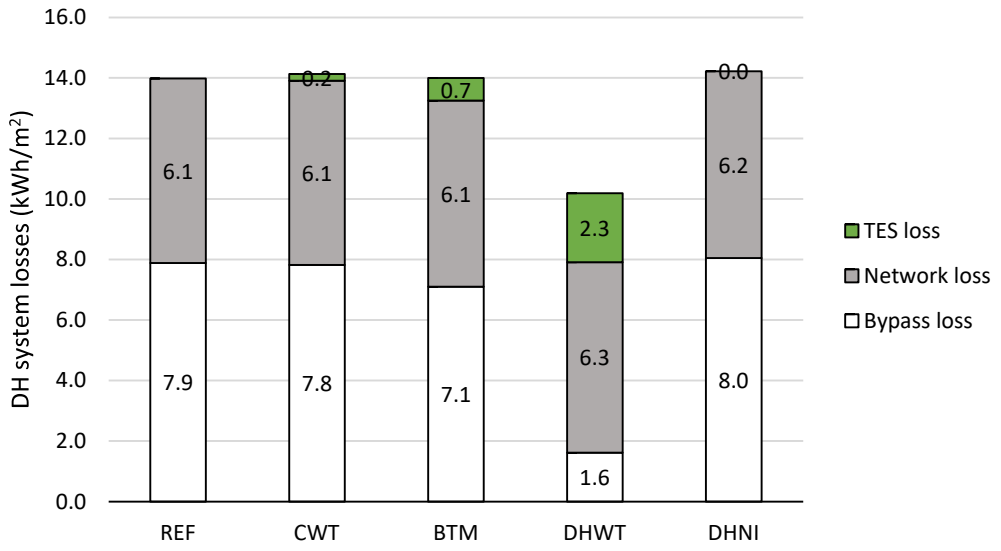

Figure 3.10. Breakdown of annual heat losses in the case system with different TES units under peak scenario.

In the VRE scenario, the CWT has the largest potential for integrating VRE and thus has the largest cost-saving rate, as presented in Table 3.6. Although the DHWT is designed to have a larger storage capacity than the CWT, as presented in Table 3.1, its actual capacity to integrate the excessive VRE is not proportionally larger. This can be explained by the larger heat losses and temperature restrictions from the DHWT when charged in idle state for a longer period.

Table 3.6. VRE integration rate under VRE scenario.

	REF	CWT	BTM	DHWT	DHNI
VRE integration rate	42%	59%	49%	44%	43%

The number of occasions when the state-of-charges of the TES units are higher than 70% of their design capacities, classified by the number of consecutive hours that each occasion has, are shown in Figure 3.11. The TES with a longer storage period can better deal with the variations in the VRE generation caused by weather conditions. The average consecutive hours for the CWT, BTM, DHWT, and DHNI are 10.0 h, 5.9 h, 5.8 h, and 3.1 h, respectively.

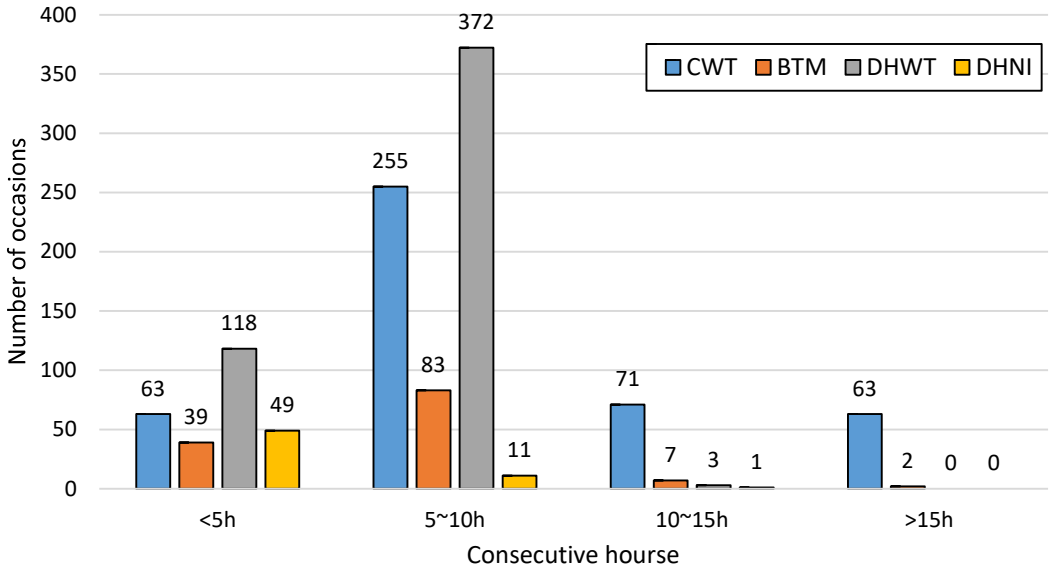

Figure 3.11. Number of occasions for different TES options when state-of-charges are higher than 70% of their design capacities.

As for the IWH scenario, the efficiency of IWH resources is more sensitive to the return water temperature compared to the heat pumps. The daily average return water temperature is 25.8°C in REF system and is slightly increased to 26.2°C in the CWT system. However, the DHWT system has the highest return water temperature, which is 28.6°C. This is explained by the control complexities for distributed small tanks and the mixtures of water inside the tank, as an opposite effect of the bypass loss reduction. Consequently, the recovered waste heat from industrial processes is reduced and the peak boiler usage is therefore increased in the DHWT system.

3.4.2 The influence of substation design

The performances of TES technologies with the triple-pipes design are also presented in Figure 3.9. The results indicate that the benefits of the CWT and the BTM are only slightly changed by the substation design, while the use of DHWT is in some ways contradict with the triple-pipes design. The cost-savings of the DHWT can be even negative due to the reasons such as the high heat loss, explained in above sections. Thus, in the future LTDH systems, the choice between the DHWT design and the triple-pipes design is required. The heat losses in the systems with the triple-pipes design are presented in Table 3.7.

Table 3.7. Heat losses in the systems with the triple-pipes design.

Cases	Network loss (kWh/m^2)	TES loss (kWh/m^2)	Total (kWh/m^2)	Loss rate (%)
REF	7.7	0.0	7.7	7.8%
CWT	7.6	0.2	7.9	8.0%
BTM	7.6	0.5	8.1	8.2%
DHWT	6.6	2.3	8.9	8.9%
DHNI	10.3	0.0	10.3	9.8%

3.4.3 The influence of SH demand

The annual cost-savings of the investigated systems with the future low-energy building stock are presented in Figure 3.12. Due to the infeasible usage of DHNI as proved in the above sections, the results for the DHNI are not presented.

From the current building stock to the future low-energy buildings, the annual cost-saving rates for all systems are increased to some levels. However, for the system with BTM, the cost-saving rate is only slightly changed because there is less storage potential from the better insulated buildings. In the current building stock, there are totally 150 days, where the BTM is actively used. In the future low-energy building stock, since the SH demand is greatly reduced, BTM is only used in 100 days. Thus, the number of full-load storage cycles in the low-energy building stock scenario is approximately half of the number in current scenario, as shown in Table 3.8.

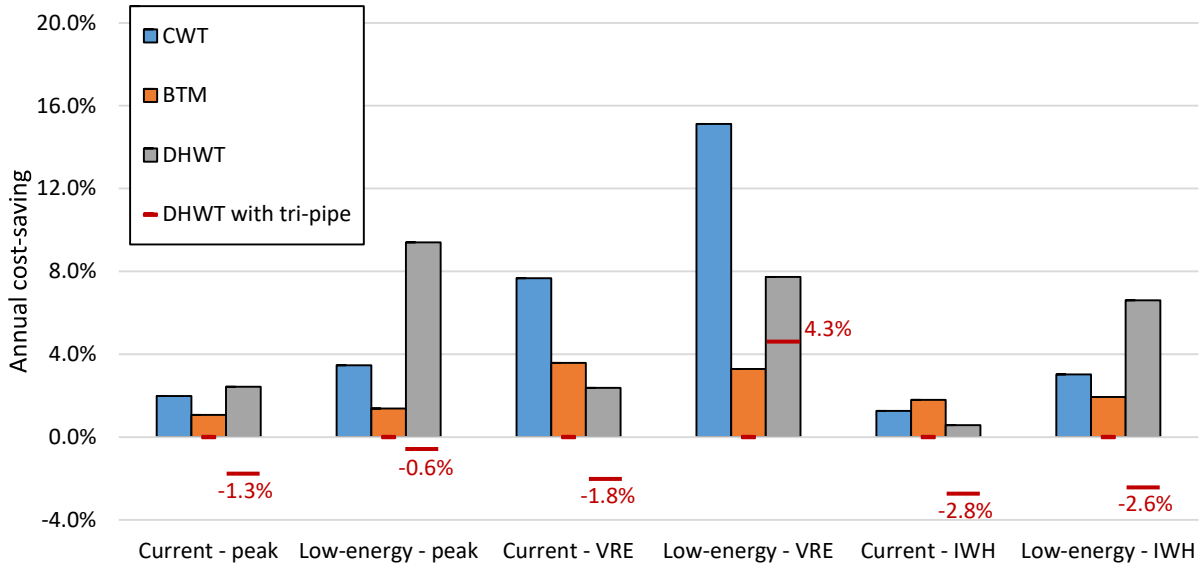

Figure 3.12. Annual cost-savings under different heat source scenarios and building stock scenarios.

Table 3.8. Full-load storage cycles of the BTM in current and future low-energy building stocks.

Scenarios	Peak	VRE	IWH
Current	76	102	57
Future low-energy	40	47	28

The system with the DHWT also has large difference between the two building stock scenarios. In the future building stock, due to the reduced demand for SH, the bypass loss becomes higher in the whole system, as shown in Figure 3.8. The benefit of reduced bypass loss can even to some extent offset the extra cost related to the DHWT in the IWH scenario.

Comparing the four TES technologies, the use of CWT is most favourable in the VRE scenario, with an annual cost-saving rate of 15.1% in the future low-energy building stock.

3.5 Discussion and conclusions

Based on the results from multi-scenarios analysis, the performance map of TES technologies under the future DH changes is shown in Figure 3.13. The current DH system has relatively low VRE integration and high SH demand. Changes in the end-use demand side and the changes in the heat source supply side are considered as two main variables during the analysis. The central idea is that the future design and usage of TES technologies should be highly in accordance with the characteristics of the future energy systems. Several instructive suggestions for the TES applications are summarized as follows. A more detailed quantitative analysis of the TES technologies in different systems is presented in Chapter 4.

①: Major changes take place in the end-use buildings. This transition is likely to happen in middle and large cities where the VRE resource is scarce. As the renovation works are conducted in the buildings, changes in the substations are also needed. Both DHWT design and the triple-pipes design can reduce the unnecessary bypass loss and increase system efficiency, but only one option is enough. The former design requires more strict control of the water temperature, and the latter design requires renovations of the pipe system.

②: Major changes take place in the heat sources, with increased VRE generations. This transition refers to the DH systems where heat and power networks are connected through heat pumps or CHP plants. Comparing the TES technologies, central and compact unit with small heat loss rate and high control flexibility, such as the CWT in this study, can better balance the supply and demand and, thus, has the largest potential for applications.

③: The share of renewable energy is also increased in this transition but, unlike transition ②, the DH systems have less interactions with the power system. Possible heating sources include the direct use of industrial waste heat and biomass boilers. The prospective benefits for TES technologies are mainly related to the peak load reduction and smooth system operation, which can be lower than the benefits in transitions ① and ②.

④: A direct transition towards the future LTDH system, which is likely to happen in newly built district with good building insulations and abundant VRE production. A combination of the supply side central TES option and the demand side measures is required, which is further explained in Chapter 4.

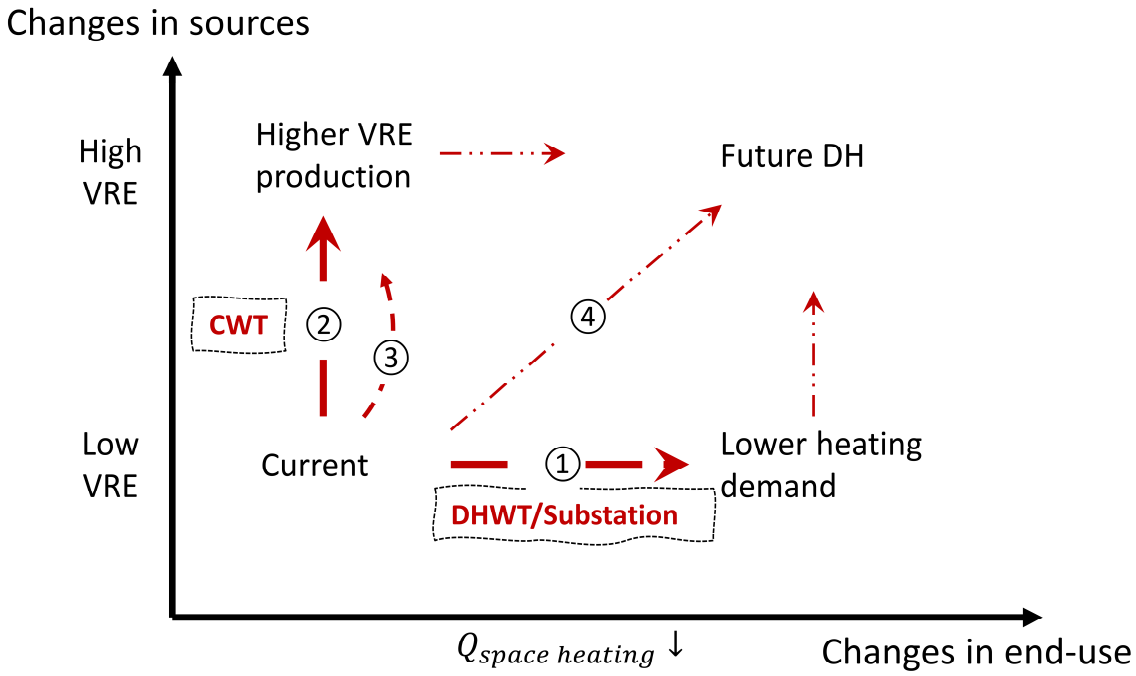

Figure 3.13. Performance map of the TES technologies under the future changes of the DH systems.

4 Comparisons between different DH systems

Based on the methodologies illustrated in Chapter 3, the applications of TES technologies in a case LTDH system were evaluated under multiple scenarios. By comparing the TES performances in two case systems, LTDH and MTDH, recommendations on the future applications of TES units are provided. This chapter also discusses the optimal choice between the supply side and demand side management measures. The case MTDH system is based on the appended Paper II.

4.1 MTDH case description

Due to the scarcity of European DH system information, a MTDH system from a town with approximately 50,000 inhabitants [49], located in the Hebei province in Northern China, is used as case study. To be consistent with the analysis for the LTDH system, only the network layout from the original Chinese DH system is used, while other parameters, such as the weather conditions, building components and DHW demand profiles, are revised according to the Swedish conditions. This town represents a vast number of middle-sized cities in Northern Europe. The end-use buildings, with the total heated floor area of 4.48 million m^2, are grouped into 71 substations, as shown in Figure 4.1. The simplifications for modelling the DH networks are the same as the LTDH case. The total length of the primary networks is 52.3 km. Three energy-efficient levels of apartment buildings are considered in the MTDH, as shown in Table 4.1. Similar as the Chapter 3, the building stocks at the current condition and future low-energy condition are investigated.

The case MTDH system has design supply and return water temperatures of 90°C and 50°C, respectively. Unlike the LTDH system, the heat source in the MTDH system is the extraction type combined heat and power (CHP) plant, located in the Northwest part of the town. It shall be noted that improvements for CHP plant, such as the recovery of waste heat from the exhaust steam by absorption heat pump, have been widely studied in recent years [50,51]. However, only the extraction CHP plant is considered, as representative of the traditional MTDH system. The detailed parameters are explained in Section 4.2.

Table 4.1. Building types and accumulated annual heat consumptions in the current and future scenarios.

Building types	Floor area (m^2)	Heat consumption (kWh/m^2)	
		Current	Future low-energy
Level-1	1,696,318	104	63
Level-2	2,169,586	73	45
Level-3	612,861	50	35

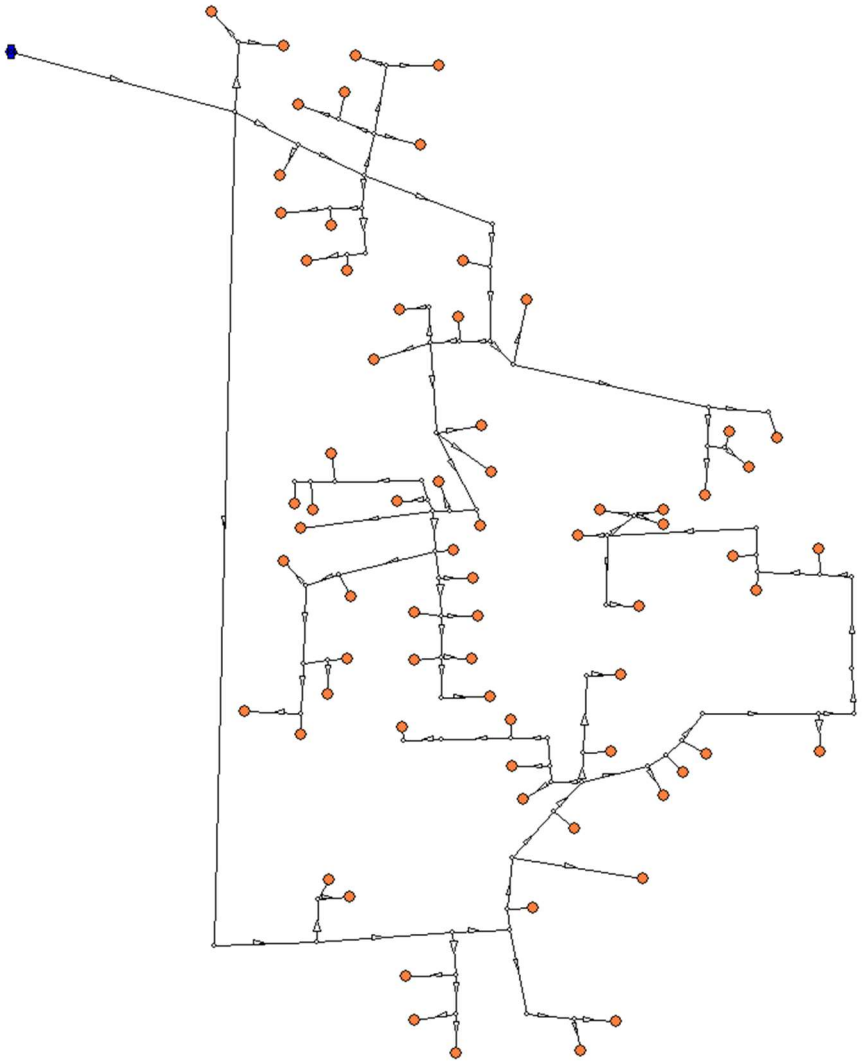

Figure 4.1. Network layout of the case DH system.

Similar as Chapter 3, four TES technologies are investigated, as shown in Table 4.2. The design storage capacities for the CWT and DHWT are the same. Compared to LTDH case, the network inertia in the MTDH case has more storage potentials. The active deviation of indoor air temperature to utilize the BTM is set to 1 K in this chapter, which represents the scenario with the best economic performance, as is further explained through sensitivity analysis in Section 4.3.2. Further analysis on the different storage capacities can also be found in Section 4.3.2.

Table 4.2. Design parameters of the TES units in MTDH system

Parameters	CWT	DHNI	DHWT	BTM
Size (m^3)	5,000	12,618	2,986	-
Storage temperature difference (K)	45	10	75	1
Storage capacity (MWh)	262	147	262	366
Percent in average daily load (%)	13%	7%	13%	18%

4.2 Methods

The modelling of the MTDH system is also based on the dynamic DH model, as explained in Section 3.2. The supplementary model for the CHP plant is introduced in this section. The method for the life-cycle cost (LCC) analysis, to quantitatively compare the performance of TES units in two systems, is also explained.

4.2.1 Models for the CHP plant

In the extraction plant, the middle pressure steam with the temperature of approximately 150°C is extracted from the steam turbines to heat the circulating water. Therefore, the active use of the network inertia is simply considered to have no influence on the source efficiency. The heating and electricity output can be adjusted by the amount of extracted steam, within certain minimum and maximum limits. Meanwhile, the main steam flowrate can be adjusted by changing the boiler load, as shown in the feasible operation range in Figure 4.2. Any operating point within this range can be expressed by the convex combination of the coordinates of the corner points [19,52], using the Eqs. (15) - (17). In this study, the selected extraction plant has a maximum power generating capacity of 270 MW.

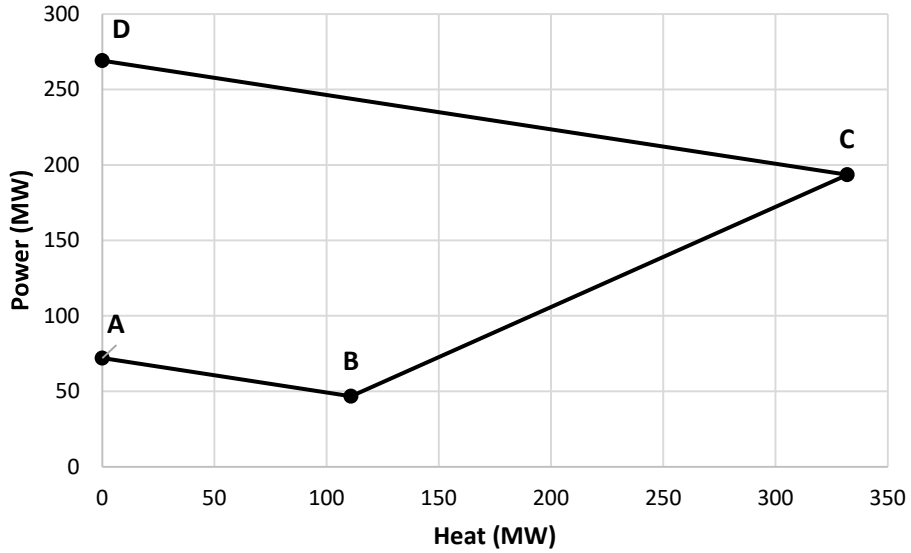

Figure 4.2. Feasible operation range of the extraction CHP plant.

$$Q_{CHP,\tau} = \sum_{N=1}^{4} (\alpha_{N,\tau} \cdot Q_{CHP,N}) \tag{15}$$

$$P_{el,CHP,\tau} = \sum_{N=1}^{4} (\alpha_{N,\tau} \cdot P_{CHP,N}) \tag{16}$$

$$F_{el,CHP,\tau} = \sum_{N=1}^{4} (\alpha_{N,\tau} \cdot F_{CHP,N}) \tag{17}$$

$\alpha_{N,\tau}$ combination factors of four corners, complying with the constraints written in Eq. (18)

$Q_{CHP,N}$ Heating power at corner N (kW)

$P_{CHP,N}$ Electricity generating power at corner N (kW)

$F_{CHP,N}$ Fuel consumption rate at corner N (kW)

$$\sum_{N=1}^{4} \alpha_N = 1 \tag{18}$$

4.2.2 LCC analysis

The installation of TES units influences not just the operation cost, but also the investment for network facilities. Thus, the life-cycle cost (LCC) is calculated to evaluate the economic performances of different systems, as presented in Eq. (19). During the analysis, the capacities of the heat sources are set the same for all systems, so the investment for the heat sources is not considered.

$$LCC = C_{inv,network} + C_{inv,TES} + f(C_{ope} + C_{manage}) \tag{19}$$

$C_{inv,network}$ Investment for the network, according to appended papers and ref [53]

$C_{inv,TES}$ Investment for TES units, based on Table 4.3

C_{ope} Annual operation cost for the heat sources

C_{manage} Annual management cost, calculated as 0.5% of the initial investment

Regarding the use of the DHNI, there is no available practical data about the investment for the control system. It has been pointed out that the control system is already embedded in the ordinary system design, and such investment can be neglected compared to the investment for the network pipes. Thus, the investment for DHNI is not considered.

A lifetime of 30 years is considered for all equipment [54]. Then, the annuity f is used to convert annual cost to LCC, calculated as Eq. (20).

$$f = \sum_{a=1}^{30} \frac{1}{(1+r)^a} \tag{20}$$

r Nominal interest rate, set to 5% according to current financial conditions [55]

The LCC saving rate, which is calculated by comparing the LCC of the TES system and the REF system, is used in the following analysis.

Table 4.3. Recommended investments for TES units.

Item	Unit	Investment	Ref
CWT	(SEK/m^3)	4750	[12,56]
BTM	(SEK/household)	2000	[57]
DHWT	(SEK/m^3)	16800	[12]
DHNI	(SEK)	0	-

4.3 Results

In this section, the MTDH and LTDH systems under the VRE scenario are compared, while the peak scenario and IWH scenario, as reported in Chapter 3, are omitted. Thus, the HPs and CHP plants are considered as heat sources in the LTDH and MTDH systems, respectively. The baseline energy supply and demand conditions for the two systems are presented in Table 4.4 and Table 4.5. Unlike the Chapter 3, the VRE source used in this section is wind power, which has more potentials for either small or large energy systems in Nordic countries [1]. The profile is based on the historical generation curves of the wind farms in Denmark [44].

The main focus of this part is the difference of TES applications between two case systems. This section also explains the storage benefits under different design capacities through sensitivity analysis.

Table 4.4. Energy supply and demand conditions of the LTDH system.

	VRE			Domestic electricity		Heating		
	Power (kW)	Generation (MWh)	Integration (MWh)	Power (kW)	Demand (MWh)	Power (kW)	Demand (MWh)	Eq. el (MWh)
LTDH	178	153	64	95	743	700	2070	419

Table 4.5. Energy supply and demand conditions of the MTDH system.

	VRE			Domestic electricity		Heating		
	Power (MW)	Generation (GWh)	Integration (GWh)	Power (MW)	Demand (GWh)	Power (MW)	Demand (GWh)	Eq. el (GWh)
MTDH	500	1401	897	229	1800	257	752	-

4.3.1 Comparison between MTDH and LTDH systems

A major difference between two systems is the heating demand, as shown in Figure 4.3. The LTDH has a small demand density of 1.01 MWh/m, which partly contributes to the relatively large thermal losses on the pipes. In contrary, the linear demand density of the MTDH system is 13.9 MWh/m.

The DHW demand in the LTDH case is larger than that in the MTDH case because the former includes SFHs, which have relatively higher demand level for DHW. Since there are usually

more than 30 households in an apartment in the MTDH case, the peak power of the DHW demand in the apartment is significantly lower than the power of a single end-user, known as the simultaneity effect. In contrast, such peak demand in the LTDH case still plays an important part in the total demand. These aspects influence the designs and operations of the TES units.

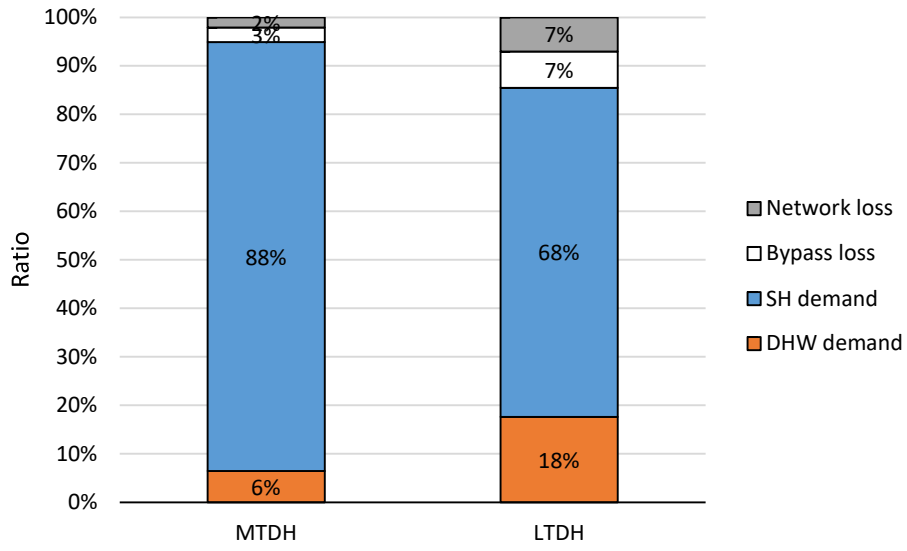

Figure 4.3. Annual heat supply for the MTDH and LTDH cases.

The difference in VRE integration rates by four TES units are presented in Figure 4.4. Although the design storage capacity of the CWT is smaller than the capacity of BTM, the CWT still has the best performance in integrating VRE. By contrast, despite having a same storage capacity, the DHWT can only integrate limited amount of VRE. As for the use of network inertia, it is only applicable in the MTDH case because the source efficiency is less sensitive to temperature changes.

Comparing the different scenarios, from the current to future passive building stocks, the VRE integration benefits are reduced to different levels. The use of the BTM is mostly influenced, as explained in the former sections. Unlike the LTDH case where the VRE integration by CWT is increased in the low-energy scenario, the MTDH case has obviously lower VRE integration in this scenario. This phenomenon could be explained by the difference of two heat sources in matching the surplus VRE with demand. For the MTDH system with CHP plant, the storage unit is discharged during the VRE surplus period and is charged during the deficit period. As the demand goes down in the future low-energy building stock, the discharged potential dropped down, so as the VRE integration potential.

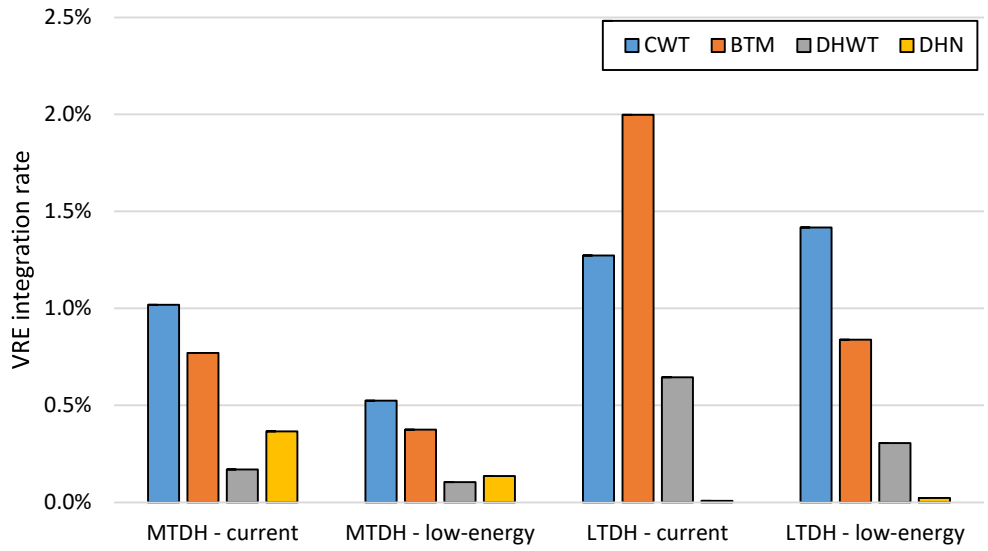

Figure 4.4. Improved VRE integration rates in the MTDH and LTDH cases.

As for the annual operational cost-saving rates, the differences between two cases lie mainly in the use of DHWT and DHN, as shown in Figure 4.5. As explained above, the benefits for the DHWT in the LTDH case comes mostly from the reduction of bypass loss. However, such benefits are no longer effective in the MTDH case due to the circulation loss inside the apartment buildings. Thus, the cost-saving benefit of the DHWT in MTDH case is basically decided by the VRE integration benefit. As for the use of the network inertia, the operation cost in LTDH system is even higher than the reference case because the COPs of the HPs are reduced, leading to more electricity consumption.

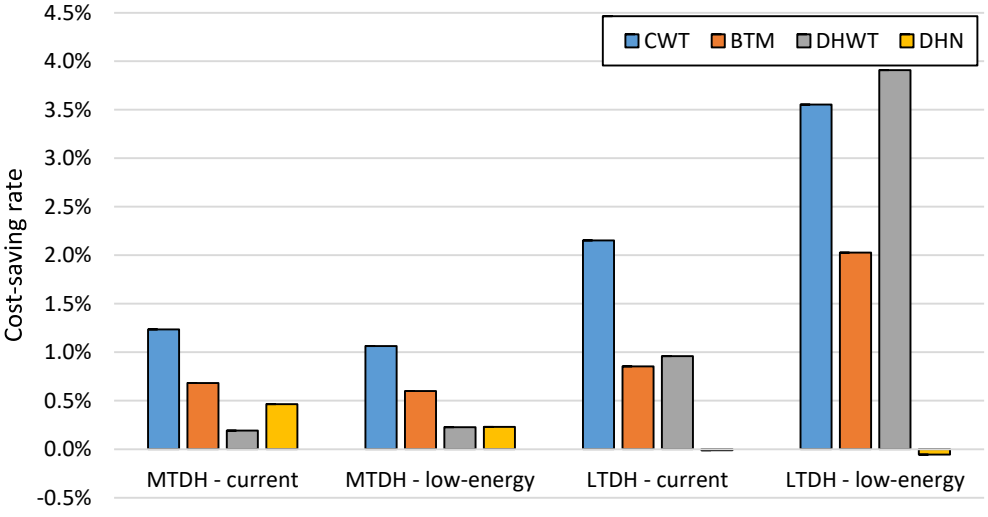

Figure 4.5. Annual operational cost-saving rates in the MTDH and LTDH cases.

With the installations of DHWTs, the sizes of the network are reduced. Thus, the comparisons of the investments for the networks are presented in Table 4.6. For the system with the other three TES technologies, the network investments are the same as the REF system. In the small-

scale LTDH case, since the peak DHW demand plays important role in the total demand, the use of DHWTs can significantly reduce the network pipes' sizes and related investment. Indeed, the reduced investment for pipes can directly offset the additional investment for DHWTs, which is 0.47 million SEK. However, in large MTDH case, such benefit is very limited. One reason is that the simultaneous effect of the DHW usage in a large group has already shaved the peak power demand. Another reason is that the share of the DHW demand is much smaller in the MTDH case. Thus, the reduction of peak DHW demand has limited effect on the total heating demand. The investment for DHWTs, which is 50.2 million SEK, still needs to be recovered by the benefits from operation costs.

Table 4.6. Network investments in the REF system and DHWT system, unit: million SEK.

Scenarios	MTDH - current	MTDH - passive	LTDH - current	LTDH – passive
REF	402.6	342.0	3.7	3.6
DHWT	394.4	334.6	3.3	3.1
Saving	8.2	7.4	0.4	0.5

The LCC saving rates for the investigated systems, compared to the REF system, are presented in Figure 4.6. Due to the high initial investment and relatively low benefits, the installation of DHWT is not feasible in the large-scale MTDH system from the economic aspect. However, it is much more attractive in LTDH systems. This result proves the suggested development pathway in the end-use demand side, presented in Figure 3.13. As for the use of DHNI, the LCC saving rates in two systems are consistent with the annual cost-savings.

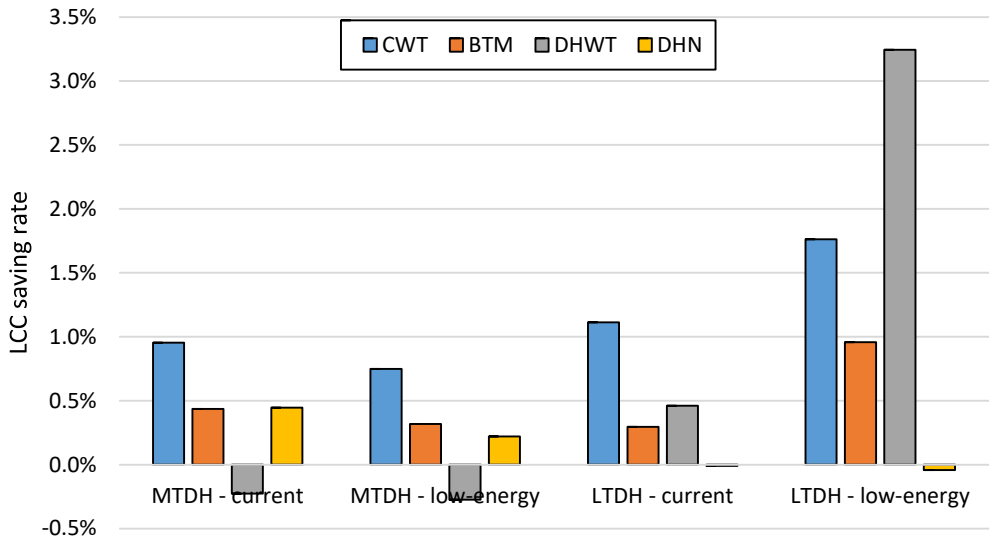

Figure 4.6. LCC saving rates in the MTDH and LTDH cases.

4.3.2 Sensitivity analysis

In this section, the storage performances were evaluated under various storage capacities, by revising the storage sizes of the CWT and DHWTs or the temperature deviations for utilizing the BTM. The main performance indicator is the LCC saving rate, as explained in above sections.

For the CWT, several storage capacities that can cover the average daily demand from 13% to nearly 65% were investigated, as shown in Table 4.7 and Figure 4.7. The LCC saving rate is increasing as the storage size is larger. However, for the MTDH and LTDH cases, there are upper limits of the VRE integration benefits and LCC saving benefits. The upper LCC saving limit in the MTDH system is much lower than that in the LTDH system, due to the large energy demand in the system. Besides, the static payback period is also longer in larger storage unit. Thus, the considerations over the initial investment, LCC, and practical issues such as the enough space for storage unit shall be balanced for decision making.

Table 4.7. Investigated CWT sizes and the ratios to the daily demand in the two case systems.

System	Size (m^3)	Capacity (MWh)	Capacity/Daily demand
MTDH	5,000	263	13%
	7,500	394	20%
	10,000	525	26%
	12,500	656	33%
	15,000	788	40%
	20,000	1,050	53%
	25,000	1,313	66%
LTDH	27.9	976	17%
	40	1,400	25%
	60	2,100	37%
	80	2,800	49%
	100	3,500	62%

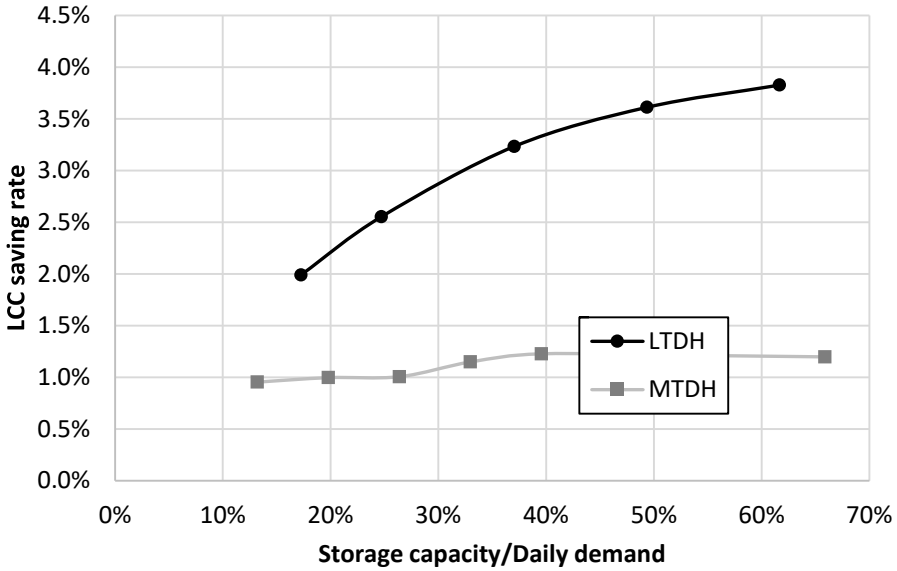

Figure 4.7. LCC saving rate for CWT with different sizes in the MTDH and LTDH cases.

Regarding the DHWT, the investigated sizes are converted to the ratio to average daily DHW demand, as presented in Table 4.8. The LCC saving rates are shown in Figure 4.8. In general, as the storage size is smaller, the LCC saving rate is higher. Several reasons can explain this result. First, as illustrated above, the capacity related VRE integration benefit is very limited, which cannot offset the initial investment. Second, as the storage size is smaller, the peak charging power is also smaller, which has a larger benefit of peak reduction. In the meanwhile,

the initial investment is also small. However, the LCC saving for DHWTs in the MTDH system is always negative because the bypass loss reduction is not applicable, as explained earlier.

Table 4.8. Investigated DHWT sizes in the two case systems.

System	DHWT Volume per household (litre)	DHWT volume/daily demand
MTDH	40	0.5
	60	0.75
	80	1
	100	1.25
	120	1.5
LTDH	90	0.6
	120	0.8
	150	1
	180	1.2
	210	1.4

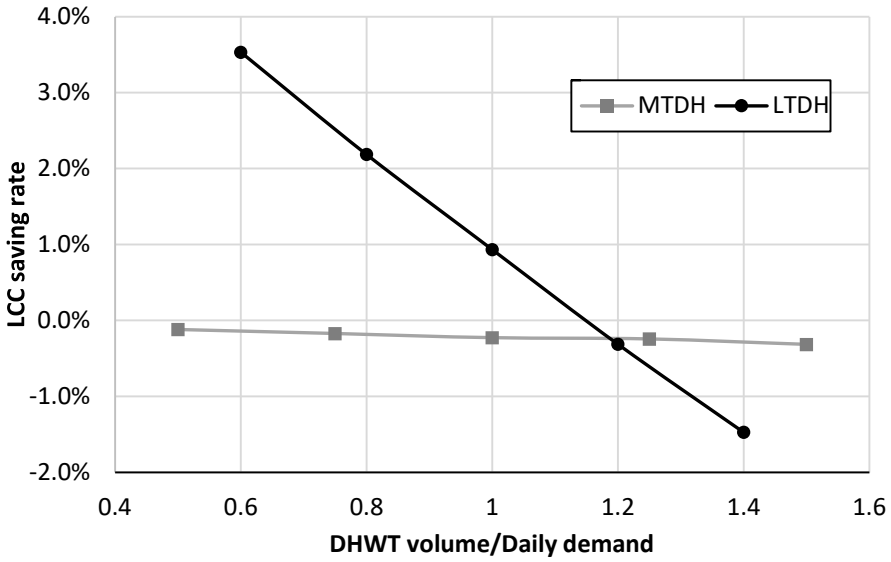

Figure 4.8. LCC saving rates for DHWTs with different sizes in the MTDH and LTDH cases.

As for the use of BTM, four typical temperature deviations from 0.5 K to 2.0 K were investigated, as shown in Table 4.9. From the LCC analysis results presented in Figure 4.9, it is found that the maximum LCC saving is achieved at the temperature deviation of around 1 K, which is also the selected value in previous analysis. For deviations larger than this value, not only the indoor thermal comfort is influenced, but the additional heat losses associated with the increased air temperature are also increased.

Table 4.9. Investigated BTM scenarios.

Cases	Temperature deviation (K)	MTDH Capacity (kWh)	Capacity/demand	LTDH Capacity (kWh)	Capacity/demand
BTM - 0.5	0.5	183075	9%	785	14%
BTM - 1.0	1	366150	18%	1570.2	27%
BTM - 1.5	1.5	549225	27%	2355	40%
BTM - 2.0	2	732300	36%	3140	53%

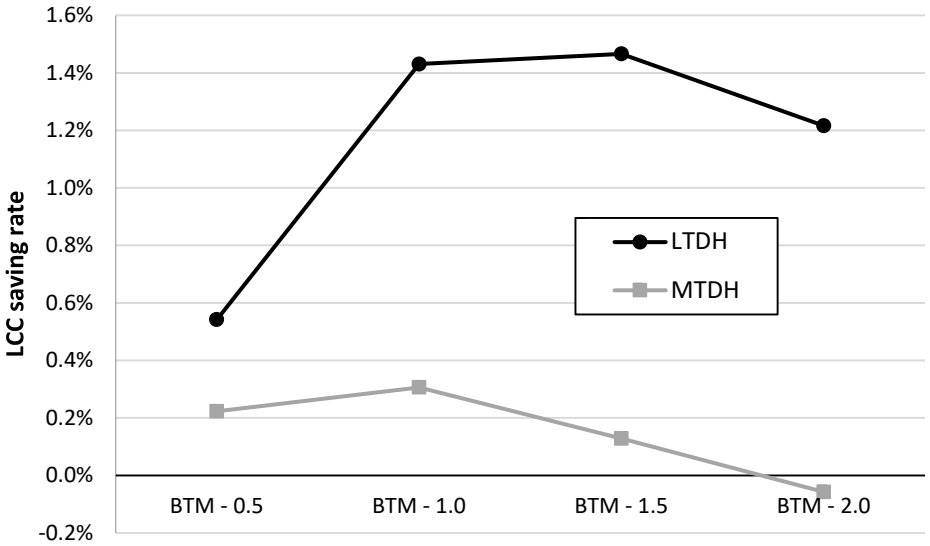

Figure 4.9. LCC saving rates for DTM with different temperature deviations in the MTDH and LTDH cases.

4.4 Discussion on the supply side and demand side management

Based on the above analysis, it is found that the active load shifting benefits of demand side DHWTs are limited. To further understand this phenomenon, the benefits of demand side measures are conceptualized in this section. In general, the benefits can be summarized into the following four points:

1) Peak reduction, including the reduced investment and operation cost

2) Load shifting. The ability to control the load from demand side to integrate more renewable energy.

3) Smooth operation of the equipment

4) Bypass loss reduction

In theory, the minimal charging power $P_{ch.min}$ can be designed as the average value of the demand side powers P_{demand}. In this baseline condition, the charging power is kept constant, and the demand is exactly fulfilled. Associated minimal storage capacity $Q_{design,min}$ can be calculated according to demand profiles.

To achieve the load shifting effect, the charging power and storage capacity shall be further increased, compared to the baseline condition with no peak demand. Correspondingly, the investment for the storage unit itself and the investment associated with the network capacity and heat source capacity are also increased, as shown in equation below:

$$\Delta Investment = (Inv_{network} + Inv_{source})\Delta P_{ch,design} + Inv_{TES} \cdot \Delta Q_{design} \quad (21)$$

$Inv_{network}$ Investment for network capacity (SEK/kW)

Inv_{source} Investment for heat source capacity (SEK/kW)

Inv_{TES} Investment for additional TES storage capacities for load shifting (SEK/kWh)

$\Delta P_{ch,design}$ Increased charging power, compared to baseline condition (kW)

ΔQ_{design} Increased storage capacity, compared to baseline condition (kWh)

The above equations can be applied to qualitatively compare the supply side measures and demand side measures. Apart from the costs, the benefits for the two types, including the reduced heat source capacity and reduced bypass losses, are similar. However, the investments for two measures are different, as shown in Table 4.10. The investment for additional storage capacities to actively shift the load is much cheaper in the supply side. Besides, based on the results in previous case studies, it can be found that the supply side storage unit can be more effectively used to shift the load, due to the less fluctuations and interference in the supply side.

Therefore, from the economical aspect, the design for extra load shifting is in some way in contradiction with the design for baseline peak shaving. Indeed, the storage capacity design for only the peak shaving benefit could be much cost-effective. However, the above discussions are only limited to traditional centralized DH systems. For multi-sources DH systems, or systems with demand-side distributed sources, the conclusions can be completely different, which are discussed in Chapter 5 as future research plans.

Table 4.10. The investment for sensible water tank in the supply side and demand side.

Investment	Supply side	Demand side
Network capacity $Inv_{network}$	No	Yes
Heat source capacity Inv_{source}	Identical	
Storage unit Inv_{TES}	1,500 SEK/m^3 (Around 5,000m^3)	15,000 SEK/m^3 (Around 1m^3)

4.5 Future combined TES design

Based on above analysis and discussions above, the future combinations of TES technologies are proposed for the LTDH and MTDH systems, as shown in Figure 4.10 and Figure 4.11, respectively. For the small-scale LTDH systems, the demand side DHWTs are applied to shave the peak demand and smoothen the demand curves. Then, the BTM is controlled to shift the demand within acceptable temperature deviations. In the source side, the CWT is directly used to balance the VRE supply and demand. Improved insulation layers and innovative storage structures can be applied to the central storage tank to assure a less heat loss and a higher storage efficiency.

For MTDH systems, the idea for using the CWT and BTM is the same as in the LTDH systems. However, as illustrated above, DHWTs are in general not widely needed. They might be only applicable in some special cases, such as the SFHs community within the large MTDH systems. Different from the LTDH systems, the DHNI inertia is utilized, by applying control systems in both the source and demand sides.

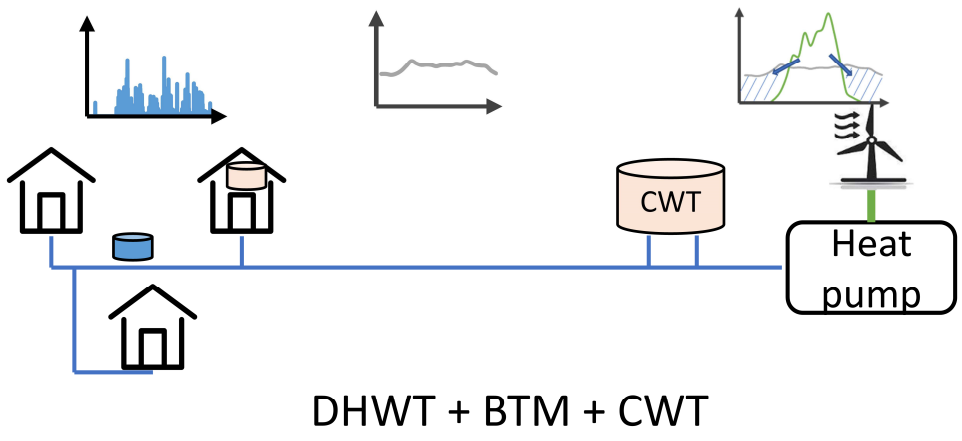

Figure 4.10. The proposed TES combinations in LTDH systems.

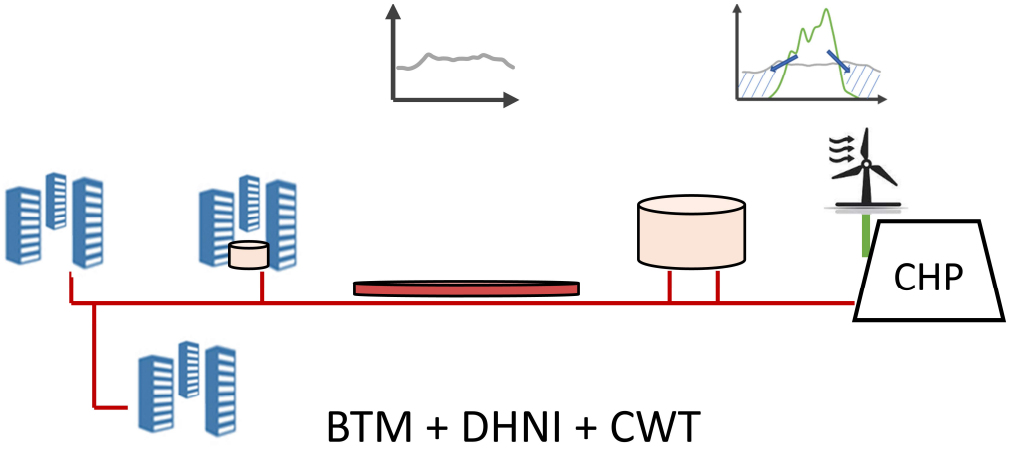

Figure 4.11. The proposed TES combinations in MTDH systems.

The TES combinations were modelled and the key performance indicators for the LTDH system and MTDH system were presented in Table 4.11 and Table 4.12, respectively. The performances of the REF system and the CWT system are used as benchmarks for comparison. It is found that the VRE integrations are improved in both systems. Concerning economic benefits, a combination of TES technologies is in general more cost-saving than single TES measure in LTDH systems. However, the combination measure has larger LCC than single CWT measure in MTDH system because the annual operation cost is only slightly improved. This is explained by the relatively small benefit of integrating VRE in the CHP plant, compared to the HP.

Table 4.11. Comparison between the CWT and the combined TES technologies in LTDH system.

	VRE integration (MWh)		Operation cost (million SEK)		LCC (million SEK)	
REF	841		0.511		11.9	
CWT	857	16.0 (1.3%)	0.486	-0.025 (-4.8%)	11.6	-0.24 (-2.0%)
DHWT+BTM+CWT	883	41.2 (3.3%)	0.468	-0.042 (-8.3%)	11.5	-0.37 (-3.2%)

Table 4.12. Comparison between the CWT and the combined TES technologies in MTDH system.

	VRE integration (GWh)		Operation cost (million SEK)		LCC (million SEK)	
REF	896		687		11,015	
CWT	910	14.3 (1.0%)	679	-8 (-1.1%)	10,910	-105.1 (-1.0%)
BTM+DHNI+CWT	923	26.9 (1.9%)	679	-8 (-1.1%)	10,999	-15.6 (-0.1%)

5 Conclusions and future research work

In this thesis, a systematic design framework is developed to identify the optimal applications of short-term TES technologies in the future. The framework considers the diverse factors from top-level targets to bottom-level implementations. The top-level target for installing TES units is theoretically analysed by matching the energy profiles. Then, the hypothetic design capacity is converted to practical TES design, through middle-level target conversions. On bottom-level, four typical short-term TES technologies were evaluated on a variety of scenarios, which are representatives of the main characteristics of the current MTDH system and future LTDH system. Based on the modelled results, the optimal combinations of TES technologies were identified, to understand the potentials and roles of short-term TES in the future. The conclusions from each part are summarized in Section 5.1. The recommendations for future research works are presented in Section 5.2.

5.1 Conclusions

By matching the energy supply and demand profiles, the load shifting target and associated storage capacity designs can be theoretically identified. Compared to complex system models, the proposed method requires only the energy profiles, to easily identify the suitable storage designs. The method is validated by results from case studies and can be applied in various scenarios, including both the heating and the electricity sectors.

The practical TES design process builds a connection between the theoretical storage target and the bottom-level TES implementations. With the proposed analysis indicators such as the heat loss efficiency and storage capacity efficiency, the practical storage capacity and sizes are acquired.

On the bottom level, the implementations of four typical short-term TES technologies were firstly evaluated in a future small-scale LTDH system. It is found that the benefits of peak load reduction and bypass heat loss reduction are much more prominent in DHWTs than the benefit of active load shifting to integrate VRE. By contrast, the CWT can store heat for longer period than the other TES technologies and is thus suitable for integrating the VRE in the future. The BTM has certain storage potentials in the current building stock but is less applicable in the future low-energy building stock due to reduced space heating demand and period. Furthermore, the use of DHNI as storage unit is proved to be infeasible in the case LTDH

system. A performance map of the TES technologies, indicating the strong links between the system characteristics and optimal TES applications, is provided in this study.

The study further compared the applications of short-term TES technologies in two DH systems with completely different system characteristics. Unlike the LTDH system, applicability of DHWTs is largely limited in the large-scale MTDH system due to the reduced benefit from peak-reduction and bypass loss reduction. Indeed, the roles of the demand-side storage units as buffer tanks and active load-shifting units are discussed in this study. As for the use of DHNI, it has much more potentials in the MTDH system. The sensitivities of the storage capacities were also evaluated. Based on the results, the future optimal combinations of TES technologies are proposed for the LTDH and MTDH systems.

5.2 Future research

As indicated in Section 1.4, a major limitation of the presented studies is that only the traditional centralized DH system is considered. However, there are growing interest for multi-sources de-centralized heating systems, including both the uni-directional type and bi-directional type, as shown in Figure 5.1. The reasons for using such system are from multiple aspects, such as the enhanced control flexibility for intermittent heating, reduced peak demand cost, recovery of low-temperature waste heat within the urban area, integration of local VRE generation, efficient supply of heating and cooling demand simultaneously and reduced penalty for return water temperatures. As the space heating demand goes down in the future, the conventional centralized district heating system will become less feasible from both the economic and technical aspects. Besides the variations of the heating load, there will also be more variations of the energy supply due to increasing amount of local VRE productions such as rooftop PV. These challenges call for flexible measures to balance the energy supply in the demand side.

Therefore, the future research focuses will be put on the optimal design and operation of de-centralized heating systems. The applicability and roles of TES technologies in these heating systems will be further investigated. Besides, since the temperature levels of the whole system will be reduced, there are less potentials for sensible TES units, while other types of storage technologies, such as latent TES utilizing the phase-change materials, could have more potentials. Together with the findings for the traditional centralized district heating systems, a bigger picture about the TES technologies in the future could be acquired.

Another issue that would be interesting to address is the applicability of long-term storage units. In this study, only the short-term TES units are considered, while the long-term storage units can be used to shift both seasonal and daily load variations. However, the applicability of the long-term storage unit is influenced by not only the DH system characteristics, but also the specific local conditions such as geographical features and available spaces. Recent reviews [58,59] have summarized the challenges for seasonal storage units and examined their applicability in future renewable energy systems from aspects of technical feasibilities. Yet, the connections between the top-level planning and bottom-level implementations are still missing. Design frameworks for the applications of long-term TES technologies can improve this understanding and facilitate further technology development.

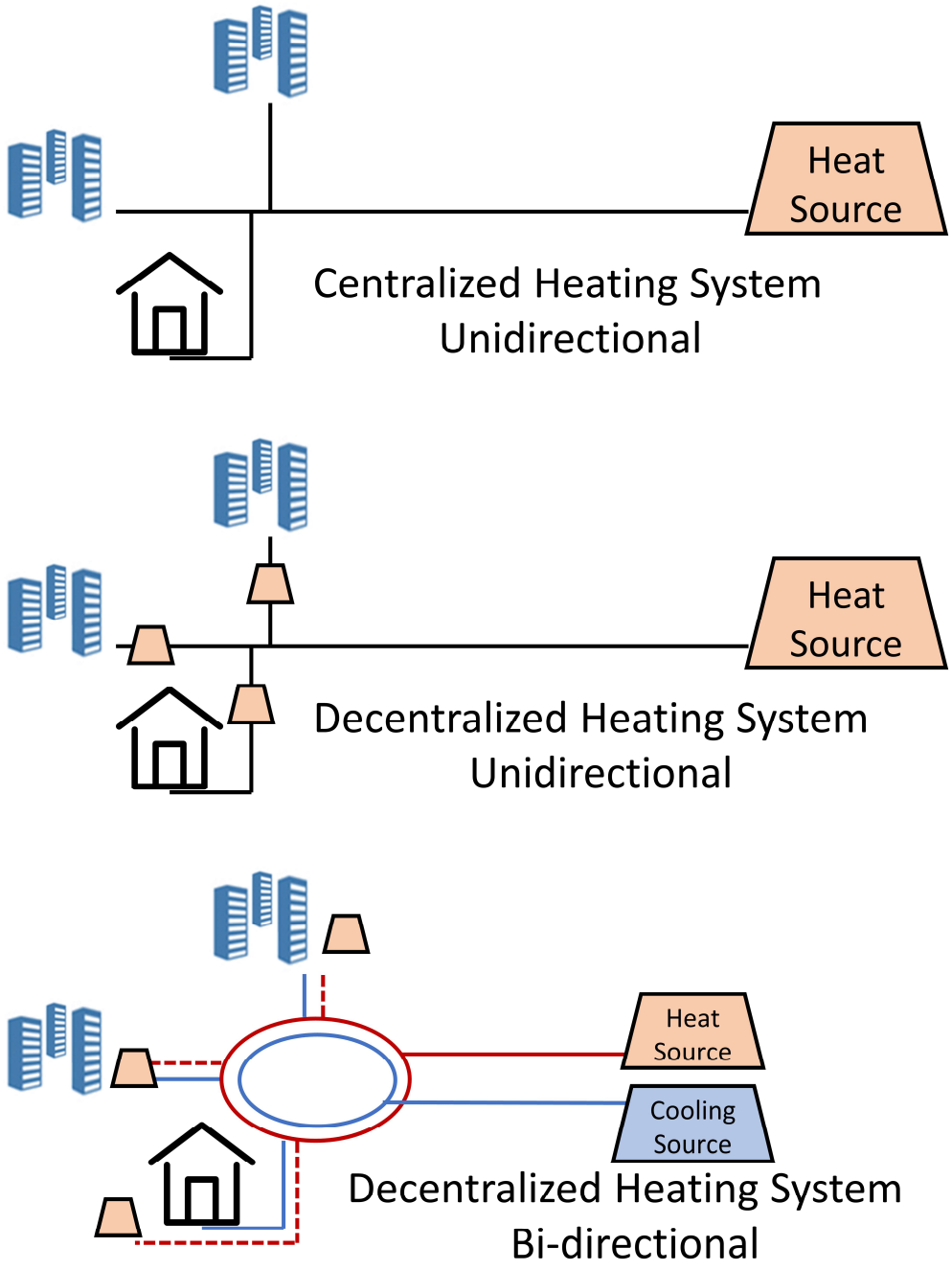

Figure 5.1. Typical heating systems classified by the locations of heat sources and energy flow directions

References

[1] Lund H. Renewable energy strategies for sustainable development. Energy 2007;32:912–9. https://doi.org/10.1016/j.energy.2006.10.017.

[2] Mathiesen B V., Lund H, Connolly D, Wenzel H, Ostergaard PA, Möller B, et al. Smart Energy Systems for coherent 100% renewable energy and transport solutions. Appl Energy 2015;145:139–54. https://doi.org/10.1016/j.apenergy.2015.01.075.

[3] Intergovernmental Panel on Climate Change, editor. Summary for Policymakers. Clim. Chang. 2013 – Phys. Sci. Basis Work. Gr. I Contrib. to Fifth Assess. Rep. Intergov. Panel Clim. Chang., Cambridge: Cambridge University Press; 2014, p. 1–30. https://doi.org/DOI: 10.1017/CBO9781107415324.004.

[4] Lund H, Werner S, Wiltshire R, Svendsen S, Eric J, Hvelplund F, et al. 4th Generation District Heating (4GDH) Integrating smart thermal grids into future sustainable energy systems. Energy 2014;68:1–11. https://doi.org/10.1016/j.energy.2014.02.089.

[5] Lund H, Østergaard PA, Chang M, Werner S, Svendsen S, Sorknæs P, et al. The status of 4th generation district heating: Research and results. Energy 2018;164:147–59. https://doi.org/10.1016/j.energy.2018.08.206.

[6] Connolly D, Lund H, Mathiesen B V., Werner S, Möller B, Persson U, et al. Heat roadmap Europe: Combining district heating with heat savings to decarbonise the EU energy system. Energy Policy 2014;65:475–89. https://doi.org/10.1016/j.enpol.2013.10.035.

[7] Lund H, Østergaard PA, Connolly D, Mathiesen BV. Smart energy and smart energy systems. Energy 2017;137:556–65. https://doi.org/10.1016/j.energy.2017.05.123.

[8] Guelpa E, Verda V. Thermal energy storage in district heating and cooling systems: A review. Appl Energy 2019;252:113474. https://doi.org/10.1016/j.apenergy.2019.113474.

[9] Hewitt NJ. Heat pumps and energy storage - The challenges of implementation. Appl Energy 2012;89:37–44. https://doi.org/10.1016/j.apenergy.2010.12.028.

[10] David A, Mathiesen BV, Averfalk H, Werner S, Lund H. Heat Roadmap Europe: Large-scale electric heat pumps in district heating systems. Energies 2017;10:1–18. https://doi.org/10.3390/en10040578.

[11] Lund H. Renewable heating strategies and their consequences for storage and grid infrastructures comparing a smart grid to a smart energy systems approach. Energy 2018;151:94–102. https://doi.org/10.1016/j.energy.2018.03.010.

[12] Lund H, Østergaard PA, Connolly D, Mathiesen BV. Energy storage and smart energy systems. Energy 2017;137:556–65. https://doi.org/10.1016/j.energy.2017.05.123.

[13] Salpakari J, Mikkola J, Lund PD. Improved flexibility with large-scale variable renewable power in cities through optimal demand side management and power-to-heat conversion. Energy Convers Manag 2016;126:649–61. https://doi.org/10.1016/j.enconman.2016.08.041.

[14] Persson U, Möller B, Werner S. Heat Roadmap Europe: Identifying strategic heat synergy regions. Energy Policy 2014;74:663–81. https://doi.org/10.1016/j.enpol.2014.07.015.

[15] Gadd H, Werner S. Thermal energy storage systems for district heating and cooling. Woodhead Publishing Limited; 2015. https://doi.org/10.1533/9781782420965.4.467.

[16] Hennessy J, Li H, Wallin F, Thorin E. Flexibility in thermal grids: A review of short-term storage in district heating distribution networks. Energy Procedia 2019;158:2430–4. https://doi.org/10.1016/j.egypro.2019.01.302.

[17] Wit J de. Heat Storages for CHP Optimisation. PowerGen Eur 2007 2007:1–18.

[18] Werner S. District heating and cooling 2013.

[19] Zheng J, Zhou Z, Zhao J, Wang J. Integrated heat and power dispatch truly utilizing thermal inertia of district heating network for wind power integration. Appl Energy 2018;211:865–74. https://doi.org/10.1016/j.apenergy.2017.11.080.

[20] Kensby J, Trüschel A, Dalenbäck JO. Potential of residential buildings as thermal energy storage in district heating systems - Results from a pilot test. Appl Energy 2015;137:773–81. https://doi.org/10.1016/j.apenergy.2014.07.026.

[21] Schmidt D, Kallert A, Blesl M, Svendsen S, Li H, Nord N, et al. Low Temperature District Heating for Future Energy Systems. Energy Procedia 2017;116:26–38. https://doi.org/10.1016/j.egypro.2017.05.052.

[22] Averfalk H, Werner S. Novel low temperature heat distribution technology. Energy 2018;145:526–39. https://doi.org/10.1016/j.energy.2017.12.157.

[23] Yang X, Li H, Svendsen S. Energy, economy and exergy evaluations of the solutions for supplying domestic hot water from low-temperature district heating in Denmark. Energy Convers Manag 2016;122:142–52. https://doi.org/10.1016/j.enconman.2016.05.057.

[24] Zheng W, Hennessy JJ, Li H. Reducing renewable power curtailment and CO2 emissions in China through district heating storage. Wiley Interdiscip Rev Energy Environ 2020;9:1–11. https://doi.org/10.1002/wene.361.

[25] Lund H, Duic N, Østergaard PA, Mathiesen BV. Future district heating systems and technologies: On the role of smart energy systems and 4th generation district heating. Energy 2018;165:614–9. https://doi.org/10.1016/j.energy.2018.09.115.

[26] Verda V, Colella F. Primary energy savings through thermal storage in district heating networks. Energy 2011;36:4278–86. https://doi.org/10.1016/j.energy.2011.04.015.

[27] Zimmermann JP. End-use metering campaign in 400 households In Sweden Assessment of the Potential Electricity Savings. Contract 2009;17:05–2743. https://doi.org/Contract 17-05-2743.

[28] Schütz T, Streblow R, Müller D. A comparison of thermal energy storage models for building energy system optimization. Energy Build 2015;93:23–31. https://doi.org/10.1016/j.enbuild.2015.02.031.

[29] Campos Celador A, Odriozola M, Sala JM. Implications of the modelling of stratified hot water storage tanks in the simulation of CHP plants. Energy Convers Manag 2011;52:3018–26. https://doi.org/10.1016/j.enconman.2011.04.015.

[30] Tol HI, Svendsen S. Improving the dimensioning of piping networks and network layouts in low-energy district heating systems connected to low-energy buildings: A case study in

Roskilde, Denmark. Energy 2012;38:276–90. https://doi.org/10.1016/j.energy.2011.12.002.

[31] Benonysson A, Bøhm B, Ravn HF. Operational optimization in a district heating system. Energy Convers Manag 1995;36:297–314.

[32] Zhao H. Analysis, modelling and operational optimization of district heating systems, 1995.

[33] de Normalización CE. EN ISO 13790: Energy Performance of Buildings: Calculation of Energy Use for Space Heating and Cooling (ISO 13790: 2008). CEN; 2008.

[34] Jordan U, Vajen K. Realistic domestic hot-water profiles in different time scales. Rep Sol Heat Cool Progr Int Energy Agency (IEA-SHC)Task 2001;26:1–18.

[35] SFS-EN 15316-3-1. Heating systems in buildings — Method for calculation of system energy requirements and system efficiencies — Part 3-1 Domestic hot water systems , characterisation of needs (tapping requirements) 2006:1–20.

[36] Gu W, Wang J, Lu S, Luo Z, Wu C. Optimal operation for integrated energy system considering thermal inertia of district heating network and buildings. Appl Energy 2017;199:234–46. https://doi.org/10.1016/j.apenergy.2017.05.004.

[37] Guelpa E, Sciacovelli A, Verda V. Thermo-fluid dynamic model of large district heating networks for the analysis of primary energy savings. Energy 2019;184:34–44. https://doi.org/10.1016/j.energy.2017.07.177.

[38] Alimohammadisagvand B, Jokisalo J, Kilpeläinen S, Ali M, Sirén K. Cost-optimal thermal energy storage system for a residential building with heat pump heating and demand response control. Appl Energy 2016;174:275–87. https://doi.org/10.1016/j.apenergy.2016.04.013.

[39] Renaldi R, Kiprakis A, Friedrich D. An optimisation framework for thermal energy storage integration in a residential heat pump heating system. Appl Energy 2017;186:520–9. https://doi.org/10.1016/j.apenergy.2016.02.067.

[40] Guadalfajara M, Lozano M, Serra L. Analysis of Large Thermal Energy Storage for Solar District Heating. Eurotherm Semin #99 Adv Therm Energy Storage 2014:1–10. https://doi.org/10.13140/2.1.3857.6008.

[41] Cruickshank CA, Harrison SJ. Heat loss characteristics for a typical solar domestic hot water storage. Energy Build 2010;42:1703–10. https://doi.org/10.1016/j.enbuild.2010.04.013.

[42] Romanchenko D, Kensby J, Odenberger M, Johnsson F. Thermal energy storage in district heating: Centralised storage vs. storage in thermal inertia of buildings. Energy Convers Manag 2018;162:26–38. https://doi.org/10.1016/j.enconman.2018.01.068.

[43] Maivel M, Kurnitski J. Heating system return temperature effect on heat pump performance. Energy Build 2015;94:71–9. https://doi.org/10.1016/j.enbuild.2015.02.048.

[44] NordPool Group. NordPool, the leading power market in Europe n.d. https://www.nordpoolgroup.com/ (accessed February 16, 2020).

[45] Commission JRCE. Photovoltaic geographical information system-interactive maps 2014.

[46] Schmidt D, Kallert A, Blesl M, Li H, Svendsen S, Nord N, et al. Annex TS1 Low Temperature District Heating for Future Energy Systems - Final report - Future low temperature district

heating design guidebook. 2017.

[47] Dalla Rosa A, Li H, Svendsen S. Method for optimal design of pipes for low-energy district heating, with focus on heat losses. Energy 2011;36:2407–18. https://doi.org/10.1016/j.energy.2011.01.024.

[48] Foteinaki K, Li R, Heller A, Rode C. Heating system energy flexibility of low-energy residential buildings. Energy Build 2018;180:95–108. https://doi.org/10.1016/j.enbuild.2018.09.030.

[49] Li Y, Xia J, Fang H, Su Y, Jiang Y. Case study on industrial surplus heat of steel plants for district heating in Northern China. Energy 2016;102:397–405. https://doi.org/10.1016/j.energy.2016.02.105.

[50] Li Y, Chang S, Fu L, Zhang S. A technology review on recovering waste heat from the condensers of large turbine units in China. Renew Sustain Energy Rev 2016;58:287–96. https://doi.org/10.1016/j.rser.2015.12.059.

[51] Li Y, Fu L, Zhang S, Jiang Y, Xiling Z. A new type of district heating method with co-generation based on absorption heat exchange (co-ah cycle). Energy Convers Manag 2011;52:1200–7. https://doi.org/10.1016/j.enconman.2010.09.015.

[52] Lahdelma R, Hakonen H. An efficient linear programming algorithm for combined heat and power production. Eur J Oper Res 2003;148:141–51. https://doi.org/10.1016/S0377-2217(02)00460-5.

[53] Best I, Orozaliev J, Vajen K. Economic comparison of low-temperature and ultra-low-temperature district heating for new building developments with low heat demand densities in Germany. Int J Sustain Energy Plan Manag 2018;16:45–60. https://doi.org/10.5278/ijsepm.2018.16.4.

[54] Danish Energy Agency. Technology data Generation of Electricity and District heating 2016:382.

[55] Sweden interest rates 2019. http://sweden.deposits.org (accessed October 13, 2020).

[56] Espagnet AR. Techno-economic assessment of Thermal Energy Storage integration into Low Temperature District Heating networks 2016:94.

[57] Hedegaard K, Mathiesen BV, Lund H, Heiselberg P. Wind power integration using individual heat pumps - Analysis of different heat storage options. Energy 2012;47:284–93. https://doi.org/10.1016/j.energy.2012.09.030.

[58] Bott C, Dressel I, Bayer P. State-of-technology review of water-based closed seasonal thermal energy storage systems. Renew Sustain Energy Rev 2019;113:109241. https://doi.org/10.1016/j.rser.2019.06.048.

[59] Dahash A, Ochs F, Janetti MB, Streicher W. Advances in seasonal thermal energy storage for solar district heating applications: A critical review on large-scale hot-water tank and pit thermal energy storage systems. Appl Energy 2019;239:296–315. https://doi.org/10.1016/j.apenergy.2019.01.189.

Part II

Appended Papers

Paper I

Applicability of thermal energy storage in future low-temperature district heating systems – case study using multi-scenario analysis

Yichi Zhang, Pär Johansson, Angela Sasic Kalagasidis

submitted to Energy Conversion and Management, May 2021

Applicability of thermal energy storage in future low-temperature district heating systems – case study using multi-scenario analysis

Yichi Zhang[1*], Pär Johansson[1], and Angela Sasic Kalagasidis[1]

[1]*Department of Architecture and Civil Engineering, Division of Building Technology,*

Chalmers University of Technology, Gothenburg 412 96, Sweden

***Corresponding author:**

Yichi Zhang

Department of Architecture and Civil Engineering, Division of Building Technology

Chalmers University of Technology

412 79, Gothenburg, Sweden

Tel: + 46 (0)31-772 68 01

Email: yichi@chalmers.se

Abstract

With the flexibilities added from thermal energy storage (TES) technologies, low temperature district heating (LTDH) system can coordinate the heat and electricity sectors in a cost-effective manner. Such combinations have therefore become an important step to achieve a 100% renewable energy system. Despite the importance of TES has been demonstrated in previous studies, giving drastic changes compared to the current systems, the practical applicability of TES in the LTDH systems remains unknown. Furthermore, the proposed benefits of TES might deviate from the expectations considering the development of future characteristics, such as the low temperature levels and small space-heating demand. This study investigates the performances and benefits of four typical short-term TES technologies, including the use of central water tank (CWT), district heating network inertia, domestic hot water tank (DHWT), and building thermal mass, based on a case LTDH system in Roskilde, Denmark. Techno-economic analysis is conducted on a variety of scenarios, based on future changes in operation of the heat sources to the end-users. An integrated model is also developed to simulate the operation dynamics of the district heating system with regards to optimizing the use of the TES units. This study provides a performance map of the TES technologies in accordance with the transitions from current to future LTDH systems, indicating the relationships between the system characteristics and optimal TES applications. The CWT is found to be most preferable for integrating the variable renewable energy due to its ability to store heat for long periods. In the end-use side, with the improved building performances and reduced space heating demand in the future, there is less potential for the use of building inertia. In contrary, the benefit of the DHWT, which mainly comes from the reduction of bypass loss during the non-space-heating period, is increased in the future. Furthermore, raising the network temperatures for active storage is found to be infeasible under all future LTDH scenarios because this measure significantly influences the heat source efficiency.

Keywords

Thermal energy storage; low temperature district heating; water tank; variable renewable energy; building thermal mass

Highlights:

- The applicability of four typical TES technologies in the future LTDH system is investigated
- Possible changes from heat sources to end-use demands in the future are represented by multiple scenarios
- Central water tank is most favourable for integrating the variable renewable energy
- The use of building thermal mass has less benefit in future low-energy building stock
- The reduction of heating demand calls for corresponding demand side measures to reduce bypass loss
- The use of network inertia is infeasible in future LTDH system

Nomenclature

Abbreviations

BTM	Building thermal mass
CHP	Combined heat and power
CWT	Central water tank
DH	District heating
DHNI	District heating network inertia
DHW	Domestic hot water
DHWT	Domestic hot water tank
IWH	Industrial waste heat
LTDH	Low temperature district heating
MILP	Mixed-Integer Linear Programming
SEK	Swedish Krona
SFH	Single-family house
SH	Space heating
TES	Thermal energy storage
VRE	Variable renewable energy

Symbols

A	Area (m^2)
$Cost$	Cost (SEK)
C	Heat capacity (kWh/K)
D	Pipe diameter (m)
F	Cross-sectoral area (m^2)
G	Flowrate (kg/s)
K	Heat transfer coefficient (W/K)
L	Length (m)
λ	Thermal conductivity (W/m·K)
P	Pressure (kPa)
Pr	Operation cost (SEK/kWh)
$\dot{Q}$	Power (W)

SOC	State-of-charge (kWh)
u	Flow velocity (m/s)

$\boldsymbol{A}$	Incidence matrix of DHN
$\boldsymbol{B}$	Route matrix
$\boldsymbol{G}$	Flowrate vector for all branches
$\Delta\boldsymbol{H}$	Pressure drop vector
$\boldsymbol{T_{out}}$	Outflow temperature vector
$\boldsymbol{R_B}$	Heat capacity matrix
$\boldsymbol{T_N}$	Node temperature vector
$\dot{\boldsymbol{Q}}_{\boldsymbol{N}}$	Energy exchange vector

Subscripts

B	Branch
ch	charge
dch	discharge
demand	Total heating demand
e	Environment
HS	Heat source
i	Inflow
in	indoor
loss	heat loss
o	*Outflow*
out	*Outdoor*
τ	Time step
x	*Coordinates*

1. Introduction

The target of a 100% renewable energy system brings drastic challenges for the whole society

[1]. With the increasing share of intermittent variable renewable energy (VRE) suppliers, the whole energy systems including the transportation networks and consumers must be re-designed and planned to efficiently utilize the VRE sources. At the same time, the secured energy supplies and acceptable economic expenditures need to be maintained. Solutions to accommodate this balance are studied and aggregated as various pathways towards the future sustainable energy system [2]. It is acknowledged that the integrated design of energy conversions and management between energy sub-sectors are becoming increasingly important for achievable and affordable strategies.

Currently, the heating sector accounts for 50% of Europe's final energy consumption [3] and is expected to remain so for the forecasted future. Among the solutions to decarbonize the heating sector and increase the renewable energy integration, the concept of the future low temperature district heating (LTDH) is discussed in several studies [4–6]. A low temperature on the circulating water in combination with low heating demands in buildings can enable key benefits including better utilization of low-temperature waste heat and integration of renewable energy sources, as well as lower losses in transportation networks. Furthermore, the heating sector of the LTDH system can be coordinated with the electricity and transportation sectors. Together they can form a smart energy system and enable an optimal transition towards the future 100% renewable energy system [2,7].

In order to achieve such synergies between sectors, thermal energy storage (TES) technologies are widely studied since they can offer flexibilities in matching the energy supply and demand on various time scales [8]. Combined with CHP plants and power-to-heat technologies such as heat pumps, TES technologies can increase the VRE integration and reduce the operational cost in existing systems [9,10] and future smart energy systems [11–14]. Common to these studies is a top-down approach where analyses are performed for an entire energy system of a country, e.g. Denmark [12], or a region like Europe [15], without detailing the sublevel systems. Thus, only cumulative storage capacities and costs of TES technologies are addressed. Compared to pathways that only consider electrical storage technologies, the smart energy system pathway with TES technologies can be achieved with significantly lower investments [11].

Despite the importance of TES and future LTDH systems imposed by previous top-down studies [4–6,11–15], relatively less attention has been put on how different TES technologies are adapted and performed in LTDH systems. In a recent review summarizing the applications of TES technologies in district heating and cooling systems [8], the majority of examples refer to the TES applications in the current middle and high temperature district heating (DH) systems. It is, however, worth noting some important changes in the future LTDH systems. Because of lower system temperatures, the heat source efficiency will be more sensitive to temperature changes. Furthermore, the networks and substations are to be re-designed to maintain the return water temperature and avoid bypass heat loses. Meanwhile, space-heating demand and heating periods will be reduced due to better energy efficiency of the future buildings. Considering the above-mentioned changes in the LTDH system, i.e. in the heat sources, networks and end-users, whether the planned TES technologies will perform as intended in the future LTDH systems still remains as an unresolved question.

From the perspective of bottom-level TES applications details in LTDH systems, as the storage temperature difference becomes smaller, the use of sensible active storage units becomes less profitable [16]. Since the system efficiency is more sensitive to temperature levels, the

current plausible storage technologies that have influence on the network working temperatures, such as the use of the district heating network inertia (DHNI) and domestic hot water tank (DHWT), might lose attractiveness in the future. Indeed, the applicability of current TES technologies needs to be well examined.

While both seasonal and short-term storage units are in focus, the latter is a common choice to deal with diurnal variations caused by the intermittent nature of VRE. These variations have strong influence on the marginal operation costs and performances of the DH systems [16]. Thus, the short-term storage units are chosen as study objects. Reviews about the applications of short-term TES units can be found in a series of previous studies [8,17,18], with focuses on the overall technology development [8], the storage potentials of BTM and DHNI [17], and the connections with the electrical grid [18]. However, as in the top-down studies mentioned above, most application studies are restricted to traditional middle and high temperature DH systems. The applicability of short-term TES units in the future LTDH systems remains unknown, which becomes the focus of this study. Detailed explanations of the advantages and challenges for short-term TES technologies in the future are further provided in the **Section 2.1**, based on the literature review of current studies.

As for the top-level planning of the TES and energy systems, most studies are still taking the current available TES technologies into account, without considering their technical details and applicability in the future. In [11], the potential of DHNI is evaluated based on a fixed temperature increase of 10 K in the network, which is not appropriate according to aforementioned reasons. Similar method is also applied in [19] to evaluate the DHNI in Chinese DH systems. Limitations also exist for evaluating the storage potential of building thermal mass (BTM) [19], since the practical storage capacity is reduced as the heating demand becomes lower in LTDH system. Without the knowledge about operational conditions of TES technologies in the future, there are risks for the exaggerated or underestimated potentials of the TES, which further influences the energy balance and overall planning of the smart energy systems. The proposed pathways towards the 100% renewable energy target might deviate from the reality. Hence, to prevent biased conclusions for the future energy systems, the technology development and planning of TES shall be in high accordance with the changes in the future LTDH systems.

Considering the knowledge gap illustrated above, this study aims to evaluate how the current TES technologies can be adapted to the changes in the future LTDH systems. Techno-economic analysis and comparisons of four typical short-term TES technologies were performed on a variety of scenarios, which are representatives of the main characteristics of the current and future DH systems. The changes of the DH systems in the source side, substations, and the end-use buildings are considered in the scenarios. The bottom-up analysis is based on an integrated dynamic model for the DH system developed in this study, which can optimize the design and operation of TES units. The model also has enough technical details to depict the characteristics and challenges of TES technologies in LTDH systems. From the results of this study, the optimal design and operation of TES units according to specific future system characteristics are derived. The study provides a clearer understanding about the possible roles of TES technologies in the transition towards the future smart and renewable energy systems.

This paper is organized as follows: **Section 2** introduces the background knowledge, including the characteristics and changes of the LTDH systems, and the associated challenges imposed

on current TES technologies. **Section 3** explains the modelling methodologies and case study. **Section 4** describes the investigated scenarios. The results of the multi-scenarios analysis are presented in **Section 5**. Based on the results, the discussions on the future applications of TES technologies are provided in **Section 6**.

2. TES technologies and LTDH designs

The concepts and characteristics of LTDH are introduced in **Section 2.1**, as knowledge basis for the investigations in this study. From the perspective of the future LTDH, an overview of the advantages and challenges with different short-term sensible TES technologies, which are the central water tank (CWT), district heating network inertia (DHNI), building thermal mass (BTM), and distributed domestic hot water tank (DHWT), are explained in the **Section 2.2**.

2.1. LTDH characteristics

The concepts and main characteristics of LTDH systems are summarized in several studies [4–6]. On the source side, due to the reduction of return water temperatures, the low-grade waste heat from multiple sources can be recovered. Besides, the integration of VRE can be improved through the implementation and smart control of power-to-heat technologies such as heat pumps. It shall be noted that the VRE discussed in this study refers to renewable electric power from intermittent sources, such as wind power and solar power. The relatively stable renewable heat sources such as biomass are not included. In the demand side, an important characteristic is the reduction of space-heating demand in existing buildings and newly built low-energy buildings. Meanwhile, the DHW demand plays more important roles in the total demand. The improved building performances also make the low-temperature heating feasible. Such changes in the demand side influence not just the heat sources, but also the transportation networks and the use of building thermal inertia.

As pointed out in previous studies [20,21], one important cause for the existing high return water temperatures is the preparation of DHW demand. The instantaneous heat exchanger and domestic hot water tank (DHWT) are two traditional designs that are widely applied in the current DH systems, as shown in **Fig. 1**. The pipes are filled with hot water to assure an acceptable waiting time, which significantly increase the heat losses and return water temperatures.

In order to maintain the required return water temperature, several solutions were provided by researchers [22–24]. One idea is based on the maximum cooling concept, that the supply water is bypassed to the floor heating pipes in the bathroom or other spaces where additional heating does not create discomfort. Thereby, the return water is cooled down to the required temperature level, as 25°C in this study. This design is also named “comfortable bathroom” in some studies [22,23]. Thus, the bypass loss is inevitably created by this design. The bypass flowrate shall be carefully designed so the supply water temperature is always within a requirement after a certain degree of temperature drops caused by heat losses on supply lines. This design is applied to the instantaneous heat exchanger and DHWT in this study. Alternatively, the triple-pipes design with a re-circulation pipe can eliminate the bypass heat loss while maintaining the thermal comfort [20], as shown in **Fig. 1 (c)**. Due to the required new investment and construction works, the triple-pipes design is suitable for newly built LTDH systems and is therefore considered as one optional scenario for the future LTDH systems. The bypass heat losses and the practical performances associated with the three typical substation types, are evaluated and presented in **Section 5.3**. There are also other

alternative designs, such as the electrical supplementary system [22]. They are currently omitted in this study since they are mostly applicable for ultra-low temperature district heating systems with supply water temperatures lower than 40°C, which is not the focus of this study. Moreover, in order to avoid legionella growth in LTDH systems, the temperature level inside the DHWT need to be strictly controlled. Otherwise, additional investments for legionella disinfection solutions, such as ultraviolet light, are required [23,25]. These measures have no influence on the performances of the heating systems but will change the economical balances.

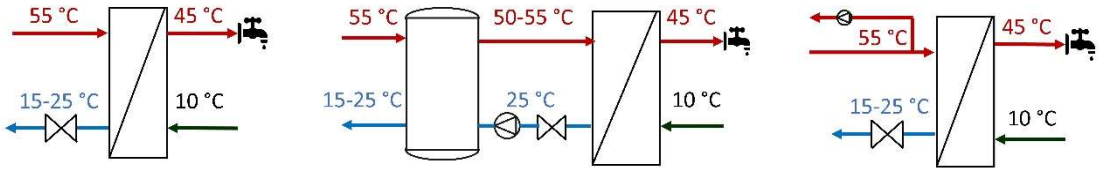

Fig. 1. *Three typical substation types for preparing the DHW demand. (a) Instantaneous heat exchanger; (b) domestic hot water tank; (c) triple-pipes.*

2.2. Advantages and challenges of typical short-term TES technologies

The central heat accumulation tank is a storage device that is often installed near the heat sources to balance the heat supply and demand. A common practice is the central water tank (CWT), due to its relatively cheap investment, stable performance, and the possibility of direct connections with the DH system [16,26]. Benefits from installing the CWT are summarized to three points: (1) reduced investment and usage of peak capacity; (2) smoother operation of equipment and reduced running costs; (3) flexible load shifting to utilize non-dispatchable VRE or electricity with lower prices [27]. In Sweden, 104 out of 167 DH systems have installed central TES units [28]. Due to the additional flexibility added to the electricity sector, it is also found that the systems with combined heat and power (CHP) plants have more incentives to install TES units than the systems with industrial waste heat (IWH) as heat sources. However, as indicated above, the energy storage density of CWT will become smaller in the future LTDH systems due to reduced temperature differences. Besides, the inevitable mixture of hot and cold water inside the tank can increase the return water temperature level and reduce the heat source efficiency [29]. The above-mentioned challenges were only qualitatively indicated in previous studies, while the quantitatively understanding is still lacking.

Distributed DHWT has the similar structure as the CWT and is placed in the consumer side to level out the intermittent DHW demand. Compared to the CWT, additional benefits of reducing the network sizes and related investments can be provided by the demand-side DHWT [30]. However, similar limitations regarding the reduced storage capacity and increased return water temperature also exist. Another important issue associated with the substation design is the bypass heat loss during the low demand period, as described in the previous **Section 2.1**. Although the improved designs have lower bypass losses and return water temperatures compared to DHWT design, the storage function and related benefits are no longer available. Comparison studies of these designs can be found on the practical substation level [31] and the whole system level [32]. However, most studies only considered the passive buffer benefit of the DHWT, while the active storage benefit is often neglected when comparing different designs. Hence, it is highly relevant to investigate the applicability of alternative substation designs in the future LTDH system

The use of building thermal mass (BTM) as a storage unit has gained increasing attentions in

recent years [17]. Compared to other active storage options, the major advantage of the BTM is the simpler system design and less investment [33]. Thus, the applications of BTM in DH systems were discussed in a variety of studies [34–36]. It is pointed out that the available storage capacity is mostly influenced by the allowed thermal comfort varying range and building types [34]. BTM has also been compared with other TES technologies, such as CWT [37] and distributed heat accumulation tanks [38]. However, the main limitation of BTM is that it can only be utilized during the space heating (SH) period. Since the energy performance of buildings is planned to be continuously improved in the future, with less SH demand and shorter SH period, the storage potential of BTM will be reduced. Moreover, well insulated buildings are prone to overheating. Residents will simply open windows to cool the indoor environment and, thereby, jeopardize the opportunities for storing the heat in the building structures. These limitations of BTM in the future LTDH systems have not been fully covered in previous application studies or energy planning works.

The DH pipelines can be considered as inherent storage units, with the charging and discharging processes achieved by adjusting the temperature levels in the pipelines. Thus, this use of district heating network inertia (DHNI) has the main attractiveness of the less investment, compared to other standalone storage options [17]. Fredriksen and Werner [39] described the limited storage capacity of DHNI and pointed out that larger storage capacity is presented in bigger DH networks, with higher heat demand density. Since the temperature levels are increased, the efficiencies of heat sources are inevitably influenced. Thus, relatively more focuses are paid on the traditional middle and high temperature DH systems in dense population areas, with CHP plants as the main heat source [13,40,41]. In these scenarios, the network supply water temperature is heated up by the extracted steam from the CHP plant and, thus, has little impact on the source efficiency. It is further indicated that the combined use of CHP plant and DHNI can increase the integration of VRE such as wind power, by expanding the regulating ability of CHP plant and reducing the VRE curtailment [41,42]. However, the above conditions that are favourable for the use of DHNI, are no longer effective in future LTDH systems. Firstly, the low temperature sources, such as the heat pump and IWH, are sensitive to both the return and supply water temperature levels. It might be economically and environmentally infeasible to heat up the network for the storage benefit. Secondly, the future heating demand density will be reduced and the LTDH systems will be built with smaller sized pipes, creating less opportunities for the use of DHNI. Besides, the network heat losses are also increased during the charging period. These challenges need to be carefully evaluated when considering the future storage potential of DHNI.

3. Methods

As reported in [6], the small-scale DH systems with small heat demand densities have promising potentials to be upgraded into the LTDH systems. Therefore, a LTDH system in a small residential community in Denmark is chosen for the case study, as introduced in **Section 3.1**. The techno-economical evaluations of TES technologies are based on numerical simulations and exemplified on the case study. In order to investigate the dynamic performance of the DH system, an integrated system model is developed. Built on the basic input parameters such as the building properties and the network layout, this model can optimize the DH system from design to operation stage. Four main steps of this model and the modelling methodologies are explained in **Section 3.2.** To investigate dynamic performances of TES units, separate TES models and control strategies are developed to represent the bottom-level technical details. These models are introduced in **Section 3.3**.

3.1. Case description

The case LTDH system is located in the suburban area of Trekroner in the municipality of Roskilde in Denmark, derived from a previous study [32]. The DH system is supplying heat through a branched network to 165 single-family houses (SFHs), aggregated into 31 substations, as shown in **Fig. 2**. This case represents a common residential area in Europe with a relatively low heating demand where the benefits of the LTDH, such as the reduction of heat losses and the improved heat source efficiency, can be investigated. The heated floor area is set as 120 m^2 for each SFH and the total heated area for the case LTDH system is 19,800 m^2. The network has a total length of 1.9 km and the pipe sizes are designed by an optimization process, explained in **Section 3.2.2**. For simplicity reasons, the secondary circulation network between the substation and the end-user SFHs is represented by a 20 m long pipe, which is not shown in the figure. Several heat source options are centred in one plant in the network and their specific characteristics are introduced in **Section 4.1** as representative scenarios of the future LTDH systems. The whole year of 2019 is selected as the study period and all external input data, such as the historical weather data and energy prices, are referring to the year 2019. This year was selected since it was the most recent year with a complete set of data at the time of the study (late 2020).

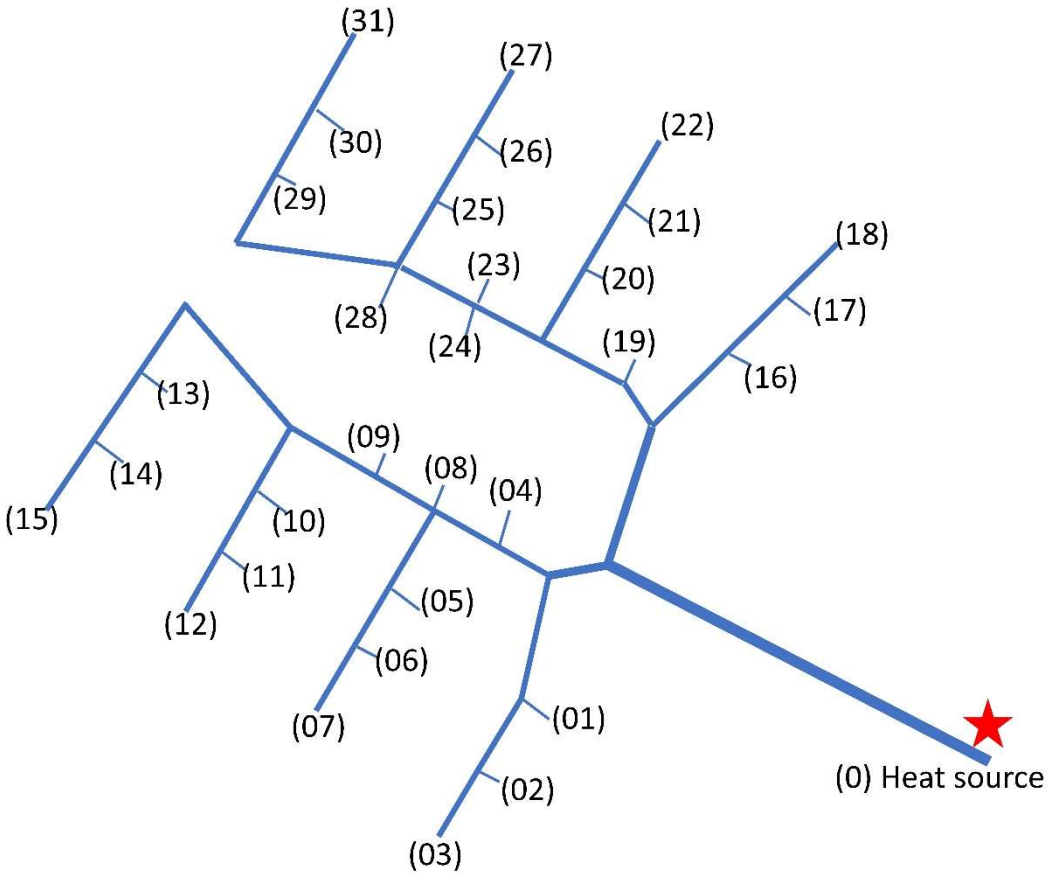

***Fig. 2**. Network layout of the case DH system, with substations and heat source marked.*

3.2. DH system model

The DH system model has four main steps, as shown in **Fig. 3**. Based on the input building properties and the weather data, the demand profiles for SH and DHW are generated by

stochastic modelling method in the first step. Then, considering the network layout and the specific design criterium for working pressures, the pipe dimensions are optimized with the objective to minimize the investment. The designs of the substations and LTDH networks are also included in the second step. For the third step, the temperature and flow dynamics of the network are modelled by the node method [43,44], with considerations of the transport delay and heat losses. Then, the operations of the TES units and the network are optimized in the fourth step. The model also has the capability of adjusting the system design according to the optimization results and, thereby, creates an iterative process between the four main steps. Based on these steps, the multi-scenarios analysis is conducted. The model is developed and performed in MATLAB.

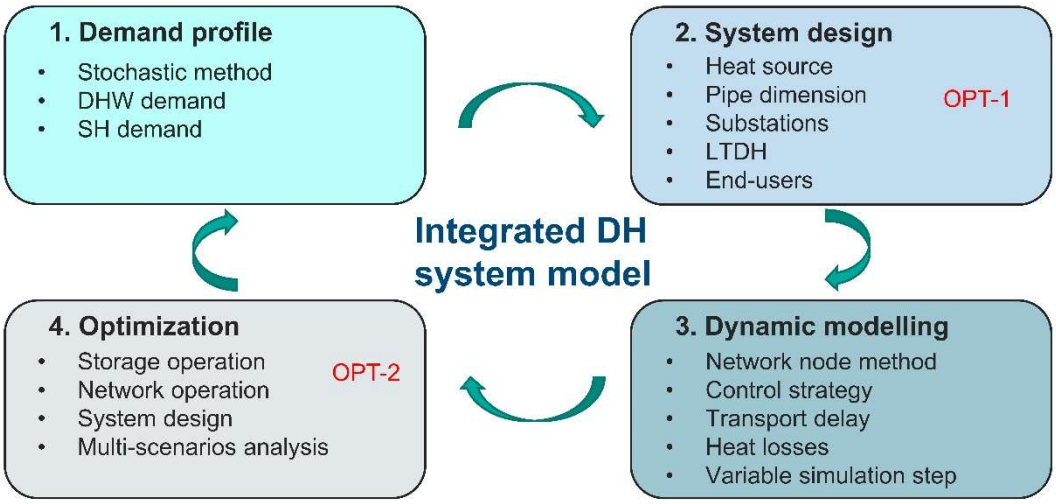

***Fig. 3**. Schematic of the main steps of the integrated DH system model developed in this study*

3.2.1. Demand profile

To simplify the computation process, the end-users connected to the same substation are aggregated into only one representative end-user. This simplification is acceptable since the end-users connected to one substation are often the buildings with similar properties and load profiles. The SH demand is calculated by a lumped capacitance building model with five resistances (5R1C), written in **Eq. (1)**, according to EN ISO 13790 [45]. In this representation, each building is considered as one thermal zone with a uniform air temperature. The specific building component properties are explained in **Section 4.2** in detail, as design scenarios in this study. The indoor setpoint temperature is 21 °C.

$$C_{eff}\frac{dT_{in}(t)}{dt} = (K_{tr} + K_{vent}) \cdot \left(T_{out}(t) - T_{in}(t)\right) + \dot{Q}_{gain} \quad (1)$$

Where the K_{tr} and K_{vent} are the total conductance for the heat transmission and ventilation part, respectively. T_{out} and T_{in} are the outdoor and indoor air temperature. $\dot{Q}_{gain}$ is the power of the total heat gains. C_{eff} is the lumped heat capacity, comprised of the capacity of indoor air, furniture and interior walls, and the effective thermal mass of the building envelope, according to EN ISO 13790 [45].

In order to consider realistic conditions of DHW usage, the draw-off profile is generated with a time-step of one minute by a stochastic modelling tool called *DHWcalc* [46], built upon

statistical methods and realistic draw-off profiles. Four categories of loads are considered in the model. For each category, the actual flowrates are sampled from a normal population with a pre-defined mean value and Gaussian distribution. The probability functions that describe the variations of the load profile during the year, weekdays, and holidays, are also defined. The daily mean DWH load for the case SFHs is randomly chosen within the range of 140 to 160 liters/day, which represents the average DHW usage for SFHs in Northern Europe [47].

Based on the above modelling approaches, the theoretical SH demand profile is calculated by the sum of the SH and DHW demand profiles. The practical issues, such as the secondary network heat losses, are illustrated in the following chapters.

3.2.2. System design

The SH part and the DHW part are designed in parallel in the substation, as shown in **Fig. 4**. To maintain low return water temperature, the SH part uses a heat exchanger with high thermal lengths, as pointed out in [20]. This design is consistent over all substations and all scenarios in this study.

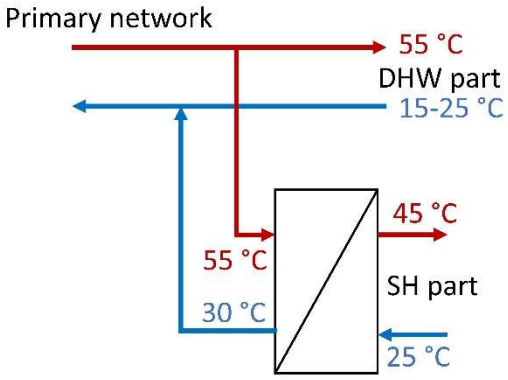

Fig. 4. *Substation design for preparing the SH demand*

With a requirement of short waiting time, the secondary circulation pipe is often filled with hot water, which causes high circulation heat losses. Compared to the SFH substation, this issue has larger impact in large substations with several end-users, such as the multi-family building substation. As mentioned above, the circulation pipe length is set as 20 m in each substation. Related heat loss for each branch pipeline is calculated according to **Eq. (2)**.

$$\dot{Q}_{B,loss} = K_B * L_B * (T_B - T_{soil}) \quad (2)$$

where K_B is the linear heat loss coefficient. L_B is the pipe length. T_{pipe} and T_{soil} are the water temperature inside the pipe and the surround soil temperature, respectively.

The case system is designed to have a fixed supply water temperature and variable flowrate. The outlet water temperature from the heat source is set as 55°C and the maximum allowable temperature drop on the primary pipeline due to heat losses is set as 5°C. The return water temperature is varying between 20 to 30°C due to the above-mentioned factors. As explained in **Section 2.1**, the comfortable bathroom design and the alternative triple-pipes design are considered to maintain the return water temperatures.

After acquiring the theoretical demand profile and network input data, the optimal pipe

dimensions are selected by the Mixed-Integer Linear Programming (MILP) process with the objective of minimal investment, written in **Eq. (3)**. Since the heat loss rate mainly depends on the temperature and pipe sizes [32], the optimization target also represents the minimal total heat loss. For each route, the maximum pressure drop limit is set as 6 bar, as is expressed in the constraint in **Eq. (4)**. The pressure drop in the branch pipe is calculated using the Darcy-Weisbach equation for circular pipes due to its simplicity and applicability in a variety of flow conditions.

$$\text{Minimize} \sum_{B} (C_B * L_B) \tag{3}$$

$$\nabla P_B = f(D_B, G_B, L_B, v, \epsilon) \leq \nabla P_{B,Max} \tag{4}$$

where C_B refers to the network construction cost of each branch pipeline, determined with the medium cost from several piping companies [48], as shown in **Appendix Table A.1**. The currency used in this study is Swedish Krona (SEK), which equals to on average 0.095 Euro for the whole year of 2019. D_B and G_B are the diameter and the design flowrate for each branch, respectively. v is the fluid viscosity and ϵ is the pipe absolute roughness height.

3.2.3. Dynamic modelling

Based on step 1 and step 2 in the integrated model, the fixed variables in the LTDH system, such as the network layout, pipe dimensions, building properties and theoretical demand profiles, are specified for following steps. In order to simulate the temperature and flow dynamics of the large DH system, an integrated node, pipe, and energy balance model is applied in this study. The basic principle is that the flow dynamics are firstly calculated by node model and the temperature dynamics and energy exchanges are updated later by the pipe model and energy balance equations.

Based on the Kirchhoff balance laws, the node model was developed in [43,44] and is since then widely applied in dynamic network models [35,40,49]. Therefore, only the general modelling approach is illustrated here, while other modelling details can be found in the cited works. The topology of the network is described by a graph approach. Each pipe is defined as a branch, with an inlet node and an outlet node. The reference flow direction is pre-defined based on the reference velocity in the branched network. The end-use substation is also simplified to a pipe that connects the supply branch and return branch, as shown in **Fig. 5**. Similar simplification is applied to the heat source. For the chosen case study, with 31 substations and one central heat source plant (see **Fig. 2**), the network model comprises of 147 branches, 118 nodes, and 31 routes. The incidence matrix, **A** (118×147), is used to express the connections between the nodes and branches. The basic element $\boldsymbol{A_{ij}}$ equals 1 or -1 if the branch *j* is leaving or entering the node i, respectively. Accordingly, the connections between the routes and branches are expressed by the route matrix, **B** (31×147), where the value 1 or -1 represents a same or inverse flow direction.

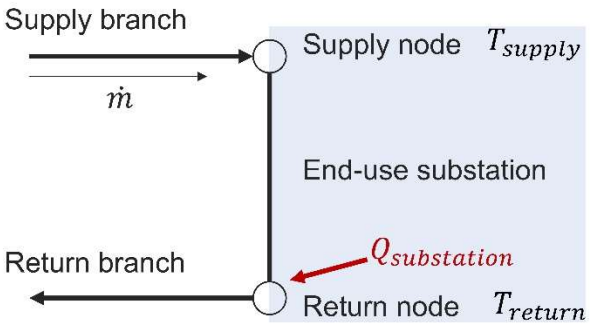

Fig. 5. Schematic diagram of the node model in end-use substations

For the entire network, the mass balance equation and pressure balance equation can be written in the matrix form in **Eqs. (5)** and **(6)**.

$$\mathbf{A}\boldsymbol{G_B} = \boldsymbol{G_{ext}} \tag{5}$$

$$\boldsymbol{B_f}\Delta\boldsymbol{H} = \mathbf{0} \tag{6}$$

where $\boldsymbol{G_B}$ is the flowrate vector for all branches. $\boldsymbol{G_{ext}}$ is the vector that expresses the mass flowrates leaving or entering the node, possibly caused by the network leakages and supplementary water in practical DH systems. $\Delta\boldsymbol{H}$ is the vector that contains the pressure drops for all branches, calculated by the Darcy-Weisbach equation as illustrated in the above section.

In order to simulate the temperature dynamics, the pipe model and energy balance equations are integrated into the network node model. Considering the heat loss and transportation delay, the outlet temperature of the branch pipe at current time step $T_{B,out}(\tau)$, can be expressed as a step response to the temperature difference between the inlet temperature and the environment temperature, written in **Eq. (7)**. A schematic diagram of the pipe model can be found in **Fig. 6**.

$$T_{B,out}(\tau) = T_{B,in}(\tau - \Delta\tau)e^{\frac{-K_p L_B}{u}} + T_e(1 - e^{\frac{-K_p L_B}{u}}) \tag{7}$$

where $T_{B,in}$ is the inlet temperature for the branch, which is also the temperature of the previous connecting node. T_e is the environment temperature for calculating the heat losses and can be regarded as soil temperature T_{soil}. $\Delta\tau$ is the transmission delay. K_p is expressed through **Eq. (8)**.

$$K_p = \frac{K_B}{A_{cross} C_p \rho} \tag{8}$$

where K_B is the linear heat loss coefficient and A_{cross} is the Cross-sectoral area of the pipes.

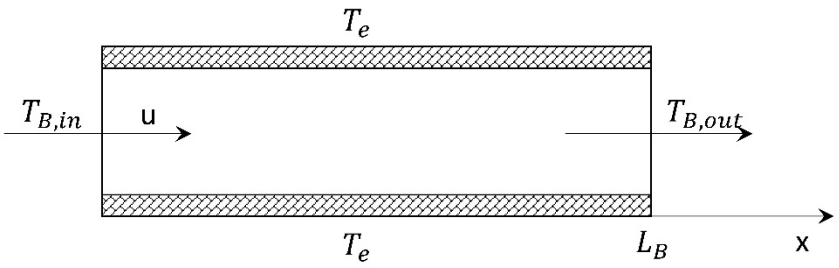

Fig. 6. Schematic diagram of the pipe model

For each node, the inlet energy equals the outlet energy. Thus, the energy balance equation for the network can be written in the matrix form as **Eq. (9)**. With the given flowrate from the node model, **Eq. (9)** has 118 unknow variables and 118 equations and, thereby, can be solved. Due to the coupling between mass and energy equations, the problem is solved by the iterative algorithm.

$$\boldsymbol{A_i R_B T_{out} - A_o R_B A_o{}^T T_N = \dot{Q}_N} \quad (9)$$

where $\boldsymbol{A_i}$ and $\boldsymbol{A_o}$ are the inflow and outflow matrix, derived from the incidence matrix $\boldsymbol{A}$ to describe the specific connections between the nodes and branches. $\boldsymbol{R_B}$ is a diagonal matrix that contains the heat capacity of branches. $\boldsymbol{T_{out}}$ is the outlet temperature of each branch, expressed by **Eq. (7)**. $\boldsymbol{T_N}$ is a vector that contains the node temperatures at current time step τ and is the unknown variable to be solved in the equation. $\dot{\boldsymbol{Q}}_{\boldsymbol{N}}$ represents the energy exchange between the node network and the exterior environment. The value could be the heating power in the source side or the substation heating demand, as shown in **Fig. 5**. As illustrated in the above **Section 3.2.2**, a fixed supply water temperature control strategy is applied in the case LTDH system. Hence, the **Eq. (9)** has 117 unknown node temperatures and 1 unknown node input power.

3.2.4. Optimization

Based on the dynamic system model, the practical demand profile and heat source supply profile can be acquired at the reference scenario, where active management is not applied. The system is operated to directly fulfil the consumers' demand. However, by utilizing the TES units, additional flexibility to shift the supply and demand profiles is implemented in the system. With a specific target of the lowest system running cost in this study, the objective of step 4 is to find the optimal operation scheme of the TES units, as well as the whole LTDH systems. The proposed model can be further improved to suit other optimization targets. The general optimization approach is explained in this section and the detailed models for the TES units are explained in the following **Section 3.3**.

Due to the non-linear characteristics of the TES units and the complex DH system, it is hard to find a global optimal result for the non-convex problem that consider the decisions of all TES units. This task becomes even more complicated in the larger system with several distributed TES units. Thus, a combined central optimization and local control strategy is applied, to simplify the optimization process while maintaining realistic characteristics of the control system. The basic idea is shown by the schematic diagram in **Fig. 7**.

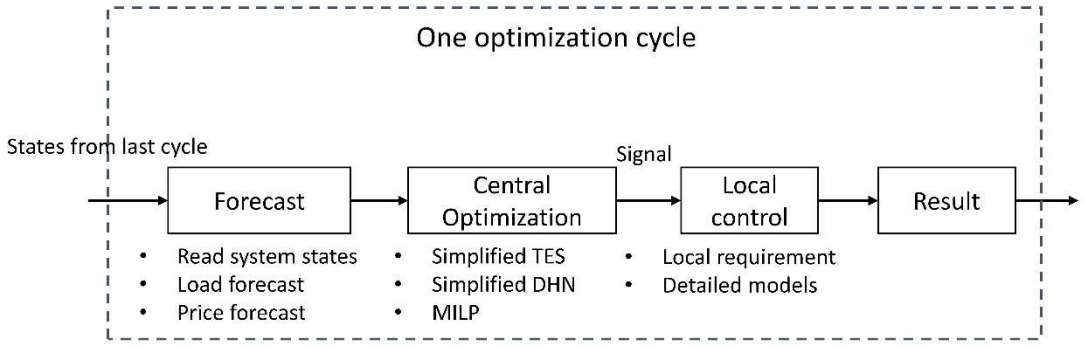

***Fig. 7**. Schematic diagram of the combined central optimization and local control strategy*

The objective function of the central optimizer is written in **Eq. (10)**. The costs of heat sources are used to represent the overall system cost, while the costs for water circulation pumps and other auxiliary equipment are omitted. As for the source cost, due to the relatively small share of the ramping and start-up cost in the small-scale LTDH system, only the energy cost is considered in this study. However, as indicated in [37], the ramping cost is a non-negligible part in city-scale DH systems with multi heat sources and, thus, has optimization potentials.

$$\min Cost_{HS} = \sum_{\tau} (Pr_{HS,\tau} * \dot{Q}_{HS,\tau}) \tag{10}$$

where $\dot{Q}_{HS,\tau}$ and $Cost_{HS}$ are the total heat supply and cost of the heat source. $Pr_{HS,\tau}$ is the operation price of the heat source at time step τ, calculated according to the efficiency and input energy cost. The specific values for the investigated heat sources are presented in detail in **Section 4.1**.

For each time step τ, the heat balance equation is expressed in **Eq. (11)**. $\dot{Q}_{TES,ch,\tau}$ and $\dot{Q}_{TES,dch,\tau}$ represent the charging and discharging power of the TES unit at time step τ, respectively. $\dot{Q}_{demand,\tau}$ is the total heating demand.

$$\dot{Q}_{HS,\tau} + \dot{Q}_{TES,dch,\tau} - \dot{Q}_{TES,ch,\tau} \geq \dot{Q}_{demand,\tau} \tag{11}$$

At time step τ, the state-of-charge of the TES unit, $SOC_{TES,\tau}$, is updated based on the state of the last time step $(\tau - 1)$, the energy exchange, and the storage heat losses $\dot{Q}_{TES,loss,\tau}$, as shown in **Eq. (12)**.

$$SOC_{TES,\tau} = SOC_{TES,\tau-1} + \dot{Q}_{TES,dch,\tau} - \dot{Q}_{TES,ch,\tau} - \dot{Q}_{TES,loss,\tau} \tag{12}$$

For TES units, there are constraints for the state-of-charge and powers, expressed in **Eqs. (13)-(15)**. These general equations are applicable for all investigated TES units in this study.

$$SOC_{TES,min} \leq SOC_{TES,\tau} \leq SOC_{TES,max} \tag{13}$$
$$0 \leq \dot{Q}_{TES,dch,\tau} \leq \dot{Q}_{TES,dch,max} \tag{14}$$
$$0 \leq \dot{Q}_{TES,ch,\tau} \leq \dot{Q}_{TES,ch,max} \tag{15}$$

To assure a reasonable use of the storage capacity, the state-of-charge of the TES unit shall return to the state at the starting point after a complete optimization cycle. In this study, the

optimization time step is one hour, and the dynamic calculation step is one minute, in accordance with the demand profile. The length of an optimization cycle is set as 5 days, considering the accuracy of forecast and the control complexity.

3.3. Thermal energy storage models

This study focuses on how the specific TES technology is adapted to the future changes, thus, the combined use of several TES units integrated within one system is currently not considered. Four typical short-term TES technologies, which are the CWT, DHNI, DHWT and BTM, are investigated separately. Together with the reference (REF) system with no TES unit, the five systems were individually simulated in all scenarios.

Although the simplified plug-flow model has been generally introduced for central optimization, the specific constraints related to each TES designs have also been considered and presented in this section together with the detailed TES models. **Table 1** summarizes the design parameters of the TES units. To make the evaluations fair, the volume of the CWT and the total volume of the distributed DHWTs are set the same. However, since the DHWT is placed in the consumer side with a 10°C inlet cold water, it has a higher storage temperature difference and a larger designed storage capacity compared to the CWT. The design parameters of the DHNI and the BTM are derived from the network structures and the building properties, illustrated in the following sections.

Table 1 *Design parameters of the TES units.*

Parameters	CWT	DHNI	DHWT	BTM
Size (m^3)	27.9	2.2	27.9	-
Storage temperature difference (K)	25	10	40	0.5
Storage capacity (kWh)	814	26.1	1302	785
Percent in average daily load (%)	14.3%	0.5%	23.0%	13.8%

3.3.1. Central water tank

The CWT has parallel connection to the heat source. A one-dimensional vertically stratified WT model with 20 layers was used , which has been commonly applied in several WT optimization studies [50,51]. For each layer, heat and mass transfer by convection and conduction are considered, as explained in **Eq. (16)**.

$$\rho V C_p \frac{\partial T}{\partial t} = A_{cross}\lambda \frac{\partial^2 T}{\partial x^2} - G\rho C_p \frac{\partial T}{\partial x} - K_{cwt,loss}A_{ext}(T - T_e) \quad (16)$$

where *x* is the vertical coordinate. Water mass flowrate G is based on a control signal of the CWT, which is consistent for all nodes. $K_{cwt,loss}$ is the heat loss factor of the CWT, which is assumed to be 0.3 (W/m^2·K)[52]. A_{cross} and A_{ext} are the cross-sectoral and exterior surface area of each layer, respectively. For simplicity, the heat losses are calculated by the temperature difference between the hot water and surrounding environment.

With the temperature sensors installed in the CWT, the temperature constraints are included in the control system to assure the thermal comfort and system performance. During the discharging period, the outlet water temperature from the CWT will gradually decrease due to inevitable mixtures of hot and cold water inside the tank. The lower limit for outlet water temperature from the top of the CWT is set as 53°C, which is 2°C lower than the design supply

water temperature. During the charging period, the upper limit for the outlet water temperature from the bottom of the CWT is set as 35°C, to keep an efficient operation of the heat sources. Hence, the state-of-charge constraints are revised based on the above limits.

3.3.2. Domestic hot water tank

The modelling approach for the DHWT is the same as the CWT. However, the DHWT only has 10 layers to suit the practical stratifications in small-sized water tank [50]. The sizes of the DHWTs in the substations are designed according to the criteria of a 150 L tank for each SFH. Hence, the total volume of the DHWTs is 27.9 m^3, which is also the design volume of the CWT. Unlike the CWT that has an extensive thermal insulation to reduce the heat loss factor to 0.3 $W/(m^2 \cdot K)$, the DHWT has less insulation due to a relatively high investment cost per volume and the extra space the insulation layer takes. Thus, the heat loss factor of the DHWT is set as 1 $W/(m^2 \cdot K)$ according to a previous field measurement study [53]. The maximum primary flowrate for a typical DHWT of 0.9 m^3 during the charging period is set as 0.18 m^3/h.

To guarantee the comfortable and safe DHW supply, a deterministic local controller is applied for the DHWT, as shown in **Fig. 8**. The controller reads the central optimization signal and decides the practical charging power P, based on the monitored temperatures at the top and the bottom of the tank. It shall be noted that, to avoid frequent charging operations, the temperature T_{top} is monitored at the second top layer. When the T_{top} is lower than 50°C, which means the storage capacity is low, the charging power is set to maximum to assure the required supply water temperature in following operations. Otherwise, if the T_{top} is higher than 51°C, the charging power is controlled according to the central optimal signal. During the idle conditions, the charging power remains the same as the previous time step. Similar as the CWT, a limit of 35°C is set for the bottom-level water temperature to maintain the required low return water temperature.

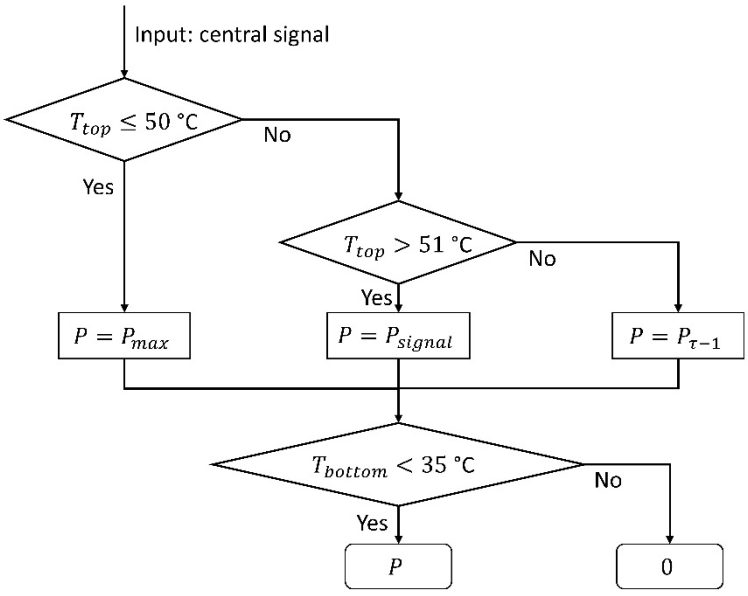

***Fig. 8**. Local control strategy for the DHWT*

3.3.3. Building thermal mass and district heating network inertia

As illustrated in **Section 3.2.1**, the SH demand is calculated by a lumped capacity building model. The available storage capacity of the BTM is decided by the effective (interior) heat

capacity of the building and the temperature deviations from the setpoint. Results from a previous field measurement of BTM in Gothenburg, Sweden [34], showed that the temperature deviation of 0.5 K above the setpoint temperature is acceptable and thus used in this study. The impact of this constrain is further analysed and discussed in **Section 5.5,** by modelling three extra temperature deviation scenarios for the BTM. Indeed, by considering only the temperature changes above the setpoint, the systems are using more energy than the reference scenario. Otherwise, if temperature changes below the setpoint are allowed, the systems tend to reduce the thermal comfort levels for lower energy consumption. This belongs to an energy-saving measure but not an active load shifting measure of the storage unit.

As for the use of DHNI as storage unit, an active temperature increase of 10 K in the transportation pipes is assumed in this study. This assumption is set the same as in previous studies (e.g. [11]), to make results comparable. However, the return water temperatures are kept the same as is illustrated in the above strategies, to avoid negative impact on the source efficiency. Thus, only half of the network storage capacity can be utilized. Based on the network layout and the optimized pipe dimensions from the model function 2, the total volume of the water in the supply transportation pipes is calculated as 2.2 m^3. Hence, the theoretical storage capacity is 26.1 kWh, which is relatively small compared to the other three TES options. Indeed, as pointed out in previous studies (e.g. [39]), the network storage capacity is larger in bigger DH networks. The state-of-charge of DHNI at time step τ, $SOC_{DHNI,\tau}$, is calculated according to the difference between the network temperature and the reference temperature. To avoid frequent changes in the network temperature, the minimum charging period is set as 5 hours, which is also in accordance with the charging period of other TES units. Then, the maximum charging power is also defined.

3.4. Analysis indicators

In order to compare the storage performances of different TES units, the number of full-load discharge cycles is defined in **Eq. (17)** in accordance with [37].

$$Full-load\ discharge\ cycles = \frac{\sum_{\tau} \dot{Q}_{TES,dch,\tau}}{SOC_{TES,design}} \quad (17)$$

During the entire year of 2019, the dynamic performances of the reference system without TES options is firstly investigated. Then, the case LTDH systems with different TES technology under different scenarios are modelled and compared. Thus, the cost-saving rate is calculated in this study to evaluate the economic benefits of the TES units, as defined in **Eq. (18)**.

$$Cost-saving\ rate = \frac{Cost_{ref} - Cost_{TES}}{Cost_{ref}} \quad (18)$$

4. Scenarios

With the aim of evaluating the applicability of TES, the performances of the LTDH system were investigated under several scenarios, which represent the possible future changes in the DH system, including the sources, substations, and end-use buildings, as shown in **Table 2**. The major changes in the substation that this study has considered are the alternative designs to reduce bypass loss, such as the triple-pipes design, which has already been introduced in the **Section 2.2**. The changes in the heat sources and the end-use buildings are also explained in this section.

Table 2 *Summary of the investigated scenarios.*

Heat sources	Substations	End-use buildings
Peak scenario	Current design with bypass loss	Current buildings
Variable renewable energy (VRE) scenario	Triple-pipes design	Future low-energy buildings
Industrial waste heat (IWH) scenario		

4.1. Heat sources

As is explained in [4], a key characteristic of the future LTDH system is the ability to recycle heat from low-temperature sources and integrate VRE sources such as solar and wind power. Thus, three typical scenarios of the heat sources are investigated and presented hereafter.

4.1.1. Peak scenario

Two baseload heat pumps and one peak boiler are installed in the modelled LTDH system. Based on the heating power duration curve in the reference scenario, the total heat capacity of the two baseload plants is designed to supply 90 % of the heat demand, while the remaining 10 % is supplied by the peak boiler. This scenario represents the current DH system where the main incentive for using the TES units comes from the reduced costs due to less usage of peak boilers.

The design parameters of the three heat sources are presented in **Table 3**. As for the two baseload heat pumps, the COP is calculated by the empirical equation with the condensing temperature and evaporating temperature [54]. The waste-water temperature at the source side is set as a stable value of 15°C. The thermodynamic efficiency is set as 0.65 and 0.55 for the source 1 and source 2, respectively. Thus, the source heat pump 1 has a higher COP than the source 2. The operation costs of the two heat pumps are the electricity bills, calculated by the hourly variable electricity prices from the NordPool spot market [55]. The average electricity price during 2019 is 1.5 SEK/kWh whereof 33% is the variable part. The reference costs under the average electricity price are also presented in **Table 3**. As for the peak boiler, considering the practical fuel cost and taxes, a fixed operation cost of 0.75 SEK/kWh_{heat}, derived from a previous study in Gothenburg [37], is applied in this study.

Table 3 *Design parameters of the heat sources in the peak scenario.*

Name	Capacity (kW)	Design COP	Reference cost (SEK/kWh_{heat})	Notation
Baseload source 1	150	4.8	0.31	Waste-water source heat pump
Baseload source 2	200	4.0	0.38	Waste-water source heat pump
Peak source 3	500	-	0.75	Wood pellets heat-only boiler

4.1.2. Variable renewable energy (VRE) scenario

VRE scenario represents the condition where the TES units are applied to increase the integration of intermittent VRE. In this scenario, 900 m^2 of crystalline solar PV panels are installed in the case system. Each panel has an area of 1.67 m^2 and a nominal system loss of 14 % [56]. There are 540 panels installed and the total power generation capacity is 178.2 kW. The hourly power generation profile at the case location is calculated by the Photovoltaic Geographical Information System-interactive (PVGIS) tools [57]. The annual power generation from the PV system is 153.3 MWh, while only 62.1 MWh can be consumed by the reference LTDH system without any TES options. The feed-in price for the residual PV power is set as 0.

The heat sources are set the same as in the peak scenario. Therefore, the optimization objective of the lowest cost is also the objective of the maximum PV integration.

4.1.3. Industrial waste heat (IWH) scenario

In contrary to the above two scenarios where power-to-heat technologies are applied, the IWH scenario uses directly exchanged waste heat from industrial processes. Therefore, the system is not connected to the electricity network and cannot integrate VRE such as solar power. However, as pointed out in several studies [4,7,15], the high efficient utilization of IWH is an important step for a sustainable future, especially in regions where IWH resources are abundant. Another characteristic of the IWH is that, the source efficiency and cost are more sensitive to return water temperature than the heat pumps [58].

In the IWH scenario, the baseload is supplied by two industrial process with a constant temperature of 60°C, which can heat the network circulation water to 55°C. The costs for the two sources are set as 0.18 SEK/kWh$_{heat}$ and 0.25 SEK/kWh$_{heat}$, respectively [58]. Due to the requirement of the heat exchanging process, maximum flowrates limits, which are calculated based on the design heating capacity, are also applied for the two sources, as shown in **Table 4**. The peak boiler is assumed to be the same as the other two scenarios. The design heating capacity is defined based on the average return water temperature of 30°C. Thus, the reduction of the return water temperature will directly increase the recovered waste heat and reduce the usage of peak boilers.

Table 4 *Design parameters of the waste heat sources in the IWH scenario.*

Name	Source (°C)	Max flowrate (t/h)	Reference cost (SEK/kWh$_{heat}$)	Design capacity (kW)	Notation
Baseload source 1	60	5.1	0.18	150	Industrial waste heat
Baseload source 2	60	6.8	0.25	200	Industrial waste heat

4.2. End-use heating demand

Another key characteristic of the future LTDH system is the improved energy performance of buildings through building renovations and newly built low-energy buildings. With less SH demand and shorter SH period, there are more variations in the demand profile, induced by the intermittent nature of the DHW demand. Besides, the storage potential of the BTM is also reduced in well-insulated buildings. To investigate the influence of the heating demand change on the TES units, two scenarios that represent the current building stock and the future low-energy building stock, are studied.

The thermal transmittances (U-values) of the building components are presented in **Table 5**. For simplicity, in all scenarios, the SFHs have the same structures and properties. A constant ventilation rate of 0.5 h^{-1} is assumed in both scenarios. However, heat recovery measures are implemented in the future low-energy buildings to further reduce the ventilation loss. The accumulated SH demand and other key performance indexes are summarized in **Table 6**.

Table 5 U-values of the building components in the current and low-energy building scenarios.

Elements	U-value (W/m^2.K)	
	Current	Low-energy
External wall	0.25	0.11
Roof	0.21	0.05
Floor	0.19	0.08
Window	1.2	0.7

Table 6 Performances of the current and low-energy buildings

Buildings	Heat loss (W/K)	Internal heat capacity (kWh/K)	Time constant (h)	SH period (h)	Heating demand (kWh/m^2)	Heating power (W/m^2)
Current	128.4	9.5	74	5715	80.6	28.2
Low-energy	67.3	9.5	141	4159	34.7	14.1

Based on the integrated DH system models, the reference systems with the current and future building stocks are simulated. A breakdown analysis of the total heat supply in two scenarios is presented in **Fig. 9**. The network loss refers to the transmission heat loss through the transportation pipes, while the bypass loss refers to the heat loss due to return water temperature requirement, as explained in **Section 3.2.2**. It can be noticed that as the SH demand decreases, the heat losses and DHW demands become increasingly important. In the future low-energy building stock, the non-space-heating period becomes longer, and a certain flowrate of hot water is required during this period, which increases the bypass loss. In general, the heat losses in two building stocks are 13% and 28% of the total heat supply, respectively.

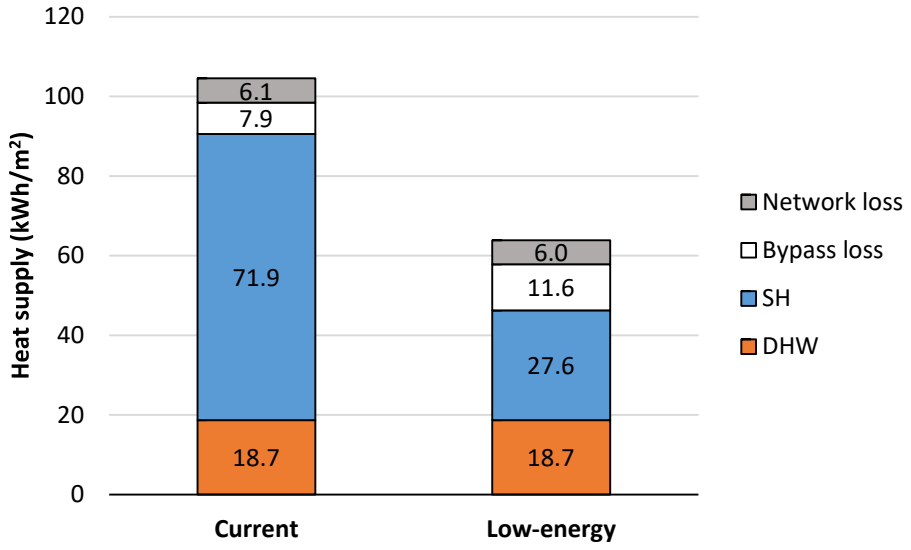

Fig. 9. Annual heat supply per unit heated area for the current and future low-energy building stocks.

5. Results

Based on the methodologies illustrated in the above sections, the scenarios designed in **Section 4** were simulated at an annual period and the results were compared. This section first shows the performance differences of TES technologies at the baseline scenario, where

current building stocks and the peak heating source scenario are applied. Then, the applicability of TES technologies under the influences of the heating sources, substation designs, and the end-use demand are analysed. Moreover, the sensitivity of the storage potentials from the BTM is further analysed and discussed.

5.1. Peak heat source scenario with the current building stock

In the peak scenario, the objective of the optimization is to reduce the use of peak boiler by shifting the demand to the baseload plants during off-peak periods. An example result of the peak-shaving effect of the CWT under typical winter days between Jan 1st and Jan 5th is shown in **Fig. 10**. Since the total heat capacity of the two baseload plants is 350 kW, the peak load above this limit, which is normally caused by the intermittent DHW demand in the morning and in the evening, is shifted to the baseloads (see the heating load differences at the 20th hour in **Fig. 10**). Yet, there is still a few hours of high-peak demand which cannot be shifted due to the limited storage capacity of the CWT. The main principle for other TES units is the same as the CWT but the practical performances and delivered benefits are quite different, which are presented in **Table 7**.

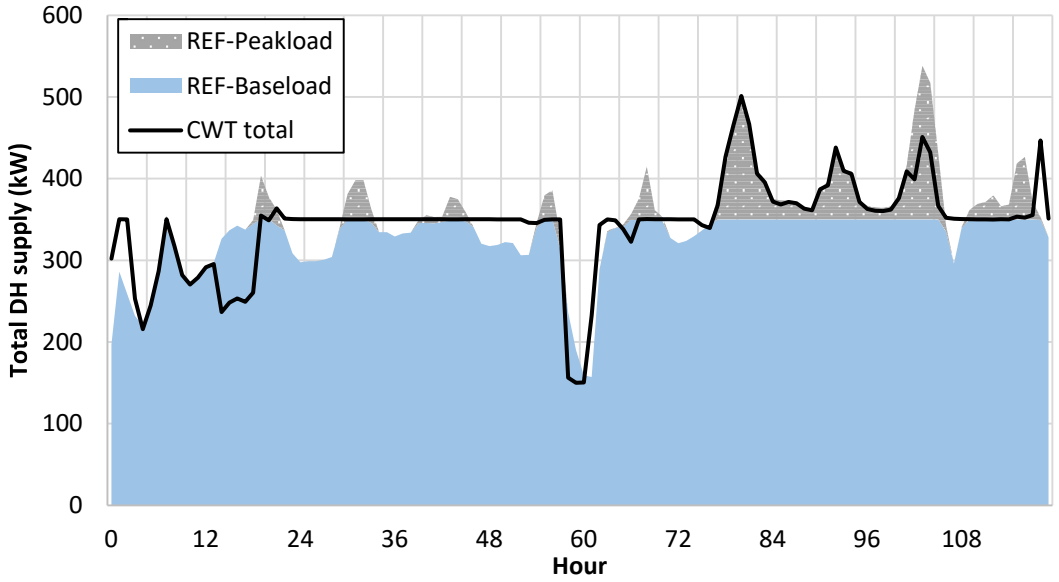

Fig. 10. Total heat supply of the REF system and the CWT system between Jan 1st and Jan 5th .

In the REF system, the peak load is 169 MWh, which is 8.2% of the total DH supply. As for the storage performances, the BTM has the lowest full-load discharge cycles because it is only used during the SH period. The CWT has the highest storage efficiency while the DHNI has the lowest, due to the network losses. The CWT also has the largest peak load reduction and thus has an annual cost-saving rate of 2%. Although the peak load reduction by the DHWT is smaller than the CWT and the BTM, the saved operation cost is the highest among the four TES units. This can be explained by the heat losses in the whole system, as shown in **Fig. 11**. Compared to the REF system, an extra TES loss is added in the four systems with TES units. The TES loss in the DHNI system is transformed to the increased network loss. Although the DHWT system has the largest TES loss, it can significantly reduce the bypass loss and thus has approximately a 4 kWh/m^2 lower heat loss compared to the other investigated systems. During the non-space-heating period, the original bypass heat loss as required to maintain the low return water temperature is collected and used in the DHWT. However, the return water temperature might be slightly increased due to inevitable mixing inside the tank. This issue is

further explained in the **Section 5.2**.

Table 7 Storage performances and annual cost-savings of the TES units.

Scenarios	Charge (kWh)	Discharge (kWh)	Efficiency (%)	Cycles (n)	Peak load (kWh)	Cost (SEK)	Cost saving rate (%)
REF	-	-	-	-	169,005	775,050	-
CWT	178,805	174,150	97%	134	-33,018	-15,374	1.98%
BTM	68,590	56,941	83%	52	-20,329	-8,256	1.07%
DHWT	363,172	317,971	88%	244	-8,066	-18,835	2.43%
DHNI	11,565	7,052	61%	267	-2,687	12,171	-1.57%

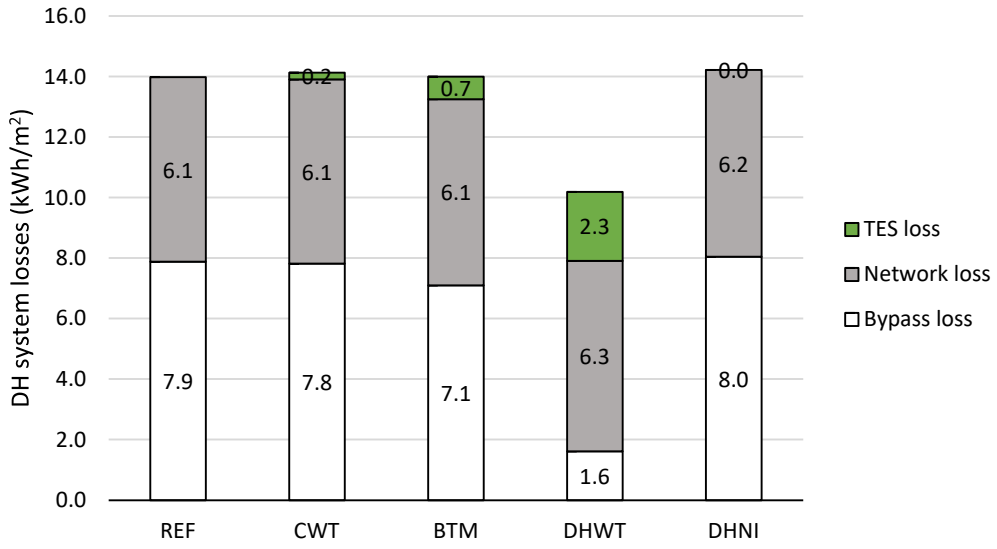

Fig. 11. Breakdown of annual heat losses in the case system with different TES units.

For the system using the DHNI as storage media, the total operation cost is even higher than the reference system without any TES options. This is mainly due to the reduced source efficiency by raising the network supply water temperature, but also due to the increased network transmission losses. The annual average COP of the two heat pumps in the DHNI system are 4.8 and 4.0, while the average COP in the REF system are 4.9 and 4.1. Besides, as shown in **Fig. 10**, the use of DHNI further increases the network loss and bypass loss due to the higher supply water temperature. Considering the relatively small storage capacity and small peak-shaving benefit, it is not economically feasible to use the DHNI in the case LTDH system. However, as indicated in the introduction, the DHNI has possible benefits in large, traditional DH system. The applicability of this technology needs to be further investigated in detail.

5.2. The influence of heat sources

The performances of TES technologies under the VRE scenario and the IWH scenario, as explained in **Section 4.1**, are compared in this Section. In the VRE scenario, the annual VRE integration rate and the cost-saving rate are presented in **Fig. 12**. The CWT has the largest potential for integrating VRE and thus has the largest cost-saving rate of 7.7%. Compared to the REF system, an additional 26 MWh of VRE is consumed by the CWT system. Although the

DHWT is designed to have a larger storage capacity than the CWT, as presented in **Table 1**, its actual capacity to integrate the excessive VRE is not proportionally larger. This can be explained by the larger heat losses and temperature restrictions from the DHWT when charged in idle state for a longer period.

The number of occasions when the state-of-charges of the TES units are higher than 70% of their design values, classified by the number of consecutive hours that each occasion has, are shown in **Fig. 13**. Due to the smaller heat loss and the control simplicity at the source side, the CWT can store energy for a longer period than the other technologies. There are 134 occasions where the CWT is used to store heat for more than 10 hours. In contrary, the DHWT is mostly used for less than 10 hours. The TES with a longer storage period can better deal with the variations in the VRE generation caused by weather conditions. The average consecutive hours for the CWT, BTM, DHWT, and DHNI are 10 h, 5.9 h, 5.8 h, and 3.1 h, respectively. Another reason for the relatively low cost-saving rate for the DHWT is that the previous benefit from the reduced bypass loss is less significant during the Summer season when VRE productions and cheap electricity prices are available.

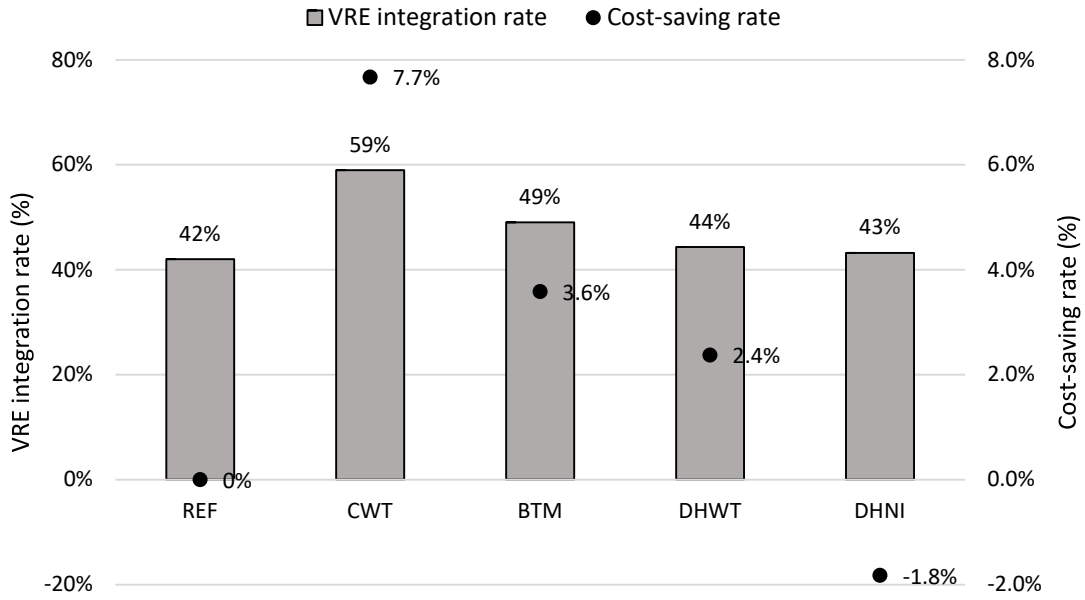

***Fig. 12**. Annual cost-saving rate and VRE integration rate in VRE scenario*

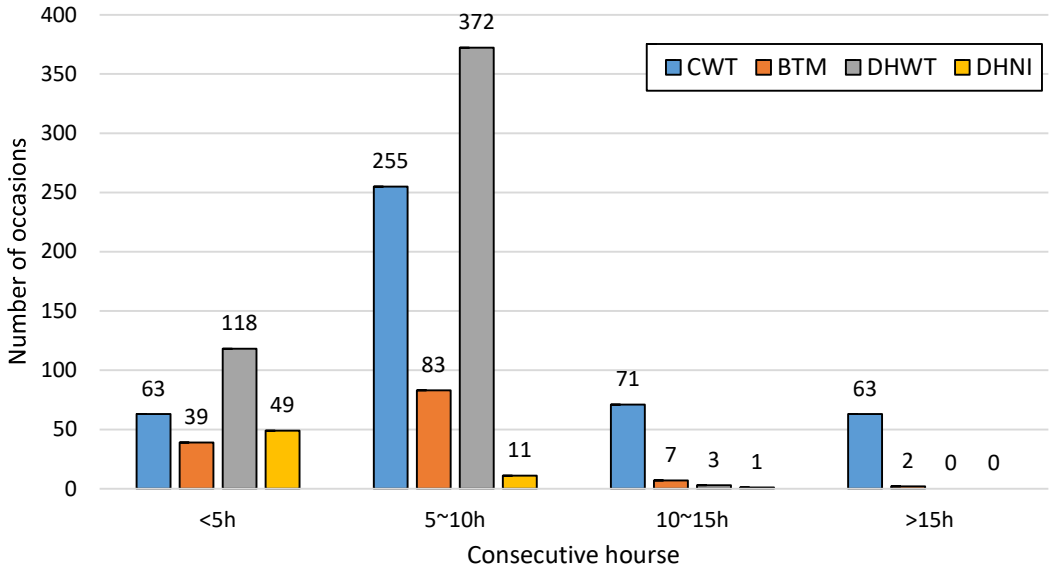

***Fig. 13**. Number of occasions for different TES options when the state-of-charges are higher than 70 % of their design values*

As for the IWH scenario, the efficiency of IWH resources is more sensitive to the return water temperature compared to the heat pumps. The daily average return water temperatures of the REF, CWT, and DHWT systems are shown in **Fig. 14**. To make the expression clear, the temperatures of the BTM and DHNI systems are not plotted. Due to strict bypass design and control, the REF system has the lowest return water temperature among the investigated systems. The return water temperatures are gradually increased from Summer to Winter, under the influence of the SH demand. The use of CWT slightly increases the temperature since a part of the return water is inevitably mixed with hot water inside the tank. However, due to the control complexities for distributed small tanks, the DHWT system has the highest return water temperature, which is about 2.8°C higher than the average temperature of the REF system. This phenomenon is more prominent during non-space-heating period. The instantaneous DHW demand is transformed into regularly controlled demand in hot water tanks. From this process, the bypass loss is significantly reduced but the return water temperature is also increased. This characteristic of the DHWT system is also reported in [20,30]. To overcome this problem, stricter controls of the return water temperatures, such as the constraints in **Eqs. (13)** to **(15)**, are needed.

As a consequence, the efficiencies of the heat sources are influenced. The key system performance indexes such as the annual usage of the peak boiler are summarized in **Table 8**. In the DHWT system, the recovered waste heat from industrial processes is reduced and the peak boiler usage is therefore increased. Indeed, the DHWT system has even higher peak boiler usage than the REF system. Thus, unlike in the peak scenario, the cost-saving rate of the DHWT is lower than the CWT and BTM systems.

Table 8 Average return water temperature, peak boiler usage and operation costs of the case system in IWH scenario.

Scenarios	Return temperature (°C)	IWH usage (MWh)	Peak boiler usage (MWh)	Cost (SEK)	Annual cost-saving rate (%)
REF	25.8	1,795	276	581,688	-
CWT	26.2	1,810	264	-7,340	1.26%
BTM	25.9	1,818	255	-10,426	1.79%
DHWT	28.6	1,696	294	-3,363	0.58%
DHNI	25.8	1,747	327	26,631	-4.58%

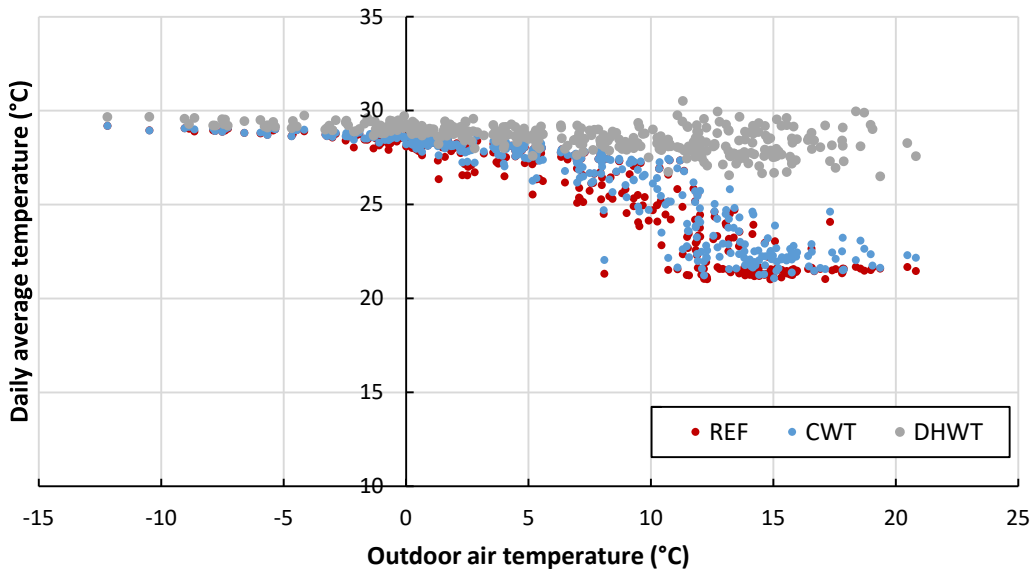

Fig. 14. Daily average return water temperature of the REF, CWT, and DHWT systems in the IWH scenario.

5.3. The influence of substation design

The three heat source scenarios were also simulated with the triple-pipes design to identify the influence of this alternative design on the TES performances. **Fig. 15** shows the comparisons of cost-savings for different substation designs. The results indicate that the benefit of the DHWT is heavily influenced by the substation design while the benefits of the CWT and the BTM are only slightly changed. With the triple-pipes design, there is no bypass loss and the cost-savings of the DHWT can be even negative due to the reasons such as the high heat loss, explained in above sections. Thus, in the future LTDH systems, the choice between the DHWT design and the triple-pipes design is required. The heat losses in the systems with the triple-pipes design are presented in **Table 9**, based on the peak source scenario. Compared to the heat losses presented in **Fig. 11**, the network loss is slightly increased due to the losses from the third pipes. However, overall heat losses are reduced.

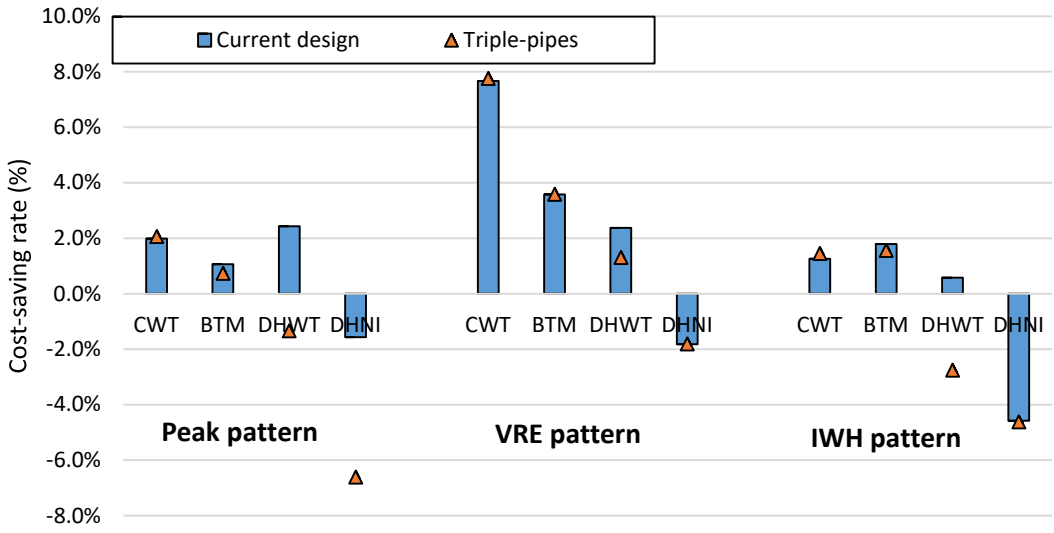

***Fig. 15**. Annual cost-savings for the systems with the current substation design and the triple-pipes design*

***Table 9** Heat losses in the systems with the triple-pipes design, under peak scenario*

Cases	Network loss (kWh/m^2)	TES loss (kWh/m^2)	Total (kWh/m^2)	Loss rate (%)
REF	7.7	0.0	7.7	7.8%
CWT	7.6	0.2	7.9	8.0%
BTM	7.6	0.5	8.1	8.2%
DHWT	6.6	2.3	8.9	8.9%
DHNI	10.3	0.0	10.3	9.8%

5.4. The influence of SH demand

The annual cost-savings of the investigated systems with the future low-energy building stock are presented in **Fig. 16**. Due to the infeasible usage of DHNI as proved in the above sections, the results for the DHNI are not presented. From the current building stock to the future low-energy buildings, the cost-saving rates for all systems are increased to some levels. However, for the system with BTM, the cost-saving rate is only slightly changed because there is less storage potential from the better insulated buildings. The use of BTM is directly influenced by the space heating demand. In the current building stock, there are totally 150 days, where the BTM is actively used. In the future low-energy building stock, since the SH demand is greatly reduced, BTM is only used in 100 days. Thus, the number of full-load discharge cycles in the low-energy building stock scenario is approximately half of the number in current scenario, as shown in **Fig. 17**.

The system with the DHWT has the largest difference between the two building stock scenarios. This is also explained by the bypass losses. In the future low-energy building stock, due to the reduced demand for SH, the bypass loss becomes higher in the whole system, as shown in **Fig. 9**. Indeed, the annual bypass loss is 11.6 kWh/m^2, which is around 18% of the total heat supply. The benefit of reduced bypass loss can even to some extent offset the extra cost related to the DHWT in the IWH scenario, with the annual cost-saving rate reached 6.6% in the low-energy building stock. Thus, the original DHWT design has more benefits while the DHWT with the triple-pipes design has basically negative cost-savings. Compared to the peak

scenario, the influence of bypass loss is less significant in the VRE scenario, as illustrated in the **Section 5.2**.

Comparing the four TES technologies, the use of CWT is most favourable in the VRE scenario, with an annual cost-saving rate of 15.1 % in the future low-energy buildings.

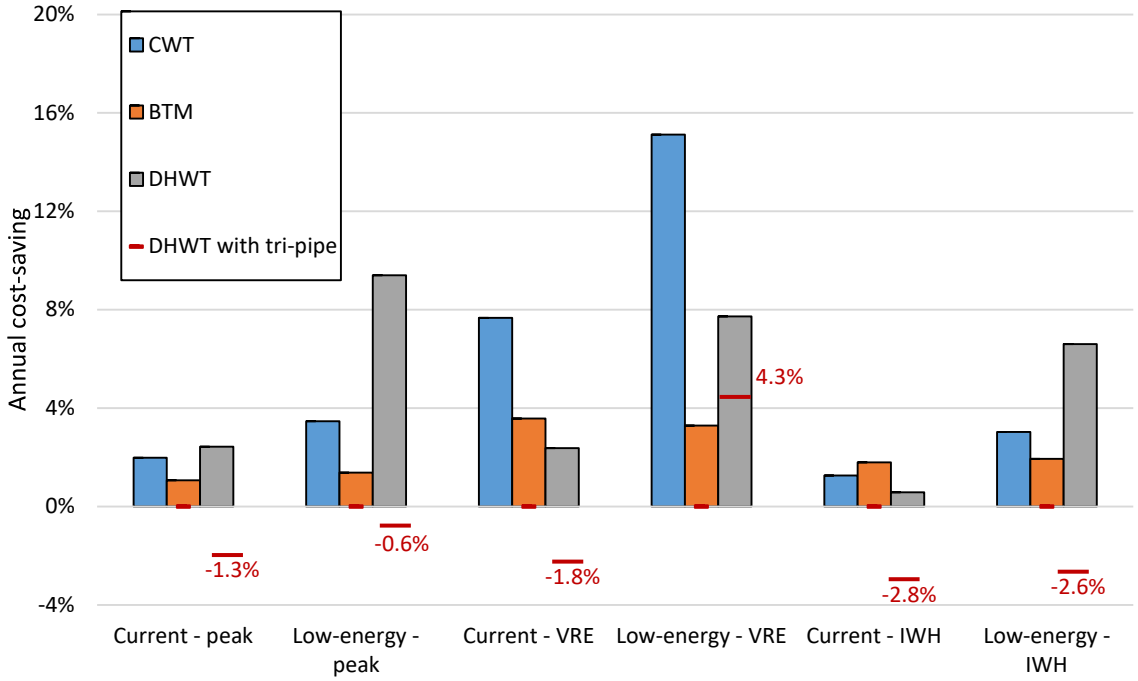

Fig. 16. Annual cost-savings under different heat source scenarios and building stock scenarios

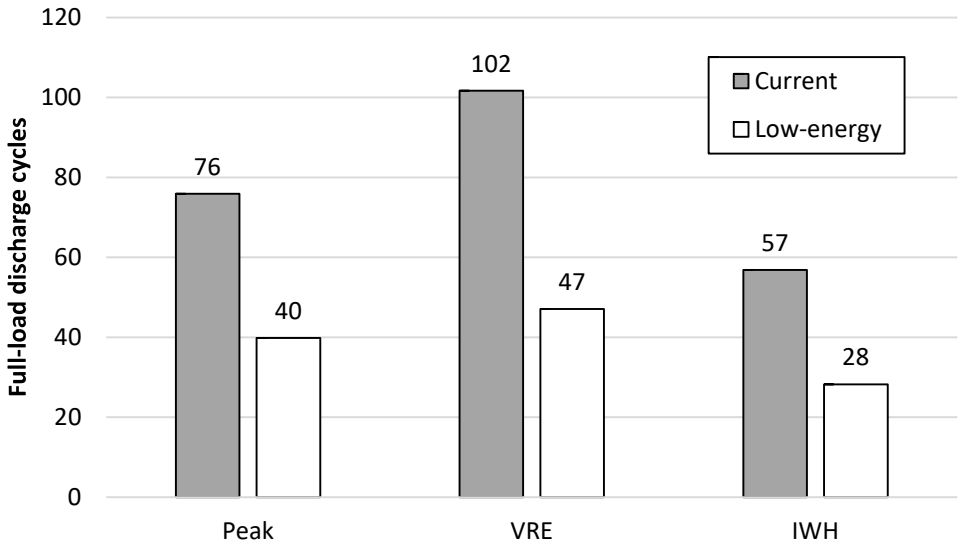

Fig. 17. Full-load discharge cycles of the BTM in current and low-energy building stocks

5.5. Sensitivity analysis

In the above analysis, a 0.5 K temperature deviation is considered for using the BTM, as a conservative evaluation of the residents' acceptance for temperature changes, according to the field measurement [34]. However, the storage potential can still be further increased by allowing larger temperature deviations. Thus, three scenarios, with deviations of 1 K, 1.5 K

and 2 K, are modelled and compared, as shown in **Fig. 18**.

The benefits of using the BTM is not linearly related to the temperature deviations. Little benefits are found from the increased use of the BTM in the peak heat source scenario since the peak load is mainly induced by the instantaneous DHW demand instead of the SH demand. A temperature increase of more than 1 K can even lead to negative impact due to the increased space heating demand. In contrary, in the VRE scenario, the larger temperature deviation increases the storage potential and, thus, increases the VRE integration and enlarges the benefits. However, similar as the case in the peak scenario, the benefit of the BTM only increases slightly when the temperature deviation is larger than 1 K. Therefore, in the investigated cases, a suitable choice of the temperature deviation level would be 1 K, to maximize the benefits while maintaining an acceptable thermal comfort range.

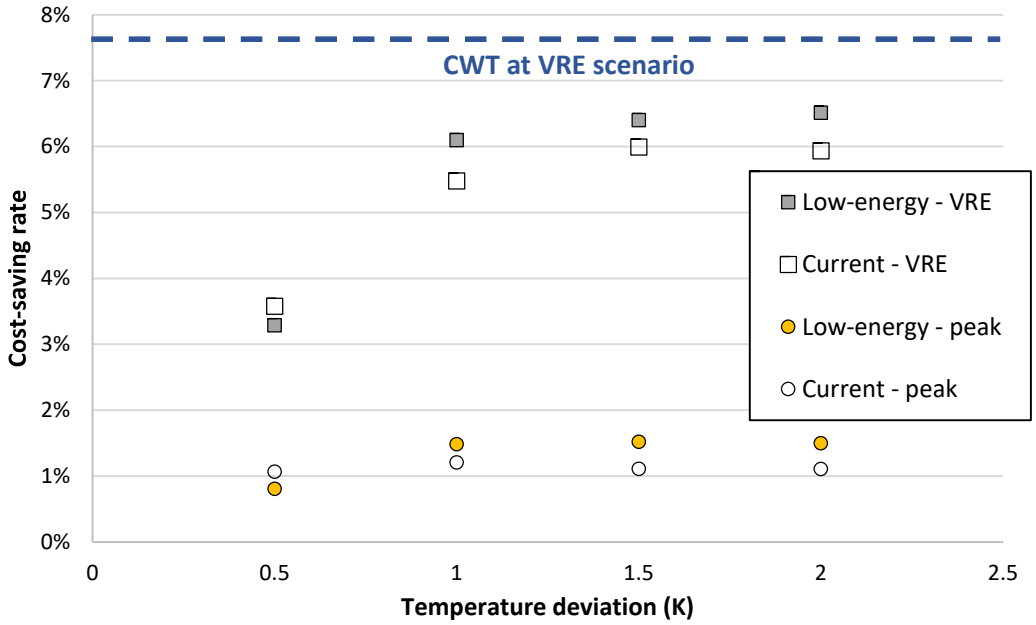

Fig. 18. Sensitivity analysis of the temperature deviations for using the BTM

As for the use of the DHWT, a prominent limitation is the high thermal loss due to a poor insulation. However, as the technology develops, there is possibility of a cheaper and space-saving thermal insulation, with less heat loss factor, for the small-scale DHWTs in the future. Thus, the sensitivity of the heat loss factors is analysed on different scenarios and shown in **Fig. 19**. It is apparent that the benefit of the DHWT becomes larger when the heat loss factor is reduced. As explained in **Section 5.1**, since the major benefit of the DHWT comes from the reduction of bypass loss, the DHWT has similar cost-saving rates in the peak scenario and VRE scenario. Compared to the CWT, the DHWT still has less potential for integrating the VRE, even though the heat losses can be reduced by improved thermal insulations.

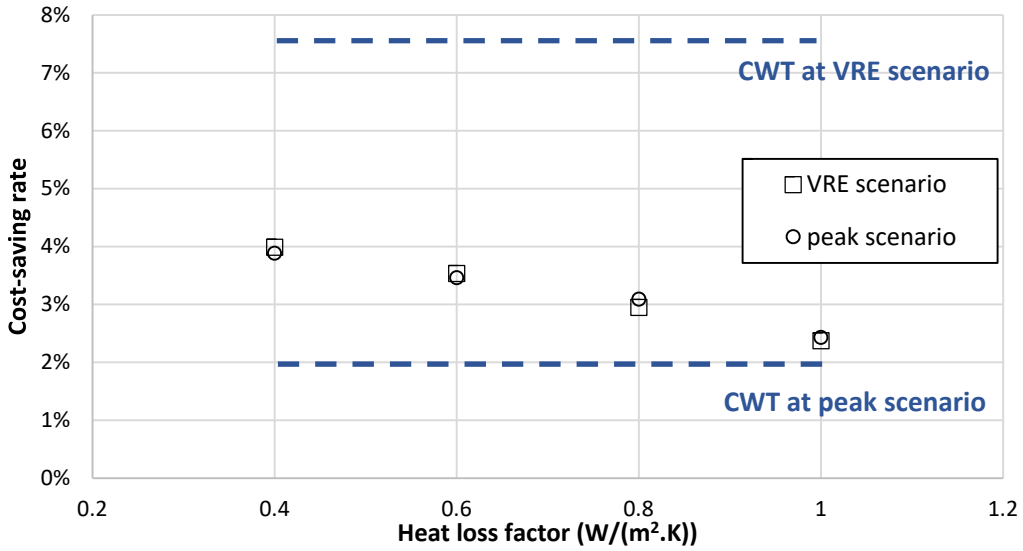

***Fig. 19**. Sensitivity analysis of the heat loss factors of the DHWT*

6. Discussion

6.1. Applicability of TES technologies in the future

Based on the simulated results from all the scenarios in this study, a performance map of TES technologies under the future DH changes is shown in **Fig. 20**. Possible transitions from the current heating system to the future heating system can be classified into changes in three parts as explained in **Section 4**, of which the changes in the end-use demand side and the changes in the heat source supply side are considered as two main variables during the analysis. The central idea is that the future design and usage of TES technologies should be highly in accordance with the characteristics of the future energy systems. Several transitions for the TES applications are summarized as follows:

①: Major changes take place in the end-use buildings. This transition is likely to happen in middle and large cities where the VRE resource is scarce. As the renovation works are conducted in the buildings, changes in the substations are also needed. As discussed in **Section 5.3**, both DHWT design and the triple-pipes design can reduce the unnecessary bypass loss and increase system efficiency, but only one option is enough. The former design requires more strict control of the water temperature, and the latter design requires renovations of the pipe system.

②: Major changes take place in the heat sources, with increased VRE generations. This transition refers to the DH systems where heat and power networks are connected through heat pumps or CHP plants. Comparing the TES technologies, central and compact unit with small heat loss rate and high control flexibility, such as the CWT in this study, can better balance the supply and demand and, thus, has the largest potential for applications.

③: The share of renewable energy is also increased in this transition but, unlike transition ②, the DH systems have less interactions with the power system. Possible heating sources include the direct use of industrial waste heat and biomass boilers. The prospective benefits for TES technologies are mainly related to the peak load reduction and smooth system operation, which can be lower than the benefits in transitions ① and ②. As shown in **Fig. 16**, the differences between TES options are relatively small.

④: A direct transition towards the future LTDH system, which is likely to happen in newly built districts with good building thermal insulation and abundant VRE production. A combination of the supply side central TES option and the demand side measures is required.

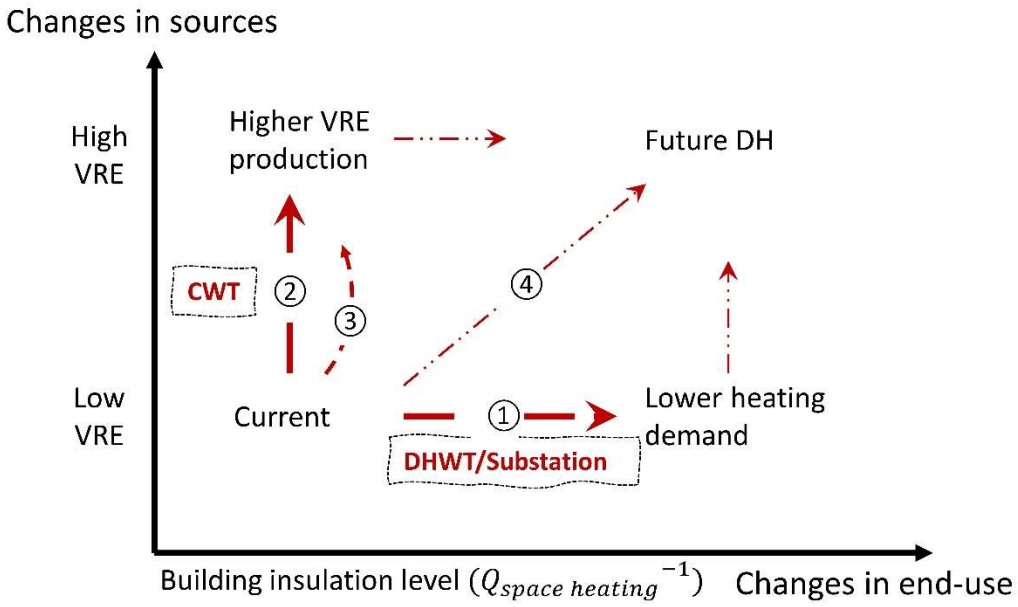

***Fig. 20**. Performance map of the TES technologies under the future changes of the DH systems*

6.2. Limitations

The results of this study are based on a small-scale LTDH system in the case residential community, with 165 SFHs. This case represents the typical small community in the suburban or rural area in the Northern Europe. However, the conditions in large DH systems in urban area can be quite different, with more differences between end-users and more control complexities. It is also indicated in the Introduction part that there are potentials for the use of DHNI in traditional high-temperature DH systems. Besides, in the multi-sources DH systems, the costs related to the start-ups and the ramping of heat sources are important parts in the total operation cost and thereby become one of the main incentives to install TES units [37]. Considering the above aspects, the applications of TES technologies in the large DH systems shall be further examined. Together with the results in this study, a better understanding about the roles of TES technologies in the future can be acquired.

As is mentioned in the above **Section 6.1**, the analysis indicators used in this study are focusing on the TES unit itself, such as the discharge cycles and cost-saving rate. However, TES units also has important influences on the sizes of the network and heating source, as indicated in [59]. The benefits of reduced investments in the pipes and heat sources are not considered in this study.

7. Conclusion

With the aim of evaluating the applicability of TES technologies in the future LTDH systems, a case LTDH system was simulated and compared under various representative scenarios of the future changes, including the changes in the source side, network side, and the end-use

demand side. For each scenario, this study compared the operating performances and cost-savings of four typical short-term TES technologies. Considering the growing need in the transitions from the current energy systems to the future sustainable and smart energy systems, conclusions on how the specific TES technologies are adapted to the future systems are summarized as follows:

1) The results show that the four TES technologies can balance the heat supply and demand to some extent. Besides the benefits of load shifting, the use of distributed domestic hot water tanks (DHWTs) can also reduce the bypass loss in the substations and, thereby, has the largest cost-savings in the current peak source scenario. It is proved that the triple-pipes design in the substation can also solve this issue, implying a choice between the two substation designs.

2) Due to the relatively small heat loss and the control flexibility, the central water tank (CWT) is able to store heat for longer period than the other TES technologies and is thus suitable for integrating the VRE in the future. In contrary, since the energy price is basically low during the summer when the VRE is abundant, the previous benefits associated with the DHWT for reducing the bypass loss is less significant.

3) As the space heating demand goes down in the future, there is less storage potential from the use of building thermal mass (BTM). Since the space-heating period is reduced, the BTM is only used for less than 100 days in the future low-energy buildings. However, the bypass loss becomes even more prominent during the non-space-heating period, calling for measures in the demand side.

4) The use of district heating network inertia (DHNI) as storage unit is proved to be infeasible in all scenarios based on the case LTDH systems. The main reason is that the heat source efficiency is significantly reduced by raising the supply water temperature. Besides, since the storage capacity of the networks in small-scale systems is as small as less than 1% of the daily heat load, the proposed benefits cannot even offset the increased network heat losses.

Finally, based on the results from all analysed scenarios, it is pointed out that the designs and applications of TES technologies shall be designed in accordance with the characteristics of the future LTDH systems to avoid under-estimations or over-estimations of the roles of TES technologies.

Acknowledgement

This work was supported by the Swedish Research Council for Environment, Agricultural Sciences and Spatial Planning (FORMAS) [Grant No. 2018-01228].

Appendix

Table A.1 *Linear heat loss coefficient and network construction cost* [48].

Nominal diameter	Linear heat loss coefficient (W/m·K)		Cost
	Supply	Return	(SEK/m)
DN12	0.095	0.040	1200
DN16	0.100	0.045	1500
DN20	0.105	0.054	1769
DN25	0.110	0.071	1909
DN32	0.115	0.127	2002
DN40	0.120	0.140	2149
DN50	0.125	0.143	2416
DN65	0.130	0.150	2608
DN80	0.135	0.160	2958
DN100	0.140	0.170	3189
DN125	0.145	0.180	3523
DN150	0.150	0.190	4082

Reference

[1] Lund H. Renewable energy strategies for sustainable development. Energy 2007;32:912–9. https://doi.org/10.1016/j.energy.2006.10.017.

[2] Mathiesen B V., Lund H, Connolly D, Wenzel H, Ostergaard PA, Möller B, et al. Smart Energy Systems for coherent 100% renewable energy and transport solutions. Appl Energy 2015;145:139–54. https://doi.org/10.1016/j.apenergy.2015.01.075.

[3] Intergovernmental Panel on Climate Change, editor. Summary for Policymakers. Clim. Chang. 2013 – Phys. Sci. Basis Work. Gr. I Contrib. to Fifth Assess. Rep. Intergov. Panel Clim. Chang., Cambridge: Cambridge University Press; 2014, p. 1–30. https://doi.org/DOI: 10.1017/CBO9781107415324.004.

[4] Lund H, Werner S, Wiltshire R, Svendsen S, Eric J, Hvelplund F, et al. 4th Generation District Heating (4GDH) Integrating smart thermal grids into future sustainable energy systems. Energy 2014;68:1–11. https://doi.org/10.1016/j.energy.2014.02.089.

[5] Lund H, Østergaard PA, Chang M, Werner S, Svendsen S, Sorknæs P, et al. The status of 4th generation district heating: Research and results. Energy 2018;164:147–59. https://doi.org/10.1016/j.energy.2018.08.206.

[6] Connolly D, Lund H, Mathiesen B V., Werner S, Möller B, Persson U, et al. Heat roadmap Europe: Combining district heating with heat savings to decarbonise the EU energy system. Energy Policy 2014;65:475–89. https://doi.org/10.1016/j.enpol.2013.10.035.

[7] Lund H, Østergaard PA, Connolly D, Mathiesen BV. Smart energy and smart energy systems. Energy 2017;137:556–65. https://doi.org/10.1016/j.energy.2017.05.123.

[8] Guelpa E, Verda V. Thermal energy storage in district heating and cooling systems: A review. Appl Energy 2019;252:113474. https://doi.org/10.1016/j.apenergy.2019.113474.

[9] Hewitt NJ. Heat pumps and energy storage - The challenges of implementation. Appl

Energy 2012;89:37–44. https://doi.org/10.1016/j.apenergy.2010.12.028.

[10] David A, Mathiesen BV, Averfalk H, Werner S, Lund H. Heat Roadmap Europe: Large-scale electric heat pumps in district heating systems. Energies 2017;10:1–18. https://doi.org/10.3390/en10040578.

[11] Lund H. Renewable heating strategies and their consequences for storage and grid infrastructures comparing a smart grid to a smart energy systems approach. Energy 2018;151:94–102. https://doi.org/10.1016/j.energy.2018.03.010.

[12] Lund H, Østergaard PA, Connolly D, Mathiesen BV. Energy storage and smart energy systems. Energy 2017;137:556–65. https://doi.org/10.1016/j.energy.2017.05.123.

[13] Salpakari J, Mikkola J, Lund PD. Improved flexibility with large-scale variable renewable power in cities through optimal demand side management and power-to-heat conversion. Energy Convers Manag 2016;126:649–61. https://doi.org/10.1016/j.enconman.2016.08.041.

[14] Child M, Bogdanov D, Breyer C. The role of storage technologies for the transition to a 100% renewable energy system in Europe. Energy Procedia 2018;155:44–60. https://doi.org/10.1016/j.egypro.2018.11.067.

[15] Persson U, Möller B, Werner S. Heat Roadmap Europe: Identifying strategic heat synergy regions. Energy Policy 2014;74:663–81. https://doi.org/10.1016/j.enpol.2014.07.015.

[16] Gadd H, Werner S. Thermal energy storage systems for district heating and cooling. Woodhead Publishing Limited; 2015. https://doi.org/10.1533/9781782420965.4.467.

[17] Hennessy J, Li H, Wallin F, Thorin E. Flexibility in thermal grids: A review of short-term storage in district heating distribution networks. Energy Procedia 2019;158:2430–4. https://doi.org/10.1016/j.egypro.2019.01.302.

[18] Enescu D, Chicco G, Porumb R, Seritan G. Thermal energy storage for grid applications: Current status and emerging trends. Energies 2020;13. https://doi.org/10.3390/en13020340.

[19] Zheng W, Hennessy JJ, Li H. Reducing renewable power curtailment and CO2 emissions in China through district heating storage. Wiley Interdiscip Rev Energy Environ 2020;9:1–11. https://doi.org/10.1002/wene.361.

[20] Averfalk H, Werner S. Novel low temperature heat distribution technology. Energy 2018;145:526–39. https://doi.org/10.1016/j.energy.2017.12.157.

[21] Schmidt D, Kallert A, Blesl M, Svendsen S, Li H, Nord N, et al. Low Temperature District Heating for Future Energy Systems. Energy Procedia 2017;116:26–38. https://doi.org/10.1016/j.egypro.2017.05.052.

[22] Yang X, Li H, Svendsen S. Energy, economy and exergy evaluations of the solutions for supplying domestic hot water from low-temperature district heating in Denmark. Energy Convers Manag 2016;122:142–52. https://doi.org/10.1016/j.enconman.2016.05.057.

[23] Schmidt D, Kallert A, Blesl M, Li H, Svendsen S, Nord N, et al. Annex TS1 Low Temperature District Heating for Future Energy Systems - Final report - Future low temperature district heating design guidebook. 2017.

[24] Dalla Rosa A, Li H, Svendsen S. Method for optimal design of pipes for low-energy district heating, with focus on heat losses. Energy 2011;36:2407–18. https://doi.org/10.1016/j.energy.2011.01.024.

[25] Yang X. Supply of domestic hot Water at comfortable temperatures by low-temperature district heating without risk of Legionella. 2016.

[26] Nielsen JE. IEA-SHC Task 45: Large solar heating/cooling systems, seasonal storage, heat pumps. Energy Procedia 2012;30:849–55. https://doi.org/10.1016/j.egypro.2012.11.096.

[27] Verda V, Colella F. Primary energy savings through thermal storage in district heating networks. Energy 2011;36:4278–86. https://doi.org/10.1016/j.energy.2011.04.015.

[28] Eriksson R. Heat storages in Swedish district heating systems. An analysis of the installed thermal energy storage capacity 2016:40.

[29] Wit J de. Heat Storages for CHP Optimisation. PowerGen Eur 2007 2007:1–18.

[30] Li H, Svendsen S. Energy and exergy analysis of low temperature district heating network. Energy 2012;45:237–46. https://doi.org/10.1016/j.energy.2012.03.056.

[31] Yang X, Li H, Svendsen S. Evaluations of different domestic hot water preparing methods with ultra-low-temperature district heating. Energy 2016;109:248–59. https://doi.org/10.1016/j.energy.2016.04.109.

[32] Tol HI, Svendsen S. Improving the dimensioning of piping networks and network layouts in low-energy district heating systems connected to low-energy buildings: A case study in Roskilde, Denmark. Energy 2012;38:276–90. https://doi.org/10.1016/j.energy.2011.12.002.

[33] Hedegaard K, Mathiesen BV, Lund H, Heiselberg P. Wind power integration using individual heat pumps - Analysis of different heat storage options. Energy 2012;47:284–93. https://doi.org/10.1016/j.energy.2012.09.030.

[34] Kensby J, Trüschel A, Dalenbäck JO. Potential of residential buildings as thermal energy storage in district heating systems - Results from a pilot test. Appl Energy 2015;137:773–81. https://doi.org/10.1016/j.apenergy.2014.07.026.

[35] Gu W, Wang J, Lu S, Luo Z, Wu C. Optimal operation for integrated energy system considering thermal inertia of district heating network and buildings. Appl Energy 2017;199:234–46. https://doi.org/10.1016/j.apenergy.2017.05.004.

[36] Guelpa E, Barbero G, Sciacovelli A, Verda V. Peak-shaving in district heating systems through optimal management of the thermal request of buildings. Energy 2017;137:706–14. https://doi.org/10.1016/j.energy.2017.06.107.

[37] Romanchenko D, Kensby J, Odenberger M, Johnsson F. Thermal energy storage in district heating: Centralised storage vs. storage in thermal inertia of buildings. Energy Convers Manag 2018;162:26–38. https://doi.org/10.1016/j.enconman.2018.01.068.

[38] Vanhoudt D, Claessens BJ, Salenbien R, Desmedt J. An active control strategy for district heating networks and the effect of different thermal energy storage configurations. Energy Build 2018;158:1317–27. https://doi.org/10.1016/j.enbuild.2017.11.018.

[39] Werner S. District heating and cooling 2013.

[40] Zheng J, Zhou Z, Zhao J, Wang J. Integrated heat and power dispatch truly utilizing thermal inertia of district heating network for wind power integration. Appl Energy 2018;211:865–74. https://doi.org/10.1016/j.apenergy.2017.11.080.

[41] Wang J, Zhou Z, Zhao J, Zheng J. Improving wind power integration by a novel short-term dispatch model based on free heat storage and exhaust heat recycling. Energy 2018;160:940–53. https://doi.org/10.1016/j.energy.2018.07.018.

[42] Li Z, Wu W, Shahidehpour M, Wang J, Zhang B. Combined heat and power dispatch considering pipeline energy storage of district heating network. IEEE Trans Sustain Energy 2016;7:12–22. https://doi.org/10.1109/TSTE.2015.2467383.

[43] Benonysson A, Bøhm B, Ravn HF. Operational optimization in a district heating system. Energy Convers Manag 1995;36:297–314.

[44] Zhao H. Analysis, modelling and operational optimization of district heating systems, 1995.

[45] de Normalización CE. EN ISO 13790: Energy Performance of Buildings: Calculation of Energy Use for Space Heating and Cooling (ISO 13790: 2008). CEN; 2008.

[46] Jordan U, Vajen K. Realistic domestic hot-water profiles in different time scales. Rep Sol Heat Cool Progr Int Energy Agency (IEA-SHC)Task 2001;26:1–18.

[47] SFS-EN 15316-3-1. Heating systems in buildings — Method for calculation of system energy requirements and system efficiencies — Part 3-1 Domestic hot water systems , characterisation of needs (tapping requirements) 2006:1–20.

[48] Best I, Orozaliev J, Vajen K. Economic comparison of low-temperature and ultra-low-temperature district heating for new building developments with low heat demand densities in Germany. Int J Sustain Energy Plan Manag 2018;16:45–60. https://doi.org/10.5278/ijsepm.2018.16.4.

[49] Guelpa E, Sciacovelli A, Verda V. Thermo-fluid dynamic model of large district heating networks for the analysis of primary energy savings. Energy 2019;184:34–44. https://doi.org/10.1016/j.energy.2017.07.177.

[50] Alimohammadisagvand B, Jokisalo J, Kilpeläinen S, Ali M, Sirén K. Cost-optimal thermal energy storage system for a residential building with heat pump heating and demand response control. Appl Energy 2016;174:275–87. https://doi.org/10.1016/j.apenergy.2016.04.013.

[51] Renaldi R, Kiprakis A, Friedrich D. An optimisation framework for thermal energy storage integration in a residential heat pump heating system. Appl Energy 2017;186:520–9. https://doi.org/10.1016/j.apenergy.2016.02.067.

[52] Guadalfajara M, Lozano M, Serra L. Analysis of Large Thermal Energy Storage for Solar District Heating. Eurotherm Semin #99 Adv Therm Energy Storage 2014:1–10. https://doi.org/10.13140/2.1.3857.6008.

[53] Cruickshank CA, Harrison SJ. Heat loss characteristics for a typical solar domestic hot water storage. Energy Build 2010;42:1703–10. https://doi.org/10.1016/j.enbuild.2010.04.013.

[54] Maivel M, Kurnitski J. Heating system return temperature effect on heat pump performance. Energy Build 2015;94:71–9. https://doi.org/10.1016/j.enbuild.2015.02.048.

[55] NordPool Group. NordPool, the leading power market in Europe n.d. https://www.nordpoolgroup.com/ (accessed February 16, 2020).

[56] AE Solar. AE Solar Product list 2020. https://ae-solar.com/products-list/ (accessed December 25, 2020).

[57] Commission JRCE. Photovoltaic geographical information system-interactive maps 2014.

[58] Averfalk H, Werner S. Economic benefits of fourth generation district heating. Energy 2020;193:116727. https://doi.org/10.1016/j.energy.2019.116727.

[59] Jebamalai JM, Marlein K, Laverge J. Influence of centralized and distributed thermal energy storage on district heating network design. Energy 2020;202:117689. https://doi.org/10.1016/j.energy.2020.117689.

Paper II

Feasibilities of utilizing the thermal inertia of district heating networks to improve system flexibility

Yichi Zhang, Pär Johansson, Angela Sasic Kalagasidis

Preprint to be submitted, May 2021

Feasibilities of utilizing the thermal inertia of district heating networks to improve system flexibility

Yichi Zhang[1*], Pär Johansson[1], and Angela Sasic Kalagasidis[1]

[1]*Department of Architecture and Civil Engineering, Division of Building Technology,*

Chalmers University of Technology, Gothenburg 412 96, Sweden

***Corresponding author:**

Yichi Zhang

Department of Architecture and Civil Engineering, Division of Building Technology

Chalmers University of Technology

412 96, Gothenburg, Sweden

Tel: + 46 (0)31-772 68 01

Email: yichi@chalmers.se

Abstract

The use of the district heating network inertia (DHNI) has been regarded as an efficient and cost-saving method to improve the flexibility of the energy systems. However, the acclaimed benefits in most studies are limited to certain cases that are only good for the utilization. The occasions where the DHNI is not feasible are unclear and the applicability of the DHNI in future low-temperature district heating (LTDH) systems requires further notice. Therefore, this study applied a top-down method where the practical storage potentials of 134 Swedish DH networks and 25 Chinese DH networks with various sizes and demand densities are evaluated and compared. Then, bottom-level analysis from technical and economic aspects are conducted on a variety of application scenarios for DHNI, with different temperature levels, heat sources, control strategies and renewable energy profiles. It is found that in LTDH system, by raising the network temperatures to actively use the DHNI, the heat source efficiency is reduced and, thereby, making the DHNI infeasible. By contrary, the DHNI is only applicable in traditional middle-temperature systems with the heat source of the CHP plant in extraction mode. The results from multi-scenario analysis identified limited benefits of the DHNI, implying a proper consideration of its roles in future works.

Keywords

District heating; network inertia; thermal energy storage; wind power integration; combined heat and power;

Highlights:

- Networks storage potentials in 134 Swedish DH systems and 25 Chinese DH systems are investigated.
- Dynamic performances of the DHNI under a variety of application scenarios were modelled.
- DHNI is only applicable in middle-temperature systems with extraction CHP plant.
- Fixed flowrate control strategy is favorable for the best use of the DHNI.
- The annual cost-saving rate from the DHNI are less than 1% under all scenarios.
- Breakdown analysis is performed to identify the effective usage of the TES unit.

Nomenclature

Abbreviations

BP	Back-pressure
CHP	Combined heat and power
CNY	Chinese Yuan
COP	Coefficient of performance
DH	District heating

DHNI	District heating network inertia
ECR	Effective conversion ratio
LTDH	Low-temperature district heating
MTDH	Middle-temperature district heating
SOC	State-of-charge
TES	Thermal energy storage

Symbols

α	Combination factor
$Cost$	Cost (CNY)
F	Fuel consumption rate (MW)
η	Efficiency (%)
P	Electric power (MW)
Pr	Price (CNY/kWh)
Q	Heating power (MW)
T	Temperature (°C or K)
θ	Proportion (%)

Subscripts

ch	Charge
dch	Discharge
el	Electricity
grid	National electric grid
h2p	Heat to power
τ	Time step

1. Introduction

To reach the target of carbon neutral society and 100% sustainable future, accelerating growth of renewable energy is predicted in most countries and a large share of it, such as the wind and solar power, has intermittent and variable characteristics [1,2]. The efficient integration of these variable renewable energy (VRE) sources has brought serious challenges to all stakeholders in the energy systems, from energy suppliers to demand-side users [3].

The integration of VRE in the electricity sector demands an increased flexibility. This flexibility

could be provided by thermal energy storage (TES) technologies in heating systems in an efficient and cost-effective manner [4–6]. Currently, the heating sector accounts for 50% of Europe's final energy consumption [7] and is expected to remain so for the forecasted future. With the use of power-to-heat technologies such as the heat pump and the combined heat and power (CHP) plant, the integrations of VRE can be improved through the flexible management of heating load [8,9]. In recent years, various types of TES technologies have been applied in district heating (DH) systems, with the aims of shifting the load, improving the heat source efficiency and reducing the operation cost [10]. Recent applications of the TES technologies can be found in a review by Guelpa and Verda [11].

To deal with the variability and uncertainty of VRE within a short period like one day, growing interests are found in utilizing the storage potentials of the district heating network inertia (DHNI) [12]. By actively adjusting the temperature levels of the circulation water inside the pipes, additional flexibilities can be provided by the network with no extra investment. Meanwhile, the heat losses from pipes are slightly increased [13]. Commonly the supply water temperature increase is limited to several degrees, such as 10K or 15K. The storage capacity of the return pipes can be used if the temperature increases in the return pipes are allowed. Compared to the standalone TES technology such as the central heat accumulation tank, the use of DHNI is easily implemented [13]. Thus, the importance and potentials of the DHNI are gradually identified in recent studies. Lund [14,15] estimated the overall storage potentials of the Danish DH networks as 5 GWh, which is approximately 4.3% of the average daily DH load, based on the assumption of a 10K temperature increase. Zheng et al. [16] evaluated the network storage capacities in Northern China and calculated the reduced wind power curtailment and carbon emissions on provincial and regional level. Fredriksen and Werner [17] described the limited storage capacity of DHNI and pointed out that larger storage capacity is presented in bigger DH networks, with higher heat demand density. Due to the scarcity of available network information, the forecasted storage potentials are mostly based on cases from regional levels.

In addition to the issues for evaluating the storage potentials, whether the expected performances can be reached by the network inertia in practical conditions remains as a question. Several case studies were conducted in recent years to investigate the practical benefits of the DHNI, especially the improved integrations of VRE, both in China [18–23] and Europe [24–28]. Zheng et al. [18] developed an integrated heat and power dispatch model and optimized the network temperatures to actively use the storage capacity for wind power integrations, based on a case study of a real DH system with CHP plant in China. Using the same model, the storage utilization strategy was compared to other strategies such as the exhaust heat recycling, in terms of the total primary energy consumption [19]. Similar modelling methodologies were found in [21] where the DHNI was studied with the inertia of the building thermal mass. In the large DH network of Helsinki, with an average daily heating demand of 17-20 GWh, the storage potential is estimated as 1.5 GWh [24,25]. It is further proved that for a certain scheme, all the surplus VRE production could be absorbed by the power-to-heat technologies with TES. However, the coefficient of performance (COP) of the heat pumps (HPs) are assumed as constant, which is not true when raising the network temperatures for active storage.

The above-mentioned studies basically explained the benefits from the DHNI in certain cases with certain heat sources that are good for DHNI applications. Due to the different boundary conditions that were considered, the results vary between cases and the preferable

application scenarios of the DHNI are still unclear. Since the network temperatures are actively increased, the efficiencies of heat sources and the associated operational issues such as heat losses are inevitably influenced. However, most case studies [18–23,26–28] as reviewed above were limited to traditional middle and high temperature DH systems with CHP plants as the main heat source. These cases are also referred to as the third generation DH [29], where the supply and return water temperatures are around 100 °C and 50 °C, respectively. The supply water is heated by the high temperature extracted steam from the CHP plant and, thus, has little impact on the source efficiency. Other studies have assumed constant heat source efficiency when utilizing the network inertia [24,25]. However, this is not appropriate for heat sources whose efficiencies are associated with the supply water temperature [30]. Indeed, the additional costs associated with the increased temperatures might be larger than the proposed benefits.

Unlike the traditional systems, the low-temperature district heating (LTDH) system has been recognized as a key DH configuration in the future [29]. In such system, the network sizes are reduced due to lower heating demand in the future and the heat sources such as HPs are sensitive to the temperature changes in the network. Considering these changes, whether the use of the DHNI is still applicable in the LTDH systems, has not been clearly proven.

In addition to the network temperatures and the heating sources, the benefits of the DHNI are also influenced by various variables. It should be noted that the results of the above-mentioned studies are only limited to certain VRE surplus conditions. As the balance between the VRE supply and the energy demand changes, the benefit of the DHNI also changes. Besides, as pointed out in [13,23], the control strategies for the flowrate and the return water temperatures, have significant influences on the usable storage capacity and load shifting benefits. Although the different operation modes were compared in [23], the focus is more on the operational cost such as the pumping cost, while the influences on the heat source efficiency and storage capacity are less covered. With these questions unsolved, the proposed potentials and benefits of the DHNI might be over-exaggerated.

According to the above literature review, limitations and challenges exist for the use of the DHNI. Instead of the single case application as reported in previous studies, the application ranges of the DHNI are still unclear. In order to support the development of a sustainable energy system in the future, more comprehensive understandings of the DHNI are much needed. Therefore, this paper aims to answer the question of where and why is the use of DHNI feasible. The study is based on multi-scenarios analysis with the considerations of the technical and economical perspectives on the system level. The main focus is how the system performance is influenced by different conditions, including the temperature levels, heat sources, control strategies and the VRE balances. From the investigated information about various DH networks in Sweden and China, the range of storage potentials from the network inertia is also specified in this study. Based on the findings from the multi-scenario analysis, the key performance indicators of the DHNI are summarized, which can be used to identify the feasibility of the DHNI at an early design stage. This paper also provides implications for the applications of the DHNI in future energy systems.

The integrated DH system model to simulate the dynamic performance of the networks and the dispatch models of the heat sources are introduced in **Section 2**. The storage potentials of the practical DH networks are explained in **Section 3**. Based on a case DH network, the use of the DHNI under multi-scenarios is modelled and the results are shown in **Section 4.**

Implications for the future energy systems are presented in **Section 5**.

2. Methods

2.1. Case description

The multi-scenarios analysis is based on a case DH system in a town with approximately 50,000 inhabitants [31], located in the Hebei province in Northern China. The town belongs to the cold climate zone with an average temperature of -4.6 °C in January of the typical meteorology year. This town is chosen because it represents a vast number of middle-sized towns in China. For smaller DH systems such as those in the rural communities, the storage potentials of the networks can be as small as 0.5% of the daily heating demand, as pointed out in [17] and in the hereafter analysis in **Section 3**. As for larger DH systems in major cities, more complex networks with multiple heat sources are often built, which have complicated hydronic conditions to be modelled.

The total heated floor area by DH is 4.48 million m^2, comprising of residential, commercial, and industrial areas. The end-use buildings are grouped into 71 substations, as shown in **Fig. 1**. Each substation has heat exchangers that separate the secondary network from the primary network. In order to simplify the modelling process, the end-users connected to the same substation are aggregated into only one representative end-user, on which the modelling of the buildings and the secondary networks is conducted. This simplification is acceptable since the end-users connected to one substation often have similar building properties and load profiles. Correspondingly, the secondary network is represented by a pipe with certain length, according to the practical conditions. In this study, the thermal inertia of the primary network is considered. The total length of the primary networks is 52.3 km and the detailed lengths of each pipe diameter are shown in **Table 1**. As a result, the total volume of the circulating water inside the two-way pipes is 25,160 m^3. Considering a temperature increase of 10 K, the storage capacity of the primary pipes is 294 MWh.

The thermal properties of the end-use buildings are derived from the local housing department and are then used as known input parameters in the building models. In general, the heated buildings can be classified into three energy-efficient types, according to the building energy standards in Northern China [32–34]. The total heated floor area and average heat consumption at the building level of each type is shown in **Table 2**, based on the historical operation data from the local district heating company during the heating period from 2018 to 2019.

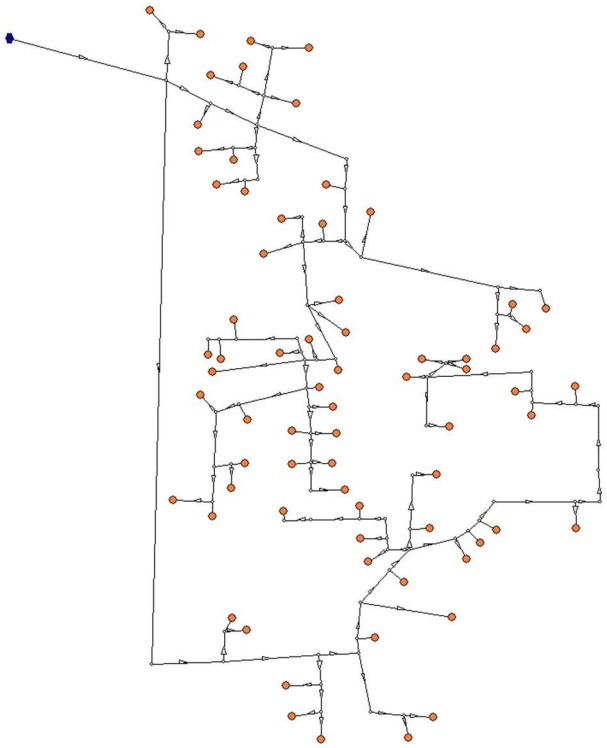

***Fig. 1**. Network layout of the case DH system*

***Table 1** Pipe diameters and total lengths of the primary network based on* [31]

Pipes	Length (m)	Volume (m^3)
DN125	24	0.3
DN150	3,820	67
DN200	6,329	199
DN250	7,047	346
DN300	4,144	293
DN350	5,371	516
DN400	4,023	505
DN450	864	137
DN500	1,852	363
DN600	7,597	2,147
DN700	600	231
DN800	1,300	653
DN900	1,324	842
DN1000	8,000	6,280
Total	52,295	12,580

Table 2 *Building types, accumulated heat consumptions and heating power demands at the building level during the heating period of 2018-2019*

Types	Floor area (m^2)	Heat consumption (kWh/m^2)	Heating power demand (W/m^2)	Ref
Non-energy-efficient building	1,696,318	140	58.3	-
Second-level energy efficient building	2,169,586	98	46.6	JGJ 26-95 [33]
Third-level energy efficient building	612,861	75	40.1	JGJ 26-2010 [34]

The investigated scenarios in this study are summarized in **Table 3**. The traditional middle-temperature district heating (MTDH) system has design supply and return water temperatures of 90 °C and 50 °C, respectively, and is the current operating system in the case town. In contrary, the LTDH represents a possible scenario in the future, with lower supply and return water temperatures of 55 °C and 25 °C, respectively. Since the focus of this study is on the DHNI, the feasibility of the LTDH system is not part of this study. Indeed, comprehensive investigations and evaluations are needed when planning for the LTDH system, as pointed out in [29]. Correspondingly, several heat sources options, located at the central heating plant in the Northwest part of the town, are available as investigated scenarios. The specific parameters and models of the heat sources are explained in **Section 2.3** in detail.

Table 3 *Summary of the investigated systems and scenarios*

Systems	Heat sources	Control strategies	VRE supply and electricity demand
MTDH	Extraction CHP, back-pressure CHP	Fixed flowrate, variable flowrate	VRE: 300MW to 700 MW
LTDH	Back-pressure CHP, large-scale HP		Demand: 50% and 100%

To investigate the application ranges of the DHNI, several scenarios with different VRE supply and electricity demand profiles are modelled, as presented in **Table 4** and **Table 5**. In this study, the available VRE is wind power, which is developing fast in Northern China but is also facing serious curtailment issues [35]. In the baseline scenario, the installed capacity of wind power is 500 MW and this scenario is also named VRE500, accordingly. Based on the actual power generating profiles in Northern China [18], the annual wind power production is 1.4 TWh, equivalent to 2801 full-load hours. In the 100% electricity demand scenario, the demand of the case town and the surrounding villages is considered, summing up to 1.8 TWh each year. The demand profile is derived from the actual profile in Jilin province [18], as shown in **Fig. 2**. The 50% electricity demand scenario is considered as the representative of a system with smaller boundary. As a result, the surplus wind power becomes higher within this scenario.

In addition to the heat supply service, the district energy company is also supplying electricity to the case town, with on-site CHP plant, wind power, or electricity from the national grid. Therefore, the main objective of using the DHNI is to minimize the operational cost for the local district energy company, by increasing the wind power share. The objective function and related energy costs are introduced in **Section 2.2**.

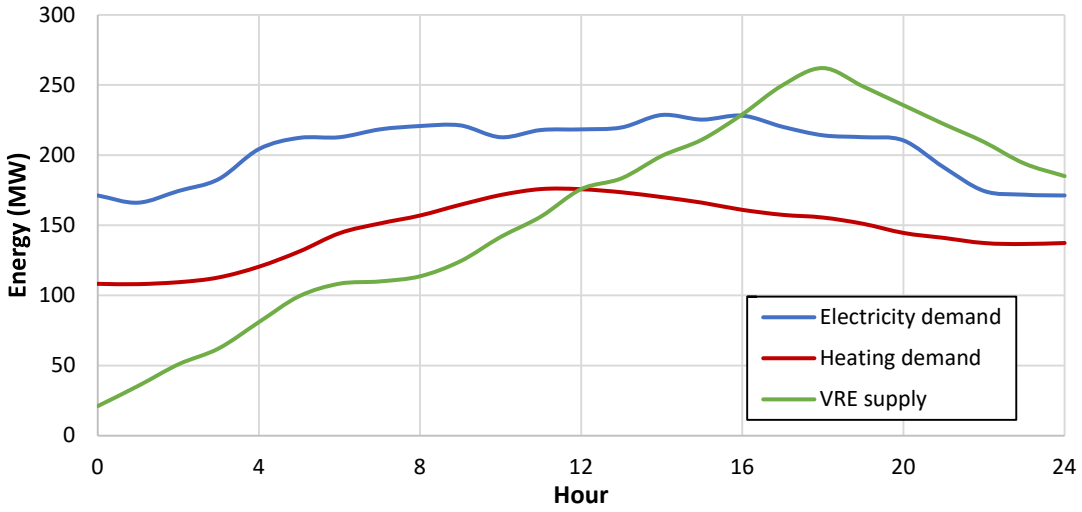

***Fig. 2**. Heating demand, electricity demand, and VRE supply profiles of the baseline scenario on the typical day of Jan 2nd*

***Table 4** Installed capacities and annual power generations for five VRE scenarios*

Scenarios	Installed capacity (MW)	Annual generation (GWh)
VRE300	300	840
VRE400	400	1,121
VRE500[1]	500	1,401
VRE600	600	1,681
VRE700	700	1,961

[1] *Baseline scenario*

***Table 5** The maximum power and annual demand for the two household electric demand scenarios*

Scenarios	Maximum power (MW)	Annual demand (GWh)
100% electric demand[1]	228.6	1,800
50% electric demand	114.3	900

[1] *Baseline scenario*

2.2. DH system models

The integrated DH system model used in this study is based on the model developed in a previous study by the authors [36]. The general modelling methodologies are briefly explained in this section, while the detailed modelling principles, variables and functions can be found in [36]. As shown in **Fig. 3**, the model has four main steps. In the first step, based on the input building properties and the weather data, the demand profiles for space-heating are calculated by a lumped capacitance building model with five resistances (5R1C), according to EN ISO 13790 [37]. Domestic hot water draw-off profiles are generated by stochastic modelling tool tool called *DHWcalc* [38]. Then, the compartments in the DH systems, such as the heat sources, substations and circulating pipes, are designed in the second step. In the

third step, the temperatures and flow dynamics of the networks are modelled by the node method [39,40], with considerations of the transport delay and heat loss. This scenario is also named the reference (REF) scenario, where the active load management is not implemented. Then, in the fourth step, the active usage of the DHNI is optimized. The multi-scenarios analysis is conducted on this model, by changing parameters according to specific designs in scenarios.

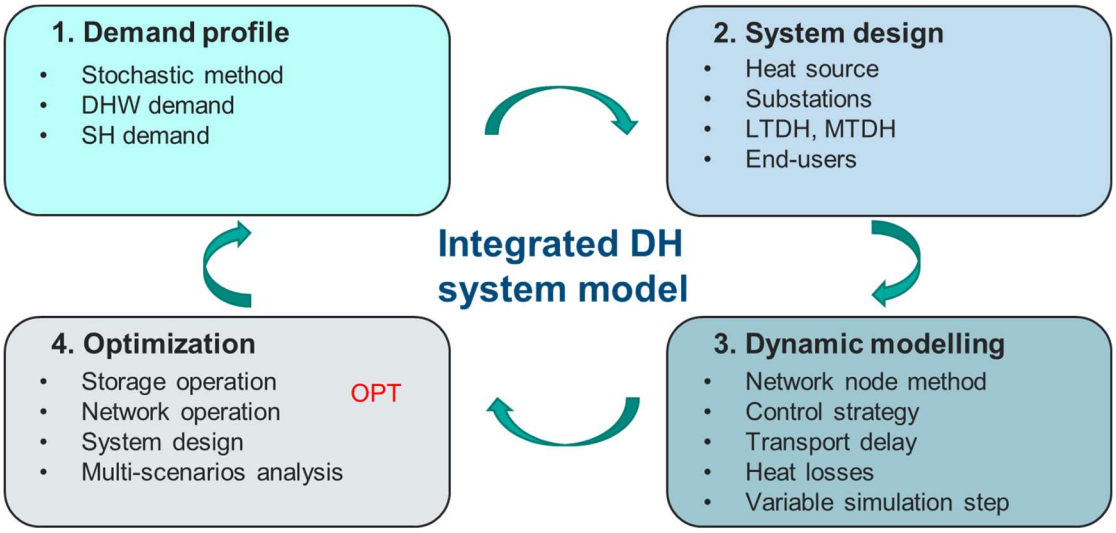

***Fig. 3**. Schematic of the main steps of the integrated DH system model*

As explained above, the target of the optimization process is to find the minimum operating cost. For simplicity reasons, this study only considered two major parts of the operating cost, which are the fuel cost of the heat source and the bill for the electricity from the grid, as written in **Eq. (1)**. The cost for water circulating pumps and the costs associated with the auxiliary equipment are neglected. Furthermore, the surplus wind power cannot be sold back to the grid. To integrate more wind power and to reduce the electricity from the grid, the electric load is changed by adjusting the heating load through the active use of the network inertia.

$$\min Cost = \sum_{\tau} (Pr_{fuel} * F_{HS,\tau} + Pr_{el,grid,\tau} * P_{el,grid,\tau}) \quad (1)$$

where $P_{el,grid,\tau}$ is the amount of electricity bought from the grid and $Pr_{el,grid,\tau}$ is the corresponding price, which is set as 0.5 Chinese Yuan (CNY)/kWh in this study, according to the average electricity price on the market. For the whole year of 2020, one Chinese Yuan (CNY) equals to on average 0.145 US dollar. $F_{HS,\tau}$ is the fuel consumption of the heat source at time τ and Pr_{fuel} is the fuel price. As for the CHP plant, the biomass fuel with an average calorific value of 16 MJ/kg is used. According to the local market, the biomass price is 440 CNY/t, which corresponds to approximately 0.1 CNY/kWh. As for the heat pump, the electricity price is set the same as the price from the grid.

For each time step τ, the heating demand and electricity demand shall be fulfilled, as written in constraint functions in **Eqs. (2)** and **(3)**.

$$Q_{HS,\tau} \geq Q_{demand,\tau} \quad (2)$$

$$P_{el,CHP,\tau} + P_{el,grid,\tau} + P_{VRE,use,\tau} \geq P_{el,demand,\tau} \quad (3)$$

where $Q_{HS,\tau}$ and $Q_{demand,\tau}$ are the heat supply and demand at time τ, respectively. $P_{el,CHP,\tau}$ is the electricity generated from the CHP plant. $P_{VRE,use,\tau}$ is the integrated wind power. $P_{el,demand,\tau}$ is the electricity demand. If the heat source is an electricity consumer, like the HP, the related demand is added to the right hand side of **Eq. (3)**.

Due to the non-linear characteristics of the complex networks, a combined central optimization and local control strategy is applied in this study, to simplify the optimization process while maintaining realistic characteristics of the DH system. As shown in **Fig. 4**, within an optimization cycle, the model first makes forecasts about the energy supply and demand, based on operation states from the last cycle. Then, the complex system and the use of the DHNI are simplified into lumped capacity models, which in total generates a mixed-integer linear problem that can be easily solved. The timely state-of-charge (SOC) of the network inertia is updated according to the temperatures inside the whole networks. Specific constraints about the maximum charging and discharging powers, storage losses, SOC limits, and the energy balance of each cycle, are implemented in the optimization problem. Detailed equations and explanations can be found in [36]. Then, the optimal operation signals of the DHNI are passed to the integrated system models. Combined with the local controllers designed to guarantee the thermal comfort and specific system requirements, the dynamic system performances with active load management are modelled. The results are passed-on to the next optimization cycle as input data.

The whole model is developed and performed in MATLAB. The dynamic calculation step is set as one minute in accordance with the demand profile, and the optimization time step is set as one hour. The length of an optimization cycle is set as 5 days, considering the accuracy of forecast and the control complexity.

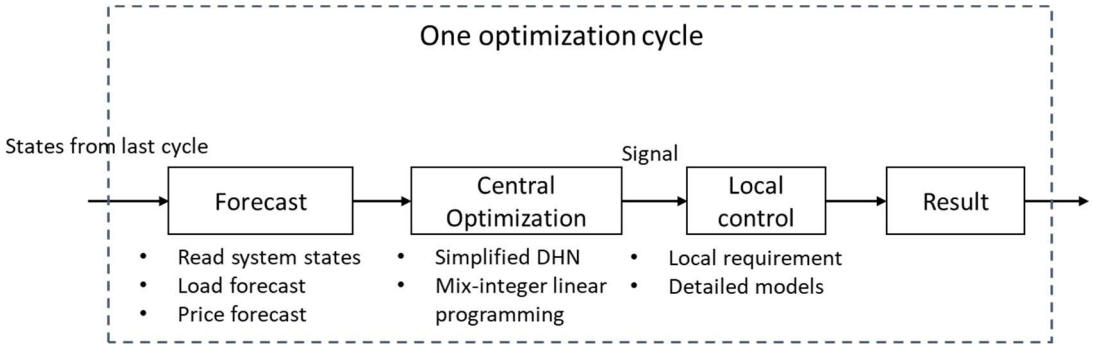

***Fig. 4**. Schematic diagram of the combined central optimization and local control strategy, from* [36].

Two control strategies for the flowrate are considered in this study, as shown in **Table 3**. Under the variable flowrate strategy, to use the network inertia, only the supply water temperature is adjusted while the return water temperature is controlled within an acceptable small range to assure the heat source efficiency. However, only half of the storage potential is used, as is indicated in previous works [13,23]. Besides, the flowrate is reduced when raising the network temperature, which further hampers the storage potential. In contrary, the “fixed flowrate, variable temperatures” control strategy can better utilize the network inertia. Due to the transportation delay in large DH networks, this control strategy is more commonly applied in systems with less frequent demand changes, such as the DH systems in China that mostly have no centralized domestic hot water supply. The hot water demand is fulfilled by household appliances like the gas boiler or electric heater.

2.3. Heat source models

Since the focus of this study is to investigate the improved VRE integrations achieved by the DHNI, the heat sources that connect the heating and electricity sectors are chosen, including the CHP plants and HPs, as shown in **Table 3**. It should be noted that the use of the storage unit can also bring in benefits from other aspects, such as the peak load shaving and the reduction of ramping costs of the heat sources [10,11]. These aspects are currently omitted in this study.

Two types of CHP plants are considered in this study, which are the extraction plant and the back-pressure plant. As for the extraction plant, the middle pressure steam with the temperature of approximately 150 °C is extracted from the steam turbines to heat the circulating water. Therefore, the active use of the network inertia is simply considered to have no influence on the source efficiency. The heating and electricity output can be adjusted by the amount of extracted steam, within certain minimum and maximum limits. Meanwhile, the main steam flowrate can be adjusted by changing the boiler load. In this study, an extraction plant with the nominal power generating capacity of 250 MW is selected. The feasible operation range of it is shown in **Fig. 5**. Any operating point within this range can be expressed by the convex combination of the coordinates of the corner points [18,41], using the **Eqs. (4)** - **(6)**. It should be noted that there are various methods to improve the efficiency of the CHP plant [42]. These methods are not considered for analysis in this study and are discussed in **Section 5**.

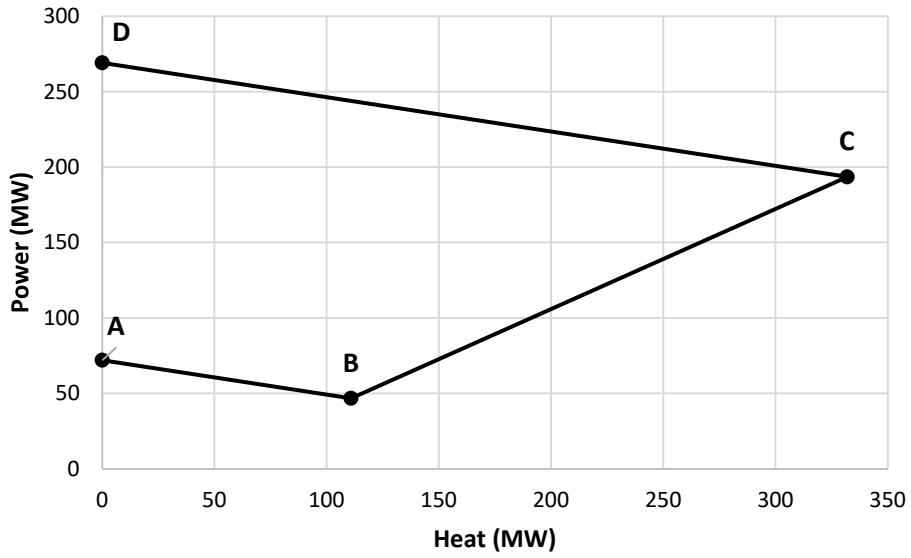

Fig. 5. Feasible operation range of the extraction CHP plant

$$Q_{CHP,\tau} = \sum_{N=1}^{4} (\alpha_{N,\tau} * Q_{CHP,N}) \quad (4)$$

$$P_{el,CHP,\tau} = \sum_{N=1}^{4} (\alpha_{N,\tau} * P_{CHP,N}) \quad (5)$$

$$F_{el,CHP,\tau} = \sum_{N=1}^{4} (\alpha_{N,\tau} * F_{CHP,N}) \quad (6)$$

where $\alpha_{N,\tau}$ are the combination factors of four corners, complying with the constraints written in **Eq. (7)**. The maximum ramping rate of the main boiler is set as 30%/hour, taken from the design brochure of the CHP plant.

$$\sum_{N=1}^{4} \alpha_N = 1 \tag{7}$$

As for the back-pressure CHP plant, the only adjustable option is the boiler load. Thus, the plant has fixed power-to-heat ratio and the feasible operation range is a straight line on **Fig. 5**, e.g. line C-B. The parameters of the chosen back-pressure plant for the MTDH scenarios are shown in **Table 6**. The circulating water is heated by the low-pressure exhaust steam from the turbine. As the required supply water temperature increases, the exhaust steam pressure and temperature shall also be increased. Correspondingly, the electric power and heating power are changed, as shown in **Table 6**. As is explained in **Section 2.2**, this change has important influences on the wind power integrations and the benefits of the DHNI.

Table 6 *Parameters of the back-pressure CHP plant for MTDH scenarios*

Load	Exhaust temperature (°C)	Main steam (t/h)	Electric Power (MW)	Heating power (MW)
Max	100	500	87.8	336.7
Min		150	26.3	101.0
Max	110	500	86.0	338.9
Min		150	25.8	101.7

Due to its low efficiency for high-temperature applications, the HP is only used in the LTDH system, with a nominal supply water temperature of 55 °C. The design parameters of the chosen waste water source heat pump are presented in **Table 7**. The practical COP is calculated by the empirical equation with the condensing temperature T_C, evaporating temperature T_E, and the thermodynamical perfectiveness of 0.65 [43], as written in **Eq. (8)**. The waste water at the source side is considered to have a stable temperature of 15 °C.

$$COP = 0.65 * \frac{T_C}{T_C - T_E} \tag{8}$$

Table 7 *Parameters of the HP for LTDH scenarios*

Name	Capacity (MW)	Outlet T (°C)	Thermodynamical perfectiveness	Design COP
Waste water source heat pump	350	55	0.65	4.8

2.4. Key performance indicators

In order to compare the storage performances of the network inertia under various scenarios, the number of full-load discharge cycles is defined in **Eq. (9)**.

$$Full-load\ discharge\ cycles = \frac{\sum_\tau Q_{dch,\tau}}{SOC_{design}} \tag{9}$$

where the $Q_{dc\ ,\tau}$ is the discharged energy at time step τ. SOC_{design} is the design SOC, which is 147 MWh is only the supply pipes are used for storage.

To evaluate the performance of improved VRE integrations, the effective conversion ratio (ECR) of the storage unit, which explains the effective usage of the discharged energy, is defined in **Eq. (10)**.

$$ECR = \frac{\Delta \sum_\tau P_{VRE,use,\tau}}{\sum_\tau Q_{dch,\tau}} \quad (10)$$

During the entire year of 2019, the dynamic performances of the reference system without active storage usage are firstly investigated. Then, the case DH systems with the use of the network inertia under different scenarios are modelled and compared. The improved VRE integration rate is calculated to evaluate the benefits of the DHNI, as defined in **Eq. (11)**.

$$Improved\ VRE\ integration\ rate = \frac{\Delta \sum_\tau P_{VRE,use,\tau} - \Delta \sum_\tau P_{VRE,use,ref,\tau}}{\sum_\tau P_{VRE,\tau}} \quad (11)$$

where the $P_{VRE,\tau}$ is the wind power production at time step τ.

3. Storage potentials

In this section, the storage potentials of the networks in Swedish DH systems and Chinese DH systems are evaluated and compared. The information about the Swedish DH systems is derived from the previous investigation of 134 DH systems [17]. Based on that, the average pipe diameters were estimated through linear heat density Q_s/L, as written in **Eq. (12),** from [44].

$$d_a = 0.0486 \cdot \ln\left(\frac{Q_s}{L}\right) + 0.0007 \quad (12)$$

Then, the storage capacities of the networks are estimated at different temperature increase scenarios. The ratio of the storage capacity in the daily heating demand is calculated and shown in **Fig. 6**, assuming on average 180 heating days in the Swedish DH systems. It should be noted that only the supply pipes are considered in the estimations. The ratio of storage capacity increases first and then decreases as the linear heat density becomes larger. Even though considering a temperature increase of 20K in the most favorable scenario, the storage capacity in the investigated DH networks is only 1.6 % of the daily heating demand. In the 10K temperature increase scenario, the storage capacity is always less than 0.8% of the daily heating demand.

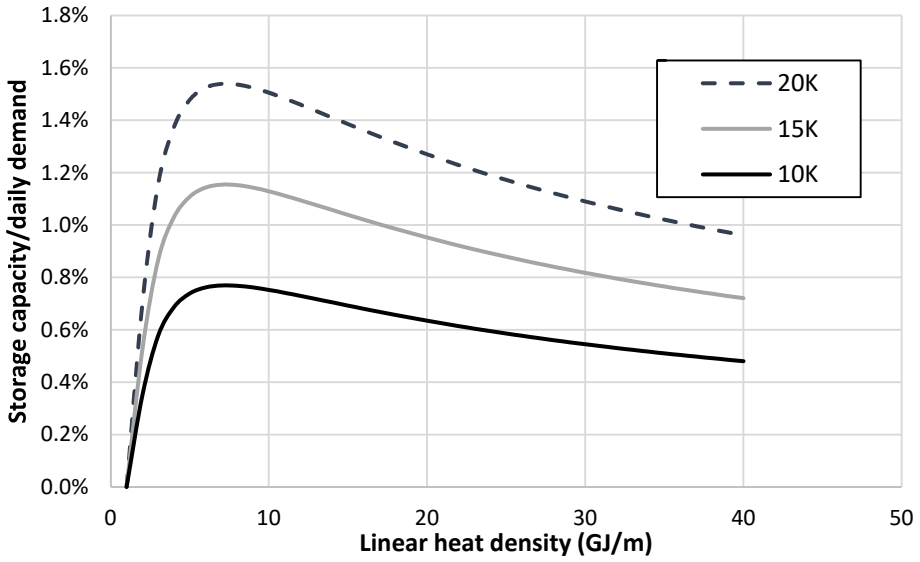

Fig. 6. The ratio of the storage capacity in the daily heating demand in Swedish DH systems

In this study, investigations were conducted about the network information and heating demand of 25 DH systems in China, located in a wide range of areas from the small towns to huge metropolitans. The relationships between linear heat densities and average pipe diameters are summarized in **Fig. 7**. Compared to Swedish DH systems, under the same heat density, the average pipe diameter in Chinese DH systems are much larger. This is explained by that the pipes are designed for the DH systems and heating loads in the future, accompanying the rapid urban development in China. Thus, from the current perspective, the pipes are over-sized to some levels. Correspondingly, the storage capacities of the supply pipes in these DH systems are calculated and summarized in **Fig. 8**. The heating periods are derived from investigations and are used for calculating the average daily demand. Similar as the Swedish DH systems, the ratio of the storage capacity increases first and then decreases in larger systems. Considering the temperature increase of 10 K, the storage capacity of the networks is on average 4 % of the daily heating demand.

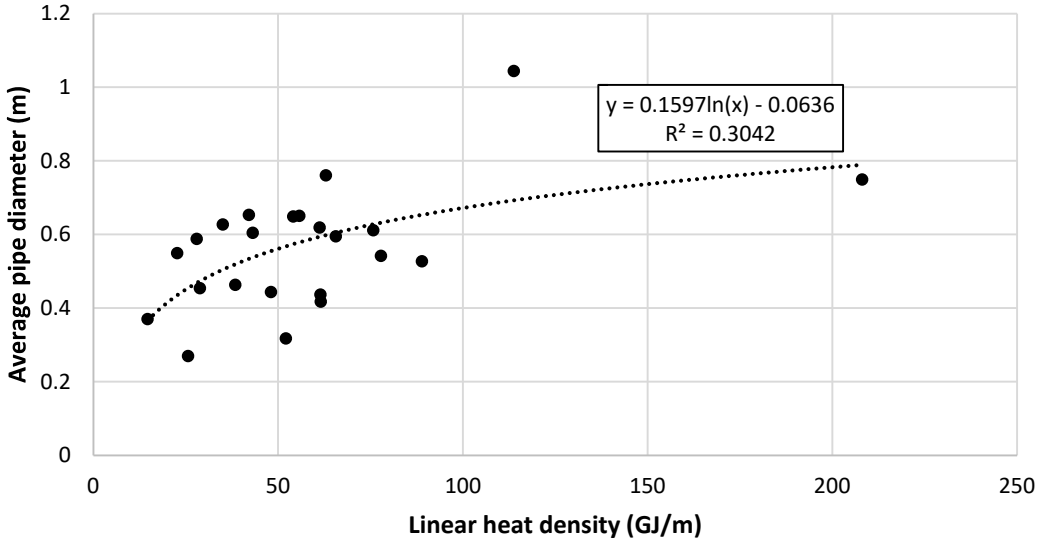

Fig. 7. The relationship between the average pipe diameter and linear heat density

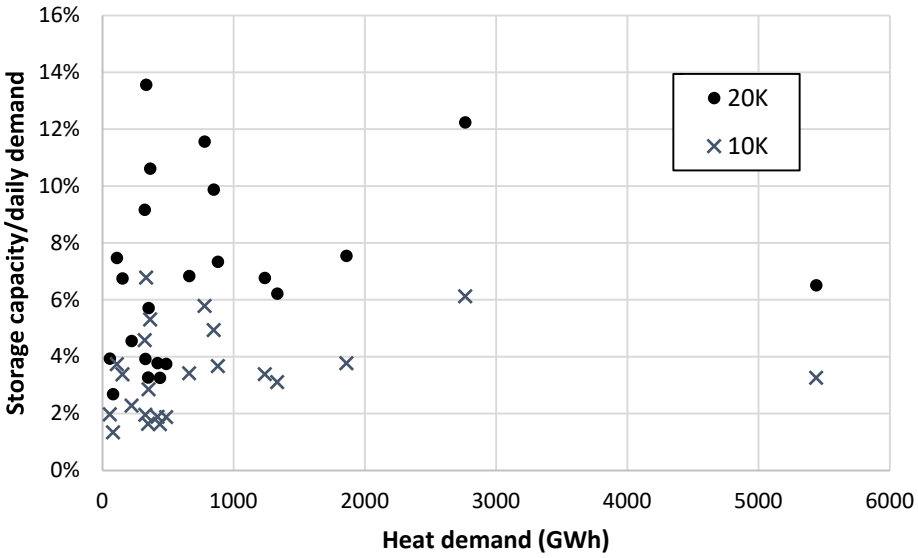

***Fig. 8**. The ratio of the storage capacity in the daily heating demand in Chinese DH systems*

4. Multi-scenario analysis results

Based on the above-mentioned methodologies, the case DH system and the scenarios explained in **Section 2** are simulated at an annual period. The performances of the network inertia under different network temperature levels, heat sources, flowrate control strategies and the VRE balances, are compared and discussed in this section.

4.1. MTDH scenarios

By comparing the MTDH systems with and without the active use of the network inertia, the performances and benefits of the network inertia are explained. Taking the system with the extraction plant as an example, the hourly heat supply and SOC of the network inertia during five winter typical days, from the Jan 1st to the Jan 5th, when there are variations in both the energy supply and demand, are shown in **Fig. 9**. Considering a time constant of 10 hours, the maximum charging and discharging powers are set as 14.7 MW for using the network inertia. When the wind power is abundant, the electric power of the CHP plant is reduced to as much as possible to integrate the surplus VRE, as shown in **Fig. 10**. Since the heat and power output are connected, the storage capacity of the network is then used to fill in the gap between the heat supply and demand, e.g. during the 8th and 16th hours of the typical days. **Fig. 11** presents the hourly supply and return water temperatures and explains how the storage capacity is utilized. Since the variable flowrate strategy is applied, the return water temperatures are kept at a relatively stable range, while the supply water temperatures are adjusted.

In the reference MTDH system, the annual total heat supply is 578.1 GWh, of which 27.7 GWh is the heat loss through pipes. In the system with active DHNI usage, although the water temperature level is increased, the circulating flowrate is reduced in the meanwhile. Thus, the total heat loss is only slightly increased to 28.6 GWh.

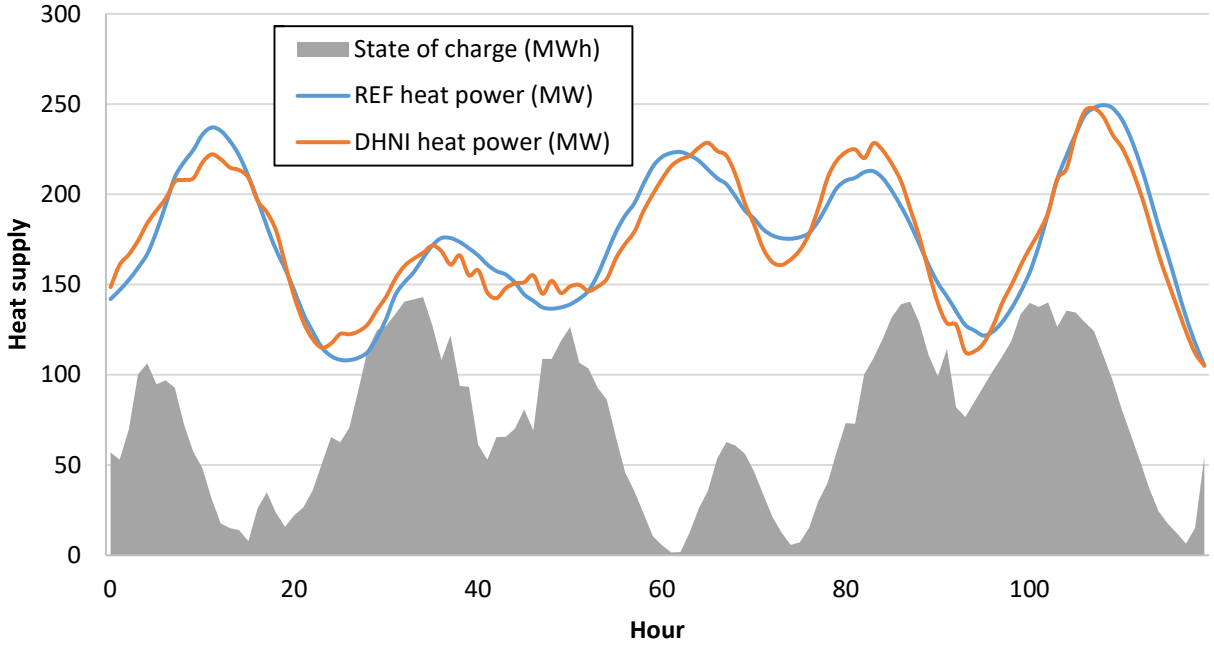

Fig. 9. Hourly heat supply and storage state of charge on five typical days from Jan 1st to Jan 5th

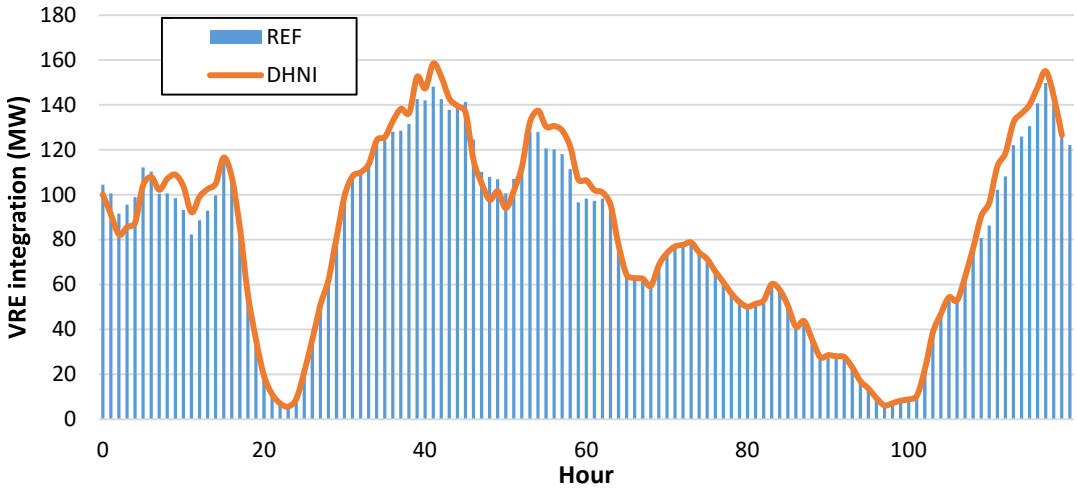

Fig. 10. Hourly VRE integrations of the REF and CHP systems on five typical days from Jan 1st to Jan 5th

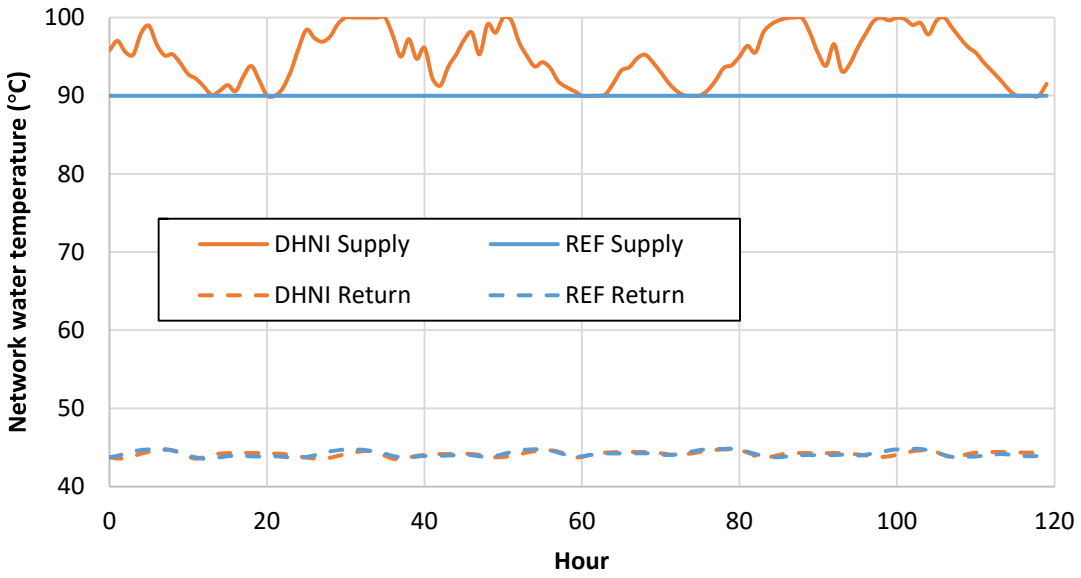

Fig. 11. Network supply and return water temperatures of the REF and CHP systems on five typical days from Jan 1st to Jan 5th

Similar modelling methodologies are applied for the MTDH system with the back-pressure plant as the heat source. The annual electricity supply and demand for the investigated systems are summarized in **Fig. 12**. The demand is constituted by the direct use of CHP power, integrated VRE and the electricity bought from the grid. By actively using the DHNI, the integrations of the VRE are improved by 6 GWh and 4.3 GWh respectively, in extraction and back-pressure systems. However, due to the restricted storage capacity, the increased VRE usage is only approximately 0.4% of the total VRE supply and 0.3% of the total electricity demand.

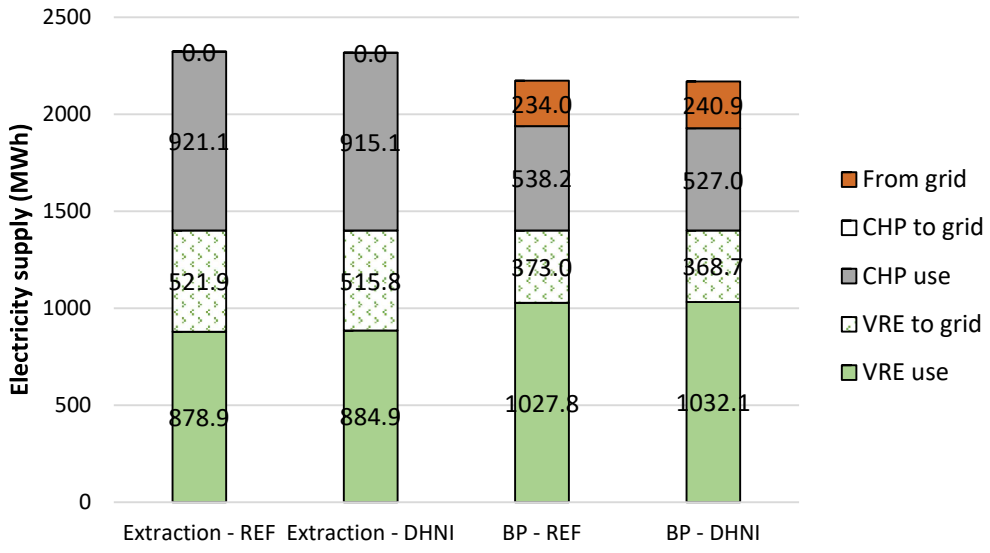

Fig. 12. Electricity supply of the extraction and back-pressure (BP) CHP systems

To evaluate the storage performance, the effective conversion ratio (ECR) of the storage unit, explained in **Section 2.4**, is calculated for the case systems. As shown in **Table 8**, in the extraction plant scenario, only around 31% of the discharged energy is effectively used to shift the electric load. This can be mainly explained by two reasons. First, the average heat-to-

power ratio of the extraction CHP plant is around 2, which is the baseline conversion factor between the heat and power sectors. Second, due to the diverse heating demand and the local control strategies, the practical control of the discharging process deviates from the ideally optimized process and, therefore, limits the storage benefits. Compared to the standalone energy storage unit such as the central water tank, the DH pipes are not only storage units but also the energy transportation carriers. Thus, the use of the storage capacity can be influenced by the fluctuations in the pipes. As for the back-pressure plant, although the heat-to-power ratio is near 4, the reduced power generating capacity has increased the VRE integrations, as is explained in hereafter paragraphs.

Table 8 *Storage efficiency and the effective conversion rate (ECR) of the DHNI in two systems*

Scenarios	Accumulated energy (GWh)		Storage Efficiency	Full-load Cycles	Improved VRE (GWh)	ECR
	Charge	Discharge				
Extraction	20.50	19.74	96.3%	134	6.0	0.31
Back-pressure	13.60	12.94	95.2%	88	4.3	0.33

The relatively small VRE integration benefit can also be explained by the limited usage of the DHNI during the low-demand period. As shown in **Fig. 13**, the optimization basically failed during Summer because it is not economical feasible to raise network temperature to just shift a small part of the load.

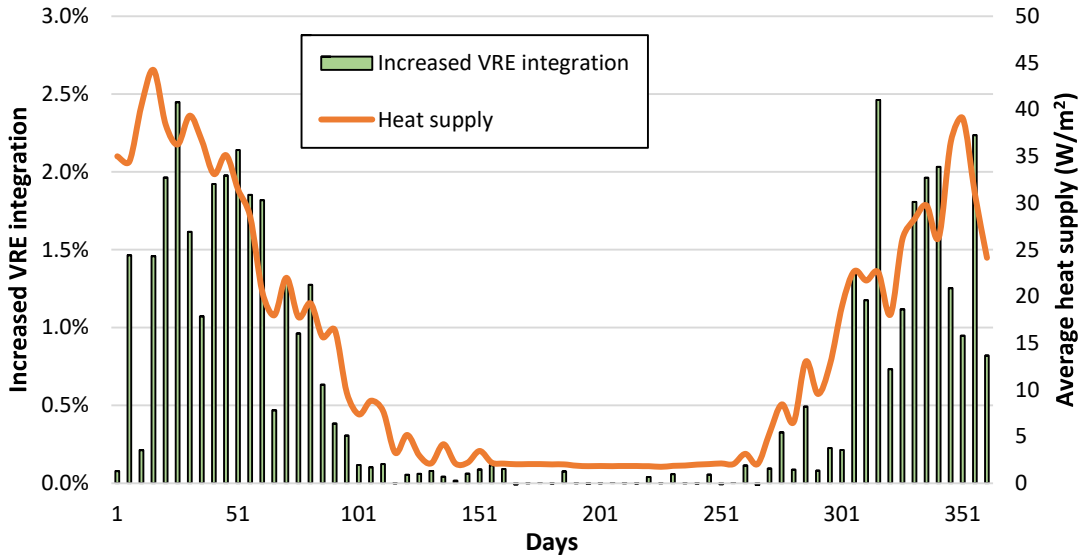

Fig. 13*. Increased VRE integration rate in the extraction CHP system during the study year. Each bar represents one optimization cycle, which equals five days.*

In the back-pressure plant, to actively raise the network supply water temperature, the saturated exhaust steam temperature is slightly increased from 100 °C to 110 °C. Consequently, the power generating capacity is reduced from 87.8 MW to 86.0 MW and the annual CHP power production is reduced by 11.2 GWh. As shown in **Fig. 12**, the reduced capacity can be partly fulfilled by the VRE, but the system still needs to buy electricity from the grid. Thus, although the use of VRE is increased by 4.3 MWh, the use of DHNI is not economically feasible in the BP system, as expressed by the total operational cost in **Table 9**. In comparison, the temperature of the extracted steam from the traditional EXTR plant is high

enough to heat up the network circulating water, causing little influences on the CHP plant efficiency. Thus, the total operating cost is reduced by 0.6% in the extraction system. Moreover, as shown in **Table 8**, the discharged energy in the BP system is also smaller than that in the EXTR system because the optimization process failed for longer period due to the lowered BP plant efficiency.

However, the above results only refer to a certain scenario where the electricity demand is higher than the total power generating capacity of the CHP plant and the VRE. The benefits and potentials of the network storage are different as the balance between the VRE supply and electricity demand changes, which are further explained in **Section 4.4**.

Table 9 *Annual operational costs and fuel consumptions of the extraction and back-pressure CHP systems*

Scenarios	CHP Fuel (GWh)	Cost (million CNY)		
		Fuel cost	Grid bought	Total
Extraction - REF	2719	680	0	680
Extraction - DHNI	2705	676	0	676
Back-pressure - REF	3042	760	119	880
Back-pressure - DHNI	3040	760	123	883

4.2. LTDH scenarios

The extraction CHP plant is not preferable in LTDH systems due to its low exergy efficiency. Using the similar methodologies as the previous section, the use of DHNI in the LTDH systems is modelled. The general results of improved VRE integration rates and the cost-saving rates of different systems are summarized in **Fig. 14**. For the system with back-pressure plant, as is in the MTDH cases, although around 5 GWh of VRE is added to the system, the use of DHNI is economically infeasible since an additional 11.3 GWh of electricity is bought from the grid.

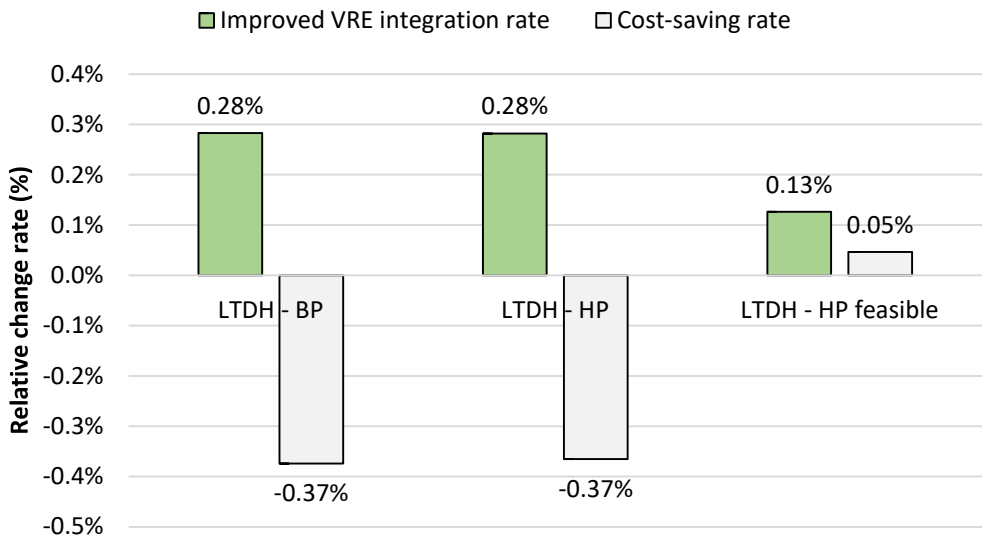

Fig. 14*. Improved VRE integration rate and cost-saving rate for the LTDH systems with back-pressure (BP) CHP plant and HP as heating sources*

As for the system with large-scale HPs, raising the network temperatures directly influences the HP efficiency. As shown in **Table 10**, the COPs are reduced, causing extra electricity

consumptions for heating, which cannot be offset by the improved VRE integrations. Thus, the operational cost becomes higher after using the DHNI. Indeed, the use of the DHNI is only feasible for 60 days, where the acquired benefits are larger than the loss of HP efficiencies. During the rest period, the operating cost is higher than that of the reference system. Thus, the DHNI can be only activated during the feasible period. The modelled results of this alternative scenario are also presented in **Fig. 14** and **Table 10**, with a short name of LTDH - HP - feasible. It is clear that with a shorter optimization period, the HP efficiencies are slightly influenced. Since the VRE integration benefits are also reduced, the general operating cost is only reduced by 0.05%.

Table 10 *Annual average COPs of the HPs and the improved VRE integrations in the LTDH systems*

Scenarios	COP	Average temperatures (°C)		Electricity demand (GWh)		VRE use (GWh)	Feasible days
		Supply	Return	Heating	Household		
LTDH - REF	4.89	55	26.8	120.6	1800	1175	-
LTDH - HP	4.64	59.2	27	128.5	1800	1180	60
LTDH - HP feasible	4.84	55.8	26.8	122.5	1800	1177	65

The storage efficiencies and the ECRs for the DHNI in the three LTDH systems are summarized in **Table 11**. As explained above, taking only the feasible optimization period into account, the use of DHNI equals to 44 complete cycles, which is significantly lower than the other scenarios. Since the HP has higher heat-to-power ratio, the ECR index in the HP system is lower than the CHP systems. A qualitative analysis about the relationships between the ECR index and the benefits of thermal energy storage units can be found in the discussion part.

Table 11 *Discharged energy of the DHNI and the storage performances*

Scenarios	Discharged energy (GWh)	Storage efficiency (%)	Equivalent cycles	ECR
LTDH - back pressure	15.8	93.7%	107	0.32
LTDH - HP	24.6	93.2%	167	0.21
LTDH - HP feasible	6.4	95.2%	44	0.35

4.3. Influence of flowrate control strategies

The MTDH systems are used as case systems in this section to investigate the influence of the flowrate control strategy. As explained above, due to the large transportation delay of the fixed flowrate strategy, the domestic hot water demand is currently omitted. The detailed supply and return water temperature profiles of the MTDH system with extraction CHP plant on Jan 4th is presented in **Fig. 15**, as an example. Compared to the variable flowrate strategy as shown in **Fig. 11**, the storage capacities of the return pipes are utilized. Consequently, the discharged energy from the network inertia is increased, as shown in the annual results in **Table 12**. However, the improved VRE integrations and associated cost-savings are not linearly increased as with the discharged energy, due to the limitations of the network storage in handling intermittent VRE. Thus, the ECR indices are reduced to approximately 0.2. As for the MTDH system with back-pressure CHP plant, the VRE integration is also improved but the operating cost is still lower than the cost in the reference scenario.

The above strategy of fixed flowrate is only applicable in traditional DH systems, where the large transportation time lag is acceptable for merely the SH demand. As the performances of the buildings are gradually improved, the instantaneous domestic hot water demand will play more important roles in the total heating demand[45,46], leaving less feasibilities for the fixed flowrate control. Besides, with the widely acknowledged benefits from reducing the return water temperatures, using the inertia of the return pipes significantly impacts the heat source efficiency and is not feasible from both the technical and economic aspects, as indicated in the previous section. Thus, the LTDH systems are not considered here.

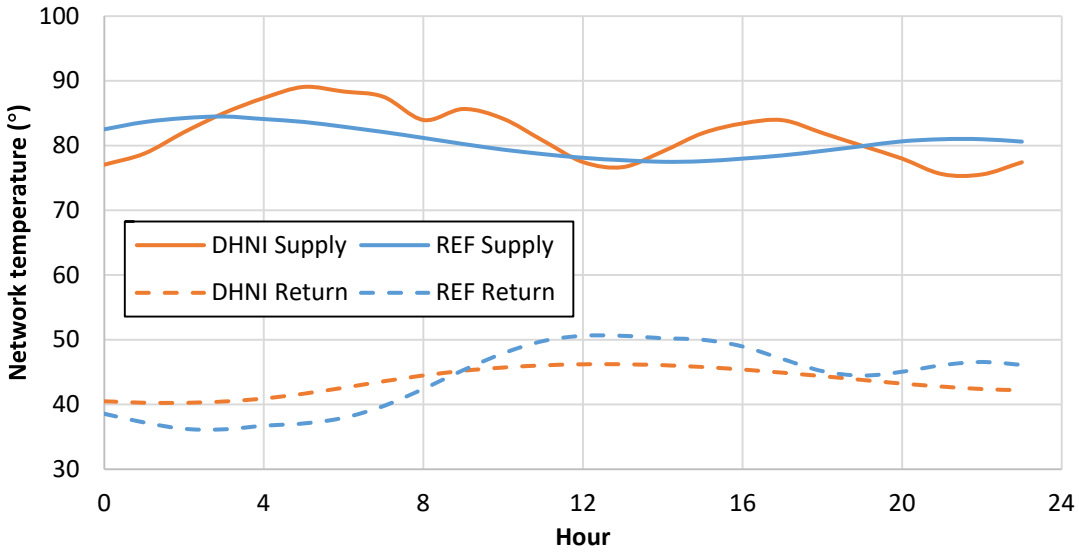

***Fig. 15**. Network supply and return water temperatures for the MTDH system with fixed flowrate control strategy*

***Table 12** The improved VRE integrations and cost-savings of the MTDH systems with two control strategies for the whole study year*

Source	Control strategy	Discharged energy (GWh)	Improved VRE (GWh)	(%)	Cost saving (Million CNY)	(%)
Extraction	Variable flowrate	19.7	6.0	0.4%	3.7	0.5%
	Fixed flowrate	44.0	8.9	0.6%	5.4	0.8%
Back-pressure	Variable flowrate	12.9	4.3	0.3%	-3.1	-0.3%
	Fixed flowrate	23.2	5.3	0.4%	-2.0	-0.2%

4.4. Influence of VRE balances

In addition to the scenarios explained above, the VRE supply profiles and household electric demand profiles are revised to understand the benefits of the DHNI under different boundary conditions. The investigated scenarios are summarized in **Table 4** and **Table 5**. The VRE scenarios represent the possible development of wind power in the future and the electric demand scenarios represent the boundaries of the investigated energy systems. Similar as the **Section 4.3**, the LTDH systems are not considered in this part due to the infeasibility of the DHNI.

Based on the simulated results, the key performance indicators for the use of the DHNI under the investigated scenarios, compared to the reference scenarios, are shown in **Fig. 16** - **Fig.**

19. The ratio between the improved integrated VRE and the total supplied VRE, becomes smaller as the energy supply is larger. The capability of the network inertia to integrate VRE is also reflected in the ECR indicator, which has an upper limit due to the heat-to-power conversion efficiencies and the storage characteristics.

As for the system with extraction plant, although the economic benefits of the DHNI is increased with a larger VRE supply, upper limits of the cost-saving rate exist, which are approximately 0.7% and 0.6% for the 50% demand and 100% demand scenarios, respectively. The upper limits are associated with the limitations to integrate the intermittent VRE. It is found that the use of the DHNI is only feasible in a certain range of application scenarios. Yet, the cost-saving benefit and VRE integration benefit are still relatively small, compared to the overall operating cost and energy consumptions of the studied whole system.

The ECR of the back-pressure plant is slightly higher than the extraction plant because the reduction of power generating capacity increases the VRE integrations, as explained in **Table 9**. Due to the same reason, the use of the DHNI in the back-pressure system is only economically feasible in the 50% demand scenario with VRE installed capacity larger than 600 MW. In this case, the installed capacity of the wind power is almost 6 times of the maximum power in the demand side, which is hard to be achieved in realistic systems.

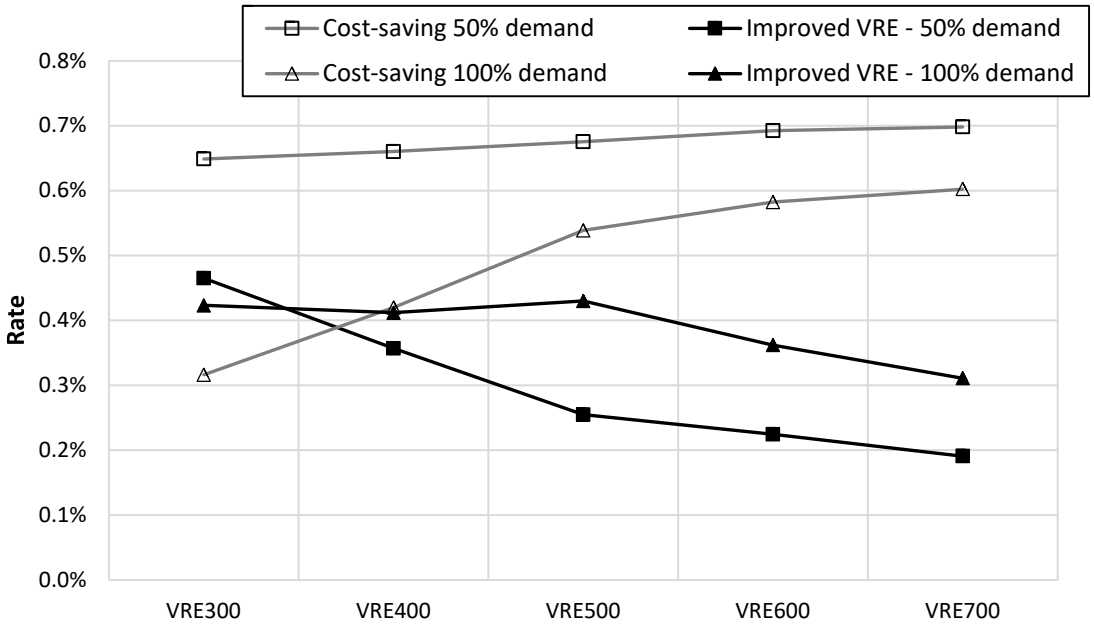

***Fig. 16**. Improved VRE integration rate and cost-saving rate for the MTDH systems with extraction plant under different conditions*

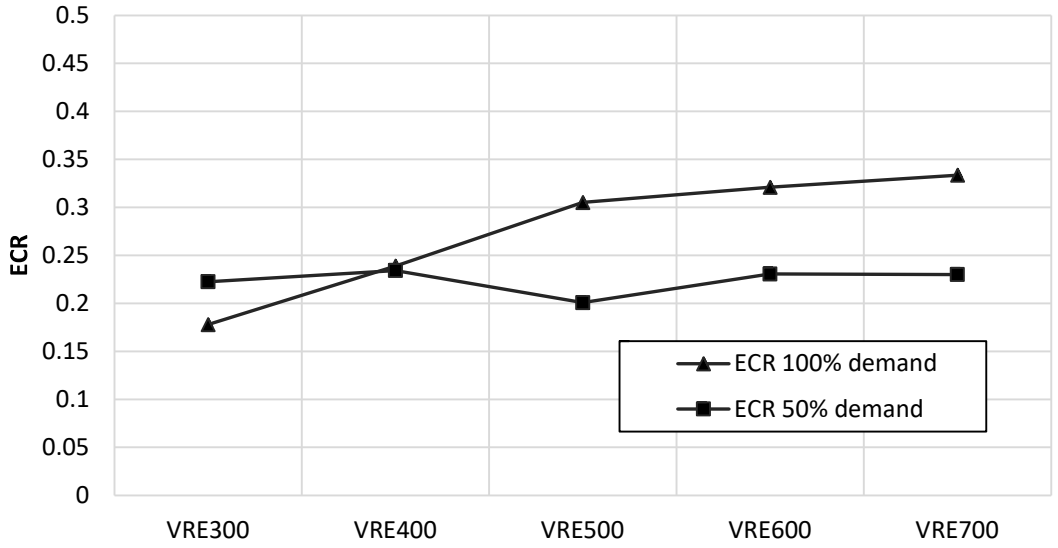

***Fig. 17**. Effective conversion ratio (ECR) for the DHNI in the MTDH systems with extraction plant*

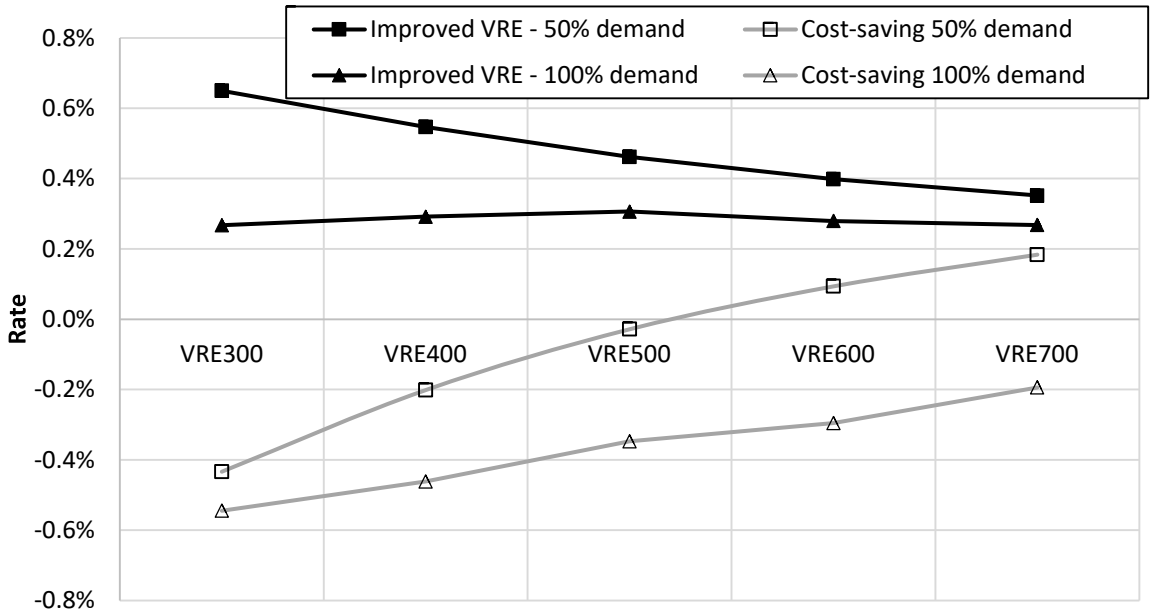

***Fig. 18**. Improved VRE integration rate and cost-saving rate for the MTDH systems with back-pressure plant under different conditions*

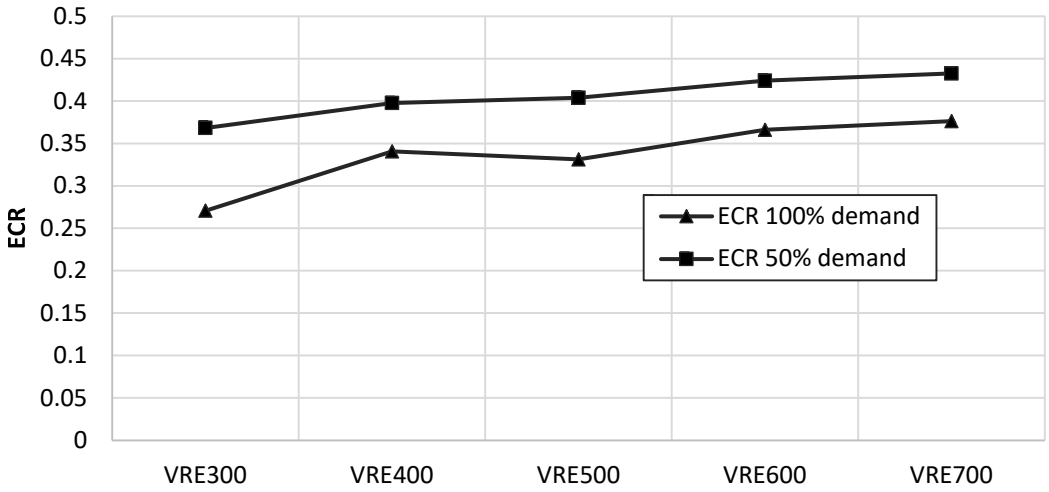

Fig. 19. Effective conversion ratio (ECR) for the DHNI in the MTDH systems with back-pressure plant

4.5. Theoretical analysis of the storage usage

From the modelled results presented in above sections, it is found that even under the most favorable scenario, the VRE integration benefit of the DHNI is still relatively small, compared to the overall energy productions and consumptions. To explore the reasons behind this result, theoretical breakdown analysis of the effective usage of the storage unit is conducted, as shown in **Fig. 20**. In this section, the analysis refers to not just the DHNI but the general TES unit. Considering a system with 100% electricity demand and 100% heating demand, the design storage capacity of the TES unit is expressed by θ_{TES}, which is for example 5% in **Fig. 20**. Then, practical issues including the heat losses and control precisions, expressed by $\eta_{heat\ loss}$ and $\eta_{control}$ respectively, have left only an usable part of the storage capacity. This part is then converted to shift the electric load with a heat-to-power conversion factor η_{h2p}, which usually has values of 2 for extraction CHP plant and 3~5 for HPs. Using the empirical values from the modelled results, the final converted electricity $\theta_{el,shift}$ is only 1.7% of the total demand. If the energy system has higher electricity demand, such as the baseline system where the electricity demand is three times of the heating demand, the benefit of the converted electricity becomes less significant, as is revealed by the results of this study. The conversion process is expressed in **Eq. (13)**. Alternatively, the ECR index can be written as **Eq. (14)**.

In the above analysis, the heat loss rate $\eta_{heat\ loss}$ is influenced by the thermal characteristics of the storage unit and has a range of 80%~95%. The control precision $\eta_{control}$ is a rather complex index that is decided by various factors such as the location of the storage unit, the system complexity and the load fluctuations, as explained in **Section 4.1**. The heat-to-power factor, η_{h2p}, is directly related to the heat sources, which are designed according to the whole energy system plans. Using the above method, the load shifting benefit of the TES unit can be easily assessed.

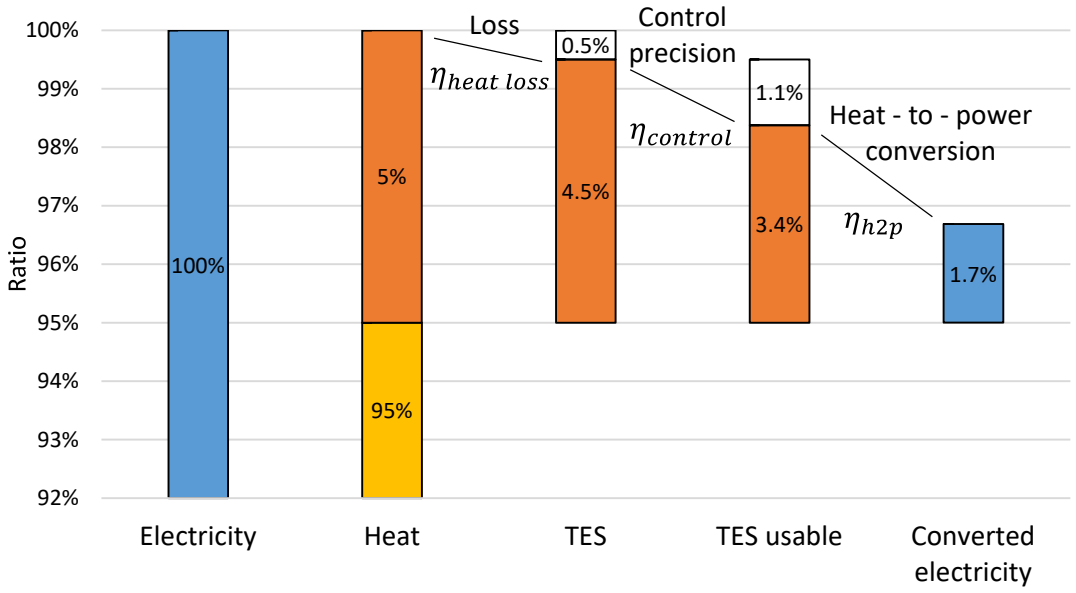

***Fig. 20**. Breakdown analysis of the effective usage of the TES for electric load shifting*

$$\theta_{el,shift} = \theta_{TES} * \eta_{heat\ loss} * \eta_{control} * \eta_{h2p} \quad (13)$$

$$ECR = \eta_{heat\ loss} * \eta_{control} * \eta_{h2p} \quad (14)$$

5. Discussion

In this study, the benefits of the DHNI are derived from the comparison of the reference scenario and the active-controlled scenario. The reference scenario is assumed to have theoretical control over the flowrate so that the network inertia is not used at all. However, in reality, due to the time delays in almost all parts of the complex DH system, the practical control strategy can hardly reach the theoretically assumed one. Therefore, the network inertia is unavoidable utilized to some levels, causing positive or even negative effects on the system performances and operating costs. Since the exact time delays and practical performances are hard to modelled, the results of this study are only limited to assumptions.

Various methods have been developed in recent years to recycle the waste heat from the exhaust steam and to increase plant efficiency [42], such as the use of the absorption heat pump [47]. However, these improvements are not considered for the extraction CHP plant in this study. Taking the system with the absorption heat pump as an example, the amount of the extracted steam and exhaust steam shall be carefully controlled, to match the high-grade and low-grade energy sources. Thus, the use of the extracted steam to raise the network temperatures might impact the overall system efficiency. The applicability of the DHNI in the newly developed CHP systems shall be further examined. Moreover, flexible heat storage options such as the two tanks design [48], have been developed in recent years to improve system flexibility while fully recovering the waste heat.

6. Conclusion

This study has investigated the storage potentials of the DH pipes in a group of representative DH systems in Sweden and China. Based on an integrated DH system model, the technical and economical feasibilities for using the network inertia as storage unit are analyzed under

various scenarios, including the different network temperature levels, heat sources, flowrate control strategies and the VRE balances. The suitable application ranges and the proposed benefits of using the network inertia are found in this study. Key conclusions are summarized as follows:

1) The investigations of the DH systems have shown that the storage capacities of the Swedish DH networks studied here are always less than 0.8% of the daily heating demand, considering a 10K temperature increase. In contrary, due to over-sized pipes, the same index in Chinese DH systems is on average 4% of the daily heating demand.

2) In traditional MTDH systems with the extraction CHP plant, since the heat source efficiency is not influenced by the raised network temperatures, the DHNI can improve the VRE integrations by 0.4% of the total VRE supply and reduce the total operating cost by 0.6%. In the scenario with the back-pressure plant, although the integrations of VRE is improved, the use of DHNI is not economically attractive because the system need to buy more electricity from the grid.

3) In future LTDH systems with HPs, the DHNI is only feasible for a short period due to reduced source efficiencies, leading to a small cost-saving rate of 0.05%. In LTDH systems with back-pressure plants, the DHNI is still economically infeasible as is in the MTDH systems.

4) The fixed flowrate control strategy can better utilize the storage capacity, compared to the variable flowrate strategy. By changing the VRE supply and electricity demand profiles, the upper limits of the cost-saving benefits for utilizing the DHNI are found, along with the upper limits of the effective conversion ratios between the storage capacity and the shifted electricity.

Finally, theoretical breakdown analysis of the effective usage of the storage unit is conducted, to explain the relatively small benefit associated with the network inertia. The proposed analysis method can be applied to all TES units. From the results of this study, it is pointed out that the DHNI can only play limited roles for improving the flexibility in future DH systems.

Acknowledgement

This work was supported by the Swedish Research Council for Environment, Agricultural Sciences and Spatial Planning (FORMAS) [Grant No. 2018-01228]. The authors also thank the Chalmers Energy Area of Advance, Profile area: Energy in Urban Development for the additional financial support. The authors would like to express sincere thanks to the DH companies for providing operational data and network information.

Reference

[1] Lund PD, Lindgren J, Mikkola J, Salpakari J. Review of energy system flexibility measures to enable high levels of variable renewable electricity. Renew Sustain Energy Rev 2015;45:785–807. https://doi.org/10.1016/j.rser.2015.01.057.

[2] Gielen D, Boshell F, Saygin D, Bazilian MD, Wagner N, Gorini R. The role of renewable energy in the global energy transformation. Energy Strateg Rev 2019;24:38–50. https://doi.org/10.1016/j.esr.2019.01.006.

[3] Alizadeh MI, Parsa Moghaddam M, Amjady N, Siano P, Sheikh-El-Eslami MK. Flexibility in future power systems with high renewable penetration: A review. Renew Sustain Energy Rev 2016;57:1186–93. https://doi.org/10.1016/j.rser.2015.12.200.

[4] Lund H, Østergaard PA, Connolly D, Mathiesen BV. Smart energy and smart energy systems. Energy 2017;137:556–65. https://doi.org/10.1016/j.energy.2017.05.123.

[5] Lund H, Østergaard PA, Chang M, Werner S, Svendsen S, Sorknæs P, et al. The status of 4th generation district heating: Research and results. Energy 2018;164:147–59. https://doi.org/10.1016/j.energy.2018.08.206.

[6] Lund H, Østergaard PA, Connolly D, Mathiesen BV. Energy storage and smart energy systems. Energy 2017;137:556–65. https://doi.org/10.1016/j.energy.2017.05.123.

[7] Intergovernmental Panel on Climate Change, editor. Summary for Policymakers. Clim. Chang. 2013 – Phys. Sci. Basis Work. Gr. I Contrib. to Fifth Assess. Rep. Intergov. Panel Clim. Chang., Cambridge: Cambridge University Press; 2014, p. 1–30. https://doi.org/DOI: 10.1017/CBO9781107415324.004.

[8] Hewitt NJ. Heat pumps and energy storage - The challenges of implementation. Appl Energy 2012;89:37–44. https://doi.org/10.1016/j.apenergy.2010.12.028.

[9] David A, Mathiesen BV, Averfalk H, Werner S, Lund H. Heat Roadmap Europe: Large-scale electric heat pumps in district heating systems. Energies 2017;10:1–18. https://doi.org/10.3390/en10040578.

[10] Gadd H, Werner S. Thermal energy storage systems for district heating and cooling. Woodhead Publishing Limited; 2015. https://doi.org/10.1533/9781782420965.4.467.

[11] Guelpa E, Verda V. Thermal energy storage in district heating and cooling systems: A review. Appl Energy 2019;252:113474. https://doi.org/10.1016/j.apenergy.2019.113474.

[12] Hennessy J, Li H, Wallin F, Thorin E. Flexibility in thermal grids: A review of short-term storage in district heating distribution networks. Energy Procedia 2019;158:2430–4. https://doi.org/10.1016/j.egypro.2019.01.302.

[13] Basciotti D, Judex F, Pol O, Schmidt R-R. Sensible heat storage in district heating networks: a novel control strategy using the network as storage. IRES - 6th Int Renew Energy Storage Conf Exhib 2011:4.

[14] Lund H. Renewable heating strategies and their consequences for storage and grid infrastructures comparing a smart grid to a smart energy systems approach. Energy 2018;151:94–102. https://doi.org/10.1016/j.energy.2018.03.010.

[15] Lund H. Corrigendum to “Renewable heating strategies and their consequences for storage and grid infrastructures comparing a smart grid to a smart energy systems approach” [Energy 151 (2018) 94–102](S0360544218304080)(10.1016/j.energy.2018.03.010). Energy 2018;153:1087. https://doi.org/10.1016/j.energy.2018.04.159.

[16] Zheng W, Hennessy JJ, Li H. Reducing renewable power curtailment and CO2 emissions in China through district heating storage. Wiley Interdiscip Rev Energy Environ 2020;9:1–11. https://doi.org/10.1002/wene.361.

[17] Werner S. District heating and cooling 2013.

[18] Zheng J, Zhou Z, Zhao J, Wang J. Integrated heat and power dispatch truly utilizing thermal inertia of district heating network for wind power integration. Appl Energy 2018;211:865–74. https://doi.org/10.1016/j.apenergy.2017.11.080.

[19] Wang J, Zhou Z, Zhao J, Zheng J. Improving wind power integration by a novel short-term dispatch model based on free heat storage and exhaust heat recycling. Energy 2018;160:940–53. https://doi.org/10.1016/j.energy.2018.07.018.

[20] Li Z, Wu W, Shahidehpour M, Wang J, Zhang B. Combined heat and power dispatch considering pipeline energy storage of district heating network. IEEE Trans Sustain Energy 2016;7:12–22. https://doi.org/10.1109/TSTE.2015.2467383.

[21] Gu W, Wang J, Lu S, Luo Z, Wu C. Optimal operation for integrated energy system considering thermal inertia of district heating network and buildings. Appl Energy 2017;199:234–46. https://doi.org/10.1016/j.apenergy.2017.05.004.

[22] Huang X, Xu Z, Sun Y, Xue Y, Wang Z, Liu Z, et al. Heat and power load dispatching considering energy storage of district heating system and electric boilers. J Mod Power Syst Clean Energy 2018;6:992–1003. https://doi.org/10.1007/s40565-017-0352-6.

[23] Zheng J, Zhou Z, Zhao J, Wang J. Effects of the operation regulation modes of district heating system on an integrated heat and power dispatch system for wind power integration. Appl Energy 2018;230:1126–39. https://doi.org/10.1016/j.apenergy.2018.09.077.

[24] Salpakari J, Mikkola J, Lund PD. Improved flexibility with large-scale variable renewable power in cities through optimal demand side management and power-to-heat conversion. Energy Convers Manag 2016;126:649–61. https://doi.org/10.1016/j.enconman.2016.08.041.

[25] Mikkola J, Lund PD. Modeling flexibility and optimal use of existing power plants with large-scale variable renewable power schemes. Energy 2016;112:364–75. https://doi.org/10.1016/j.energy.2016.06.082.

[26] Balić D, Maljković D, Lončar D. Multi-criteria analysis of district heating system operation strategy. Energy Convers Manag 2017;144:414–28. https://doi.org/10.1016/j.enconman.2017.04.072.

[27] Korpela T, Kaivosoja J, Majanne Y, Laakkonen L, Nurmoranta M, Vilkko M. Utilization of District Heating Networks to Provide Flexibility in CHP Production. Energy Procedia 2017;116:310–9. https://doi.org/10.1016/j.egypro.2017.05.077.

[28] Turski M, Sekret R. Buildings and a district heating network as thermal energy storages in the district heating system. Energy Build 2018;179:49–56. https://doi.org/10.1016/j.enbuild.2018.09.015.

[29] Lund H, Werner S, Wiltshire R, Svendsen S, Eric J, Hvelplund F, et al. 4th Generation District Heating (4GDH) Integrating smart thermal grids into future sustainable energy systems. Energy 2014;68:1–11. https://doi.org/10.1016/j.energy.2014.02.089.

[30] Averfalk H, Werner S. Economic benefits of fourth generation district heating. Energy 2020;193:116727. https://doi.org/10.1016/j.energy.2019.116727.

[31] Li Y, Xia J, Fang H, Su Y, Jiang Y. Case study on industrial surplus heat of steel plants for district heating in Northern China. Energy 2016;102:397–405. https://doi.org/10.1016/j.energy.2016.02.105.

[32] Ministry of Housing Urban-Rural Development. Standard for energy consumption of building GB/T 51161-2016. Beijing, China: Architecture and Building Press; 2016.

[33] Ministry of Housing Urban-Rural Development. JGJ 26-95 Energy conservation design

standard for new heating residential buildings. Beijing, China: Architecture and Building Press; 1995.

[34] Ministry of Housing Urban-Rural Development. JGJ 26-2010 Design Standard for Energy Efficiency of Residential Buildings in Severe Cold and Cold Zones. Beijing, China: Architecture and Building Press; 2010.

[35] Fan XC, Wang WQ, Shi RJ, Li FT. Analysis and countermeasures of wind power curtailment in China. Renew Sustain Energy Rev 2015;52:1429–36. https://doi.org/10.1016/j.rser.2015.08.025.

[36] Zhang Y, Johansson P, Kalagasidis AS. Applicability of thermal energy storage in future low-temperature district heating systems – case study using multi-scenario analysis (under review). Energy Convers Manag 2021.

[37] de Normalización CE. EN ISO 13790: Energy Performance of Buildings: Calculation of Energy Use for Space Heating and Cooling (ISO 13790: 2008). CEN; 2008.

[38] Jordan U, Vajen K. Realistic domestic hot-water profiles in different time scales. Rep Sol Heat Cool Progr Int Energy Agency (IEA-SHC)Task 2001;26:1–18.

[39] Benonysson A, Bøhm B, Ravn HF. Operational optimization in a district heating system. Energy Convers Manag 1995;36:297–314.

[40] Zhao H. Analysis, modelling and operational optimization of district heating systems, 1995.

[41] Lahdelma R, Hakonen H. An efficient linear programming algorithm for combined heat and power production. Eur J Oper Res 2003;148:141–51. https://doi.org/10.1016/S0377-2217(02)00460-5.

[42] Li Y, Chang S, Fu L, Zhang S. A technology review on recovering waste heat from the condensers of large turbine units in China. Renew Sustain Energy Rev 2016;58:287–96. https://doi.org/10.1016/j.rser.2015.12.059.

[43] Maivel M, Kurnitski J. Heating system return temperature effect on heat pump performance. Energy Build 2015;94:71–9. https://doi.org/10.1016/j.enbuild.2015.02.048.

[44] Persson U, Werner S. Heat distribution and the future competitiveness of district heating. Appl Energy 2011;88:568–76. https://doi.org/10.1016/j.apenergy.2010.09.020.

[45] Braas H, Jordan U, Best I, Orozaliev J, Vajen K. District heating load profiles for domestic hot water preparation with realistic simultaneity using DHWcalc and TRNSYS. Energy 2020;201:117552. https://doi.org/10.1016/j.energy.2020.117552.

[46] Averfalk H, Werner S. Novel low temperature heat distribution technology. Energy 2018;145:526–39. https://doi.org/10.1016/j.energy.2017.12.157.

[47] Li Y, Fu L, Zhang S, Jiang Y, Xiling Z. A new type of district heating method with co-generation based on absorption heat exchange (co-ah cycle). Energy Convers Manag 2011;52:1200–7. https://doi.org/10.1016/j.enconman.2010.09.015.

[48] Wu Y, Fu L, Zhang S, Tang D. Study on a novel co-operated heat and power system for improving energy efficiency and flexibility of cogeneration plants. Appl Therm Eng 2019;163:114429. https://doi.org/10.1016/j.applthermaleng.2019.114429.